Copyright Warning & Restrictions

The copyright law of the United States (Title 17, United States Code) governs the making of photocopies or other reproductions of copyrighted material.

Under certain conditions specified in the law, libraries and archives are authorized to furnish a photocopy or other reproduction. One of these specified conditions is that the photocopy or reproduction is not to be "used for any purpose other than private study, scholarship, or research." If a, user makes a request for, or later uses, a photocopy or reproduction for purposes in excess of "fair use" that user may be liable for copyright infringement,

This institution reserves the right to refuse to accept a copying order if, in its judgment, fulfillment of the order would involve violation of copyright law.

Please Note: The author retains the copyright while the New Jersey Institute of Technology reserves the right to distribute this thesis or dissertation

Printing note: If you do not wish to print this page, then select "Pages from: first page # to: last page #" on the print dialog screen

ABSTRACT

The Effects of Twist on Pressure Through a Teflon Vascular Prosthesis

by
Steven Alfred Olivieri

A closed loop fluid system was developed which mimics the flow curve in the human circulatory system in order to test the effects of pressure drop and flow velocity on artificial arterial implants. This device consists of a piston pump connected to a microcomputer controlled servo-motor. Fluid (in this case distilled water) flows through transparent Tygon tubing to a test chamber. The prosthetic tube is placed in the fluid but is attached through a specially constructed chamber. The pressure across the implant can be measured for different conditions. System compliance was generated by using flexible tubing in the return loop and fluid resistance was developed by using filters.

Experiments were performed using standard tubing as well as artificial grafts to test the concept that twist of the implant effects flow. The pressure drop across the implant was measured with an increasing twist. Various lengths and tensions were tested. The results indicate that there is no correlation between twist (from 0 to 180 degrees) and pressure drop.

THE EFFECTS OF TWIST ON PRESSURE THROUGH A TEFLON VASCULAR PROSTHESIS

By

Steven Alfred Olivieri

A Thesis
Submitted to the Faculty of
New Jersey Institute of Technology
in Partial Fulfillment of the Requirements
for the Degree of Master of Science in
Biomedical Engineering
May 1992

APPROVAL PAGE

The Effects of Twist on Pressure Through a Teflon Vascular Prosthesis

By

Steven Alfred Olivieri

5-7-92

Clarence W. Mayott III, Ph.D., Thesis Adviser — Date
Professor of Mechanical Engineering, NJIT

5-7-92

David Kristol, Ph.D., Committee Member — Date
Director of Biomedical Engineering, Professor of Chemistry, NJIT

5/7/92

Frank T. Padberg, Jr., MD, Committee Member — Date
Associate Professor of Surgery, New Jersey Medical School, UMDNJ, Newark, NJ
Dept. of Surgery (112), VA Medical Center, East Orange, NJ

BIOGRAPHICAL SKETCH

Author: Steven Alfred Olivieri

Degree and Date: Master of Biomedical Engineering, May 1992

Undergraduate and Graduate Education:

- Master of Biomedical Engineering,
  New Jersey Institute of Technology, Newark, NJ, 1992
- Bachelor of Science in Mechanical Engineering,
  Worcester Polytechnic Institute, Worcester, MA, 1986

Major: Biomedical Engineering

Presentations and Publications:

The Effects of Twist on Pressure of a Teflon Vascular Prosthesis, First New Jersey Symposium on Biomaterials and Medical Devices, UMDNJ, Poster Session, 1992.

Modeling the Insertion of a Zickel Rod Into the Femur, ASTM's F-4 Special Technical Publication 1008, 1989.

Positions Held:

Development Engineer, Research & Development, 6/1991-Present
Osteonics Corp., Div. of Stryker Corp., Allendale, NJ

Development Engineer, Reconstructive Product Development, 1/1991-6/1991
Graduate Co-Op Student, Reconstructive Product Development, 6/1990-12/1990
Howmedica, Div. of Pfizer, Rutherford, NJ

Mechanical Engineer, Engineering Department, 11/1986-9/1989
Hamilton Standard, Div. of United Technologies, Corp., Windsor Locks, CT

Research/Engineering Assistant, Research and Development, 6/1984-5/1986
C.R. Bard, Cardiosurgery Division, Billerica, MA

This thesis is dedicated to:

My fiancée, Renée R. Bouquard, who encouraged and supported my decision to attend graduate school full-time. Her emotional support is greatly appreciated. Renée is presently pursuing her nursing degree. I am confident that her knowledge, kindness, and genuine caring for others will be well appreciated by the medical community.

My parents, Gasper J. Olivieri & Elena M. Olivieri, who have always stressed the value of an education. I am very grateful for all that they have taught me. I would like to thank them for all the many sacrifices they have made throughout the years to ensure that my brother and I always received a quality education. Their love and encouragement have made the pursuit for higher education an easier endeavor.

My brother, David N. Olivieri, for his continual support and the many hours he spent tutoring me on various subjects during my graduate career. Dave is presently pursuing his PhD in Nuclear Physics. I wish him the best, and know that he will succeed in all that he does.

ACKNOWLEDGMENT

The author wishes to express his sincere appreciation to his advisor Clarence W. Mayott III, Ph.D., for his guidance and assistance throughout this research.

The author also wishes to acknowledge the support of David Kristol, Ph.D., Director of the Biomedical Engineering Program. His continued friendship, guidance and support throughout my career as a graduate student at the New Jersey Institute of Technology is greatly appreciated. His generosity and "open door policy" towards students seeking academic guidance benefits the many students who come in contact with him.

The author expresses sincere gratitude to Frank T. Padberg, Jr., MD. His medical knowledge, research experience, and an interest to work with students at the New Jersey Institute of Technology continually provides the clinical/medical expertise necessary to perform such research. Dr. Padberg also provided the vascular graft samples and some additional laboratory equipment which made this research possible.

Gratitude is expressed to the State of New Jersey and the Ciba-Geigy Corp. for partially funding this author's graduate career and project through support of the Biomedical Engineering Program.

Finally, a very special thank you to a good friend, John F. Andrews, M.S., currently a Ph.D. candidate at the New Jersey Institute of Technology, for his technical computer support. This author wishes him the very best on his graduate career endeavor.

TABLE OF CONTENTS

LIST OF TABLES

LIST OF FIGURES

I. CIRCULATORY SYSTEM

I-1 The Human Cardiovascular System

The human body is made up of many specialized cells (referred to as ***cell differentiation***). These differentiated cells (unlike single celled organisms such as the ameba) are incapable of carrying on a single existence. They require water, oxygen, and nutrients in order to survive. It is the function of the human circulatory system to provide the cells of the body with these essential requirements, as well as, carrying wastes (including carbon dioxide) and metabolic products from the cells. Fluid outside the cells, referred to as interstitial fluid, bathe the cells and help deliver and carry away these products and nutrients. The interstitial fluid is serviced by the blood which is delivered to the tissue sites via the circulatory system.

The flow of blood through the circulatory system occurs because of the pumping action of the heart. This flow is referred to as ***bulk flow*** since all of the constituents which make up blood move together.[1] Blood is composed of erythrocytes (red blood cells), leukocytes (white blood cells), platelets, and plasma. Platelets are fragments of cells formed when a ***megakaryocyte*** (a large white blood cell, also referred to as a platelet mother cell) matures and fragments to form small disks. Platelets play a role in blood clotting. Platelets change from a disc to spiny shape when they encounter an altered vessel wall or a non-wettable surface. Once

changed to a spiny shape, hidden adhesives sites are exposed which cause the platelets to adhere to the vessel wall. Platelets also adhere loosely and reversibly to one another. Thrombin is formed at this stage. **Figure 1** represents the process of ***hemostasis*** (the arrest of bleeding).

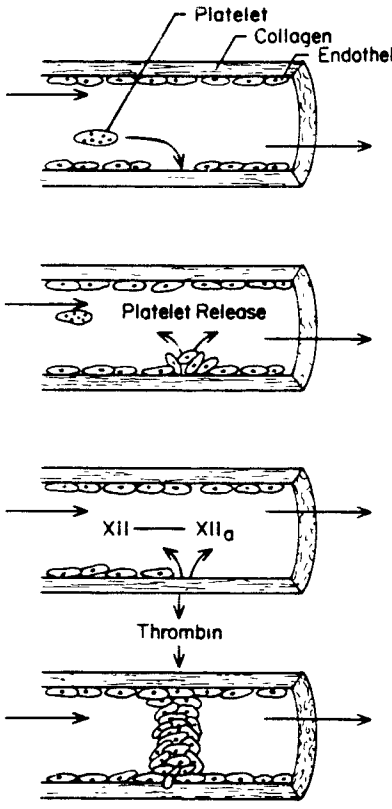

1 Vessel Injury
- a Vasoconstriction
- b. Exposure of subendothelial connective tissue

2 Platelet Responses
- a. Adhesion to vascular defect
- b Reversible aggregation to other platelets
- c. Release of substances from storage granules (ADP, serotonin, vascular permeability factor, platelet factors 3 & 4)
- d. Irreversible aggregation follows release of adenine nucleotides, primarily ADP
- e. Retraction of the platelet mass renders the platelet plug less permeable

3. Coagulation Responses
- a Coagulation cascade begins with activation of factor XII
- b Extrinsic pathway is activated by tissue thromboplastin
- c Thrombin and fibrin are formed

4 Hemostasis Completed
- a. Fibrin is incorporated into the platelet plug
- b A firm fibrin – platelet plug results in complete hemostasis

Figure 1 Process of Hemostasis[2,3]

Plasma is approximately 90% water, the other 10% comprised of various proteins. Approximately eight percent of body weight can be used as a reference to determine the ***total blood volume***.[4] For an average 70 Kg young male, the total blood volume equals 5.6 Liter (taking into account that one Kg of blood occupies approximately one Liter). The total blood volume for a female is approximately 4-5 Liters. Some properties of blood can be found in **Table I**. As a side note, many students ponder the question as to why the standard of a 70 Kg young healthy male was chosen in medical literature. The answer stems from the fact that throughout history, physicians collected much of this data from their abundant source of humans, their understudies (medical students). At the time data was gathered, medical students were predominantly young males in their early twenties with an average weight of 70 Kg.[5]

TABLE I PROPERTIES OF BLOOD[6]

Description	Values
Viscosity	4.5 - 5.5
Temperature	38°C (100°F)
pH	7.35 - 7.45
Salinity	0.9%
Total Body Weight	8%
Volume (male) Volume (female)	5 - 6 Liters 4 - 5 Liters

The circulatory system is comprised of the heart (a four chambered pump), arteries, arterioles, capillaries, venules, and veins (discussed in the next sections). All of the previously mentioned, with the exception of the heart, are tube shaped vessels, of varying diameter which act as conduits for the flow of blood to and from the body's cells and tissues. The largest diameter vessels are the arteries of which the largest is the aorta. Their function is to carry blood away from the heart. Veins, which are smaller than the arteries, carry blood from the lungs and peripheral tissues back to the heart. Throughout the circulatory system a significant amount of branching of arteries and veins exists.

I-2 The Human Heart

The heart is a four chambered pump composed of smooth muscle (***cardiac muscle***). The left and right atria are situated above their respective ventricles (**Figure 2**). Pressures which force the blood throughout the circulatory system are generated by contractions of the ventricles which are filled by the atria. As mentioned previously, arteries and veins also assist in the flow of blood.

The heart is nourished with oxygenated blood delivered to the cardiac muscle via the right and left coronary arteries. These arteries branch directly from the aorta and descend deep into the cardiac muscle. It is often blockage of the coronary arteries which causes heart attacks. Blockage results in loss of fresh blood to the cardiac

muscle, causing damage, or death (an infarct), to the cardiac muscle tissue. Coronary veins stem from the heart muscle and join into one large vein, the coronary sinus. Blood in the coronary sinus drains into the right atrium.

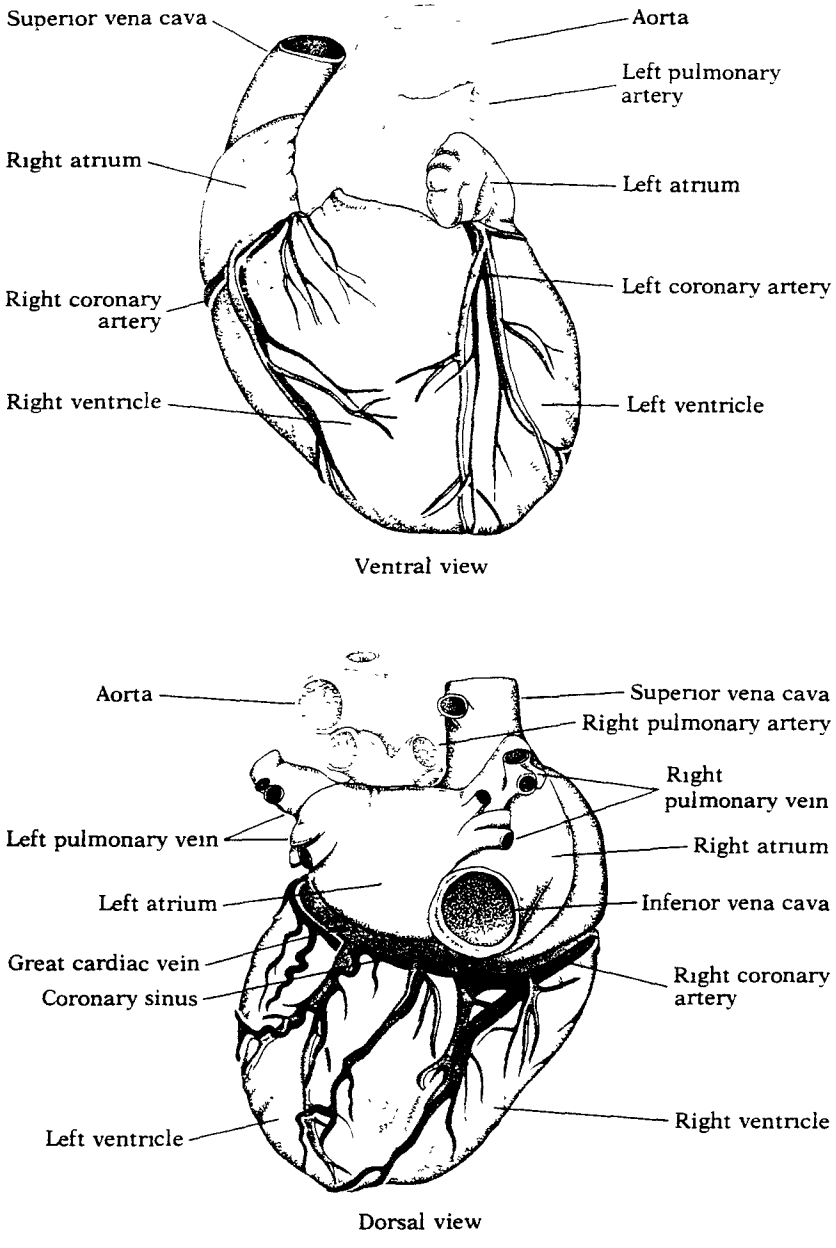

Figure 2 The Human Heart[7]

Electrical stimulation of the heart begins at the ***sino-atrial (SA) node*** (**Figure 3**). This node is often referred to as the ***pacemaker***. The impulses generated at the SA node spread over the atria causing these two chambers to contract. At this moment in time, blood in the left and right atria is forced into the left and right ventricles, respectively. The impulse travels from the atria to a second node, the ***atrioventricular (AV) node***. The impulse is regenerated at the AV node and spread down the ***ventricular septum***. The impulse spreads over the ventricles starting at the base and moving up towards the atria. At this point, the atria have completed their contraction and the ventricles contract due to the electrical stimulus.

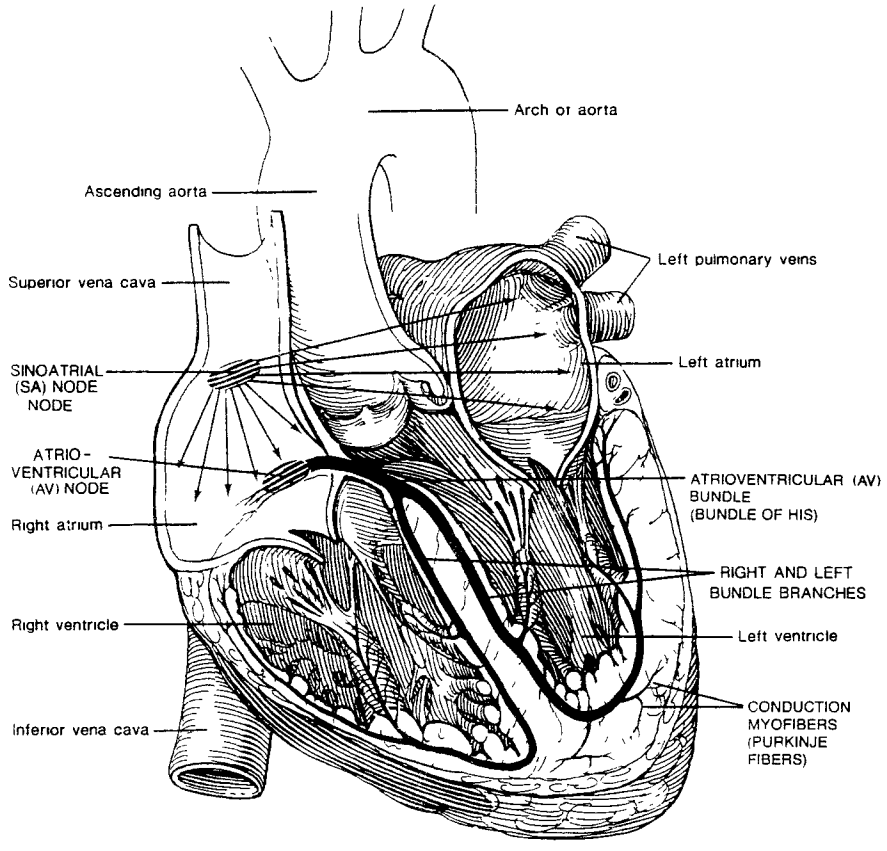

Figure 3 Location of the Various Nodes Used to Generate a Heart Beat[8]

In its route through the circulatory system, a small quantity of blood is forced from the right ventricles into the left and right pulmonary arteries. The blood on this side of the heart has returned from the various capillary networks in the body and is deoxygenated and high in carbon dioxide). The pulmonary arteries direct the blood flow to the left and right lungs. The blood flows through capillary networks in the lungs where it expels carbon dioxide and collects oxygen (the respiratory process). Oxygenated blood appears to be a bright red color due to the iron rich protein ***hemoglobin***. Hemoglobin is a crystallizable protein consisting of an iron-containing pigment, ***heme***, and a simple protein, ***globin***. There is approximately 12 to 16 g/100 mL of hemoglobin in adult females, and 14 to 18 g/100mL in adult males.[9] The freshly oxygenated blood returns from the lungs into the left atrium via the pulmonary veins. Stimulation of the atria forces blood from the left atrium into the left ventricle. Contraction of the ventricles ejects blood from the left ventricle into the aorta where it is distributed to the heart, head and body via an arterial network. Deoxygenated blood returns from the head and body into the right atria via the inferior and superior vena cava. Contraction of the atria forces the blood from the right atrium into the right ventricle, and the cycle described above repeats.

There are four valves of the heart which prevent the backflow of blood (**Figure 4**). The ***tricuspid valve*** (a three tissue flapped valve) separates the right atrium and ventricle. This valve prevents blood from entering the right atrium as the right ventricle contracts. The ***bicuspid valve***, or ***mitral valve***, (a two tissue flapped valve) separates the left atrium and ventricle. It prevents blood from entering the left

atrium as blood is ejected from the left ventricle. The tricuspid and bicuspid valves are the largest of the four heart valves. The ***aortic semilunar valve*** prevents the backflow of blood into the left ventricle after it has been ejected, while the ***pulmonary semilunar valve*** prevents the backflow of blood into the right ventricle. The aortic and pulmonary valves are smaller but heavier valves flaps than the bicuspid and tricuspid valves.

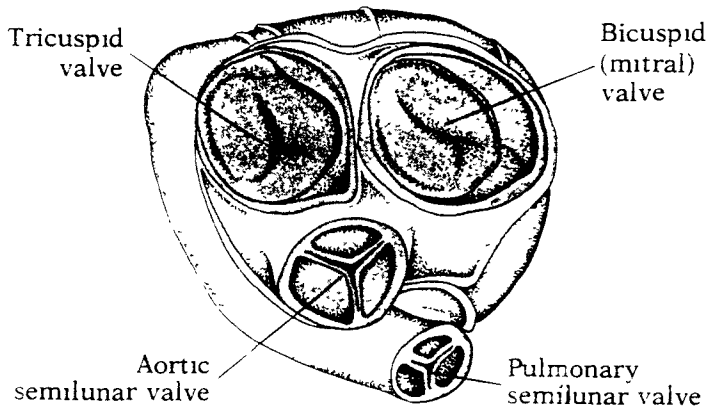

Figure 4 The Four Valves of the Human Heart[7]

The Atria are not shown in this view

The average heart rate for an adult at rest is between 72 to 75 beats per minute. During periods of exercise or physical exertion, the heart rate can rise to over 160 beats per minute. ***Ergonomists***, those who study human characteristics for the

appropriate design of living and working environments, established a guideline listing the various heart rates associated with the work involved (**TABLE II**).[10] The guidelines were derived in order to classify the categories of work. It is a useful tool in demonstrating the heart rates and the total energy expended. During light or no work, the body maintains a steady state pulse of 90 beats/minute. The levels of oxygen and glucose in the blood are sufficient enough to supply the cardiac muscle during these light periods of work. The body is able to obtain this steady state for extended periods of time. This steady state condition does not exist for periods of very heavy or extreme work where the heart rate rises to 140 or more beats per minute. Metabolic by-products, such as lactic acid, can accumulate in the blood. These high energy demanding, high heart rate periods are demanding on the body and rest or cessation of the activity will be required.

TABLE II VARIOUS HEART RATES
(As Defined by Ergonomists to Classify Work Loads[10])

Classification of Work	Total Energy Expenditure (kcal/min)	Heart Rate (beats/min)
Light Work	2.5	90 or less
Medium Work	5	100
Heavy Work	7.5	120
Very Heavy Work	10	140
Extremely Heavy Work	15	160 or more

I-3 Blood Vessels

Blood vessels are viscoelastic and do not obey Hooke's Law.[11] Their stress-strain relationship is non-linear and hysteresis does exist. They also creep under constant stress and relax under constant strain. The blood vessel wall is a composite material. There is no specific steady state (mechanical or biochemical dynamic equilibrium) to which they return when external stresses are removed. Equilibrium varies throughout the different locations in which blood vessels are located. Any change in the tissue surrounding the vessel will cause dimensional changes in the vessel until equilibrium is once again obtained. The proceeding sections focus on the anatomy and function of the various blood vessels.

I-3.1 Arteries

Arteries are thick-walled, muscular vessels of considerable elasticity (**Figure 5**). The word artery was derived from ***aer*** = air, and ***tereo*** = to carry: because arteries found empty at death were once thought to carry air.[12] A cross-sectional view of an artery will show that it is made up of three layers. The innermost layer, ***tunica interna (intima)***, is a smooth endothelium surrounded by a basement membrane and a layer of elastic tissue called the ***internal elastic lamina.*** The tunica interna is in direct contact with the blood. The hollow inner space in which blood flows is referred to as

lumen. The middle layer, or ***tunica media***, is the thickest layer. Smooth muscle and the ***external elastic lamina*** (elastic fibers) comprise its makeup. the outer layer, ***tunica externa (adventitia)***, consists of elastic and collagenous fibers.

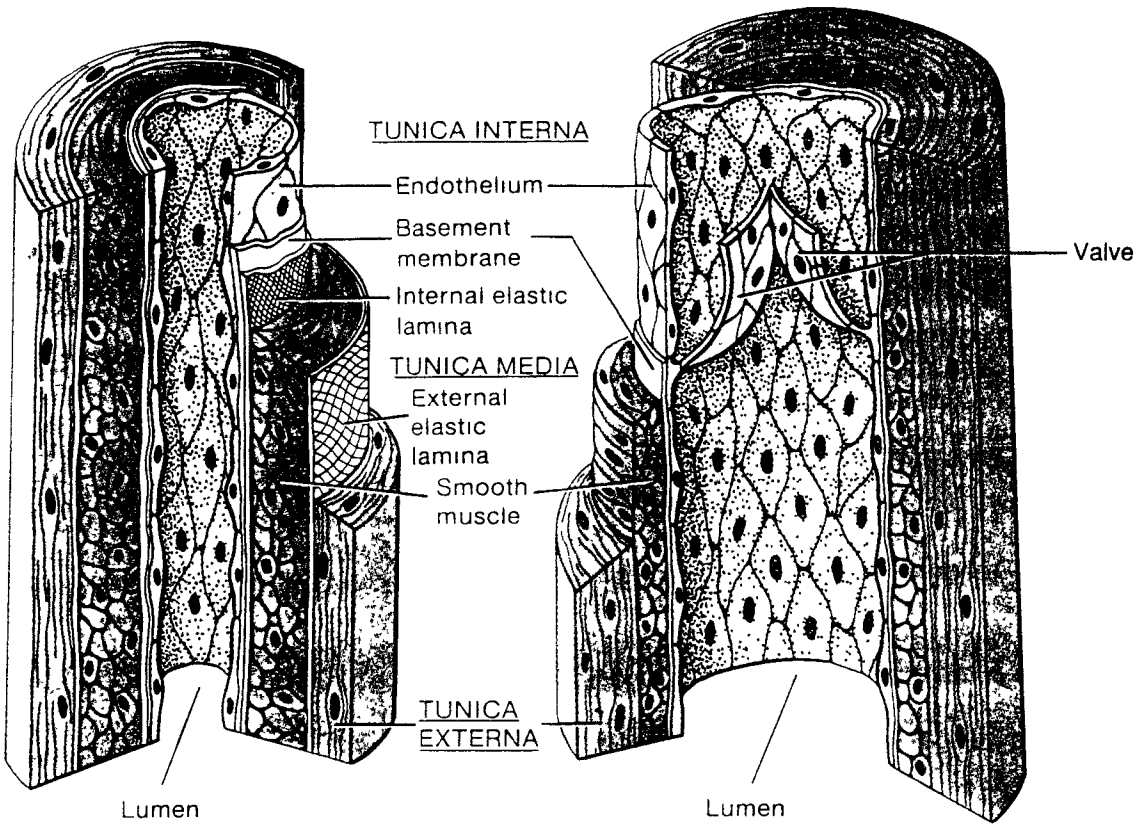

Figure 5 The Composition of an Artery and Vein[12]

Primarily as a result of the thicker middle layer, the two major properties of arteries are elasticity and contractibility. Elasticity allows vessel expansion at high pressure, however under sympathetic nervous control, the arteries can contract decreasing the size of the lumen. Sympathetic stimulations originates from the autonomic nervous system; the nerve fibers stemming from the thoracic and lumbar regions of the spinal column. This contracting action is known as ***vasoconstriction***. When the sympathetic stimulation is reduced, the smooth muscle relaxes increasing the size of the lumen and increasing the blood flow. There are three types of arteries: the larger arteries known as the ***elastic (conducting) arteries***, the medium sized ***muscular (distributing) arteries***, and the smaller arteries (the ***arterioles***).

The aorta is an example of a large artery. Their tunica media contains more elastic fibers than smooth muscle. Elastic arteries help move blood away from the heart. As the ventricles contract, blood is ejected into the aorta and pulmonary artery. These arteries swell and expand to accommodate the blood volume (or ***stroke volume***). As the ventricles relax, the aorta and pulmonary artery contract forcing the flood forward throughout the circulatory system. This results in a rise of the blood pressure throughout the system. This mechanism accounts for the arteries significant role in the maintenance of blood pressure.

Medium sized arteries, in contrast to the larger arteries, contain more smooth muscle than elastic fibers in the tunica media. These arteries are more capable of ***vasoconstriction*** and ***vasodilation*** (expansion of the artery) to adjust blood volume or pressure. Their wall is much thicker than the larger arteries, mostly due to the larger

amount of smooth muscle. These arteries are referred to as "distributing" arteries since they distribute the blood throughout the circulatory system.

Arterioles are the smallest arteries. These vessels deliver the blood to the capillaries. Arterioles vary in size. The larger arterioles are connected to the medium sized arteries, and have a tunica interna, a tunica media (containing smooth muscle and very little elastic fibers), and a tunica externa composed mostly of elastic and collagenous fibers. Arterioles closest to the capillaries consist of a single layer of endothelium cells surrounded by a few scattered smooth muscle fibers (**Figure 6**). These smooth muscles constrict the arterioles, thus regulating the flow of blood into the capillaries.

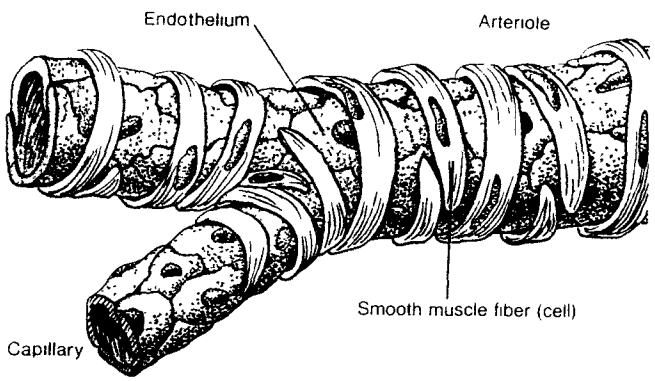

Figure 6 Structure of an Arteriole[12]

Arterioles are connected to the capillaries by a small vessel known as a ***metarteriole*** (**FIGURE 7**). The metarteriole regulates the flow of blood through the capillaries. This vessel enters the capillaries from the arteriole, passes through the capillary network and empties into the ***venule.*** The metarteriole posses scattered smooth muscle cells on the arteriole side (the side carrying the oxygen rich blood supply) but does not possess these muscles on the venule side. The deoxygenated blood enters the venule and is directed back to the right heart via the venous network. The muscle cells surrounding the arterioles are known as ***precapillary sphincters.*** The non-muscular side of the metarteriole is referred to as the ***thoroughfare channel.*** Blood flow is increased in the thoroughfare channel because vasoconstriction can not take place.

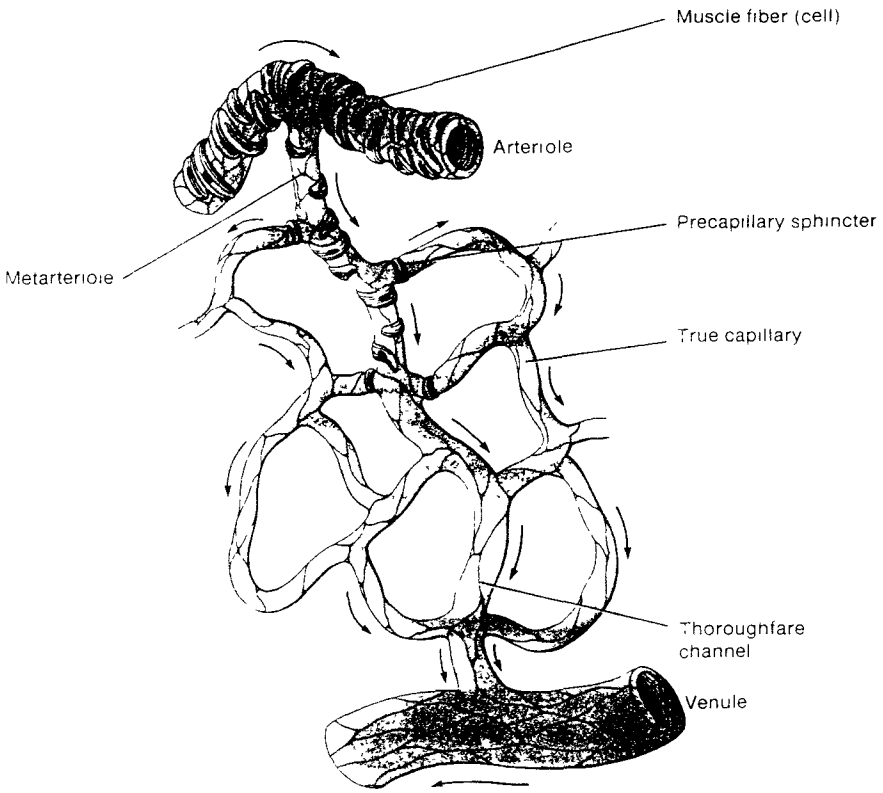

Figure 7 Representation of a Capillary Network[12]

Capillaries are microscopic vessels that usually connect arterioles and venules. Their main function is to permit the exchange of nutrients and wastes between the blood and tissue cells. They are comprised of only a single layer of endothelium cells, thus making this exchange possible. A great number of capillaries exist throughout the circulatory system because they are the sites for the exchange of materials between the cells and the blood. These large networks are referred to as ***capillary beds***. Their surface area is immense thus providing greater regions for material exchange. Blood flow can be completely restricted from one capillary bed in order that it be redirected to another area in greater demand of blood. Capillaries are also involved in the very complex process of shifting water and ions across the capillary walls. Blood entering the capillaries from an arteriole is under a hydrostatic pressure that is greater than the osmotic potential. Solutes and water are forced out of the capillaries and into the surrounding tissues as a result. The opposite is true for the venule side of the capillary network. Since water was forced out into the tissue on the arteriole side, the hydrostatic pressure outside the capillary bed on the venule side is greater. The solutes are taken up by the cells, and the remaining water diffuses back into the capillaries and then into the venules. Water reentering the capillaries carries the cellular wastes and other metabolic products. Water which does not reenter the capillaries at this site will be drained from the extracellular spaces by the lymphatic system in order that a fluid balance remain.

I-3.2 Veins

Veins are similar to arteries (**Figure 8**, also reference **Figure 5**). Their main function is to carry the deoxygenated blood back to the right side of the heart where it is then pumped into the lungs to be oxygenated. Veins are thinner walled vessels than arteries, and like the arteries are comprised of three layers. The inner layer consists of endothelium cells. The variance is noticed in the middle layer which is comprised of less muscle than an artery and is not as elastic. The outer layer consists of the same elastic and collagenous fibers as arteries, however much thicker. Despite these differences, veins can still adapt to variations in blood volume and pressure. The forward motion of blood through veins is ensured by one way valves located in the lumen. As the forward pulse of the blood ceases and the blood begins to reverse direction, the weight of the blood closes these valves.

Venous flow is assisted by muscular movements. A contracting muscle squeezes the vein, thus pushing the blood towards the heart. Breathing is another mechanism by which blood is forced through the veins. Inhalation causes a negative pressure in the chest cavity causing some blood to be drawn into the veins in this region. Exhaling causes the diaphragm to exert a force on the organs below, thus squeezing blood into the veins.

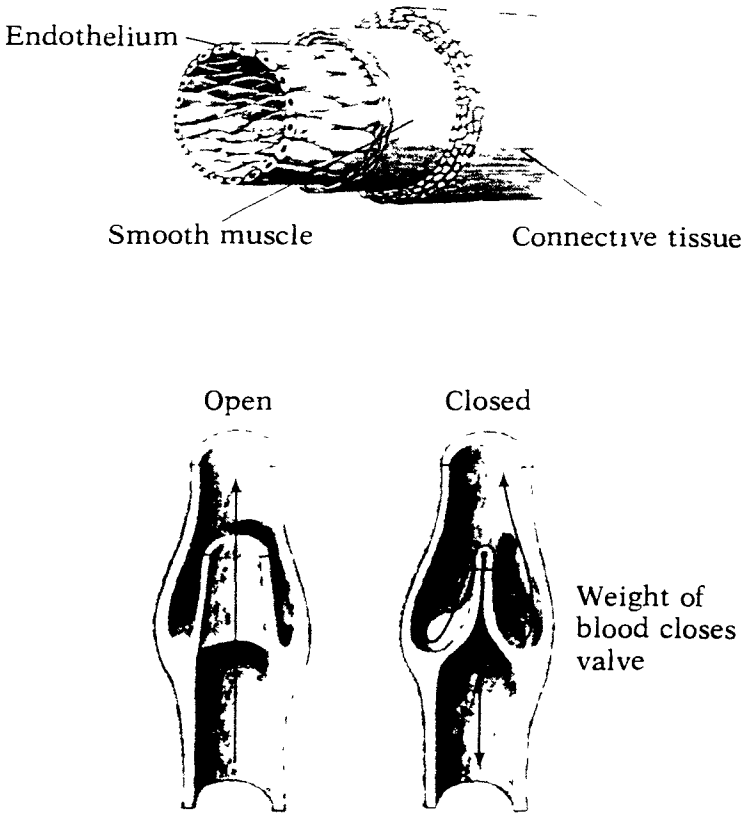

Figure 8 Composition of a Vein[7]

(Note the internal valves)

I-4 Blood Pressure

Located throughout the human circulatory system are nerve cells called ***baroreceptors***. These nerve cells are capable of responding to changes in blood pressure and act as the feedback mechanism which help maintain pressures within the circulatory system.

Blood flow is directly proportional to blood pressure. Flow through the circulatory system, as with flow through any system, takes place from a region of high pressure to one of low pressure. The units of flow are expressed in terms of liters per minute (L/min). The units of pressure are expressed clinically as millimeters of mercury (mmHg). These units are used because historically blood pressure has been measured by determining how tall a column of mercury could be supported by the pressure.[13] The instrument used to measure arterial blood pressure is a ***sphygmomanometer***. This device consists of a cuff which is wrapped around the patient's arm. The cuff consists of a bladder in which air is pumped to cut off the blood circulation through the ***Brachial Artery***. Two tubes enter this bladder. One tube is for inflating the cuff. The other is connected to a column of mercury which is used to measure blood pressure.

The pressure pulse created by the heart with each contraction travels along the arteries much more rapidly than the induced bulk movement of the blood. This rapid propagation results from the elasticity of the arterial walls, which expand with each heart beat. Arterial blood is pulsatile with Reynolds numbers ranging from 0 to 10000 and pressures ranging from 70 to 130 mmHg; while veins are quasi-steady flow with pressures ranging from 5 to 12 mmHg.[14]

The mean pressure in the aorta is about 100 mmHg. In normal resting young adults, systemic arterial pressure fluctuates between 120 mmHg during ***systole*** and 80 mmHg during ***diastole***. Systole refers to the period in the heart's cycle in which the ventricles are contracting. Diastole, the opposite of systole, refers to the period in which the heart dilates and the chambers fill with blood (atria diastole precedes

ventricle diastole). As the blood flows through the systemic circulatory path its pressure decreases progressively. Once it reaches the right heart, the pressure approaches 0 mmHg. The following graph demonstrates blood pressures throughout the various portions of systemic and pulmonary circulations of the cardiovascular system (**Figure 9**).

Pressure is reduced throughout the circulatory system because of the resistance (or opposition) and compliance to blood flow. Blood flow is inversely proportional to the resistance. Resistance in the aorta is close to zero especially when compared to the high pressure generated by the contracting left ventricle of the heart (100 mmHg). Pressure in the large arteries is reduced as the resistance is increased. Because the large arteries are close to the aorta however, the pressure in these vessels remains high (approximately 95 to 97 mmHg).

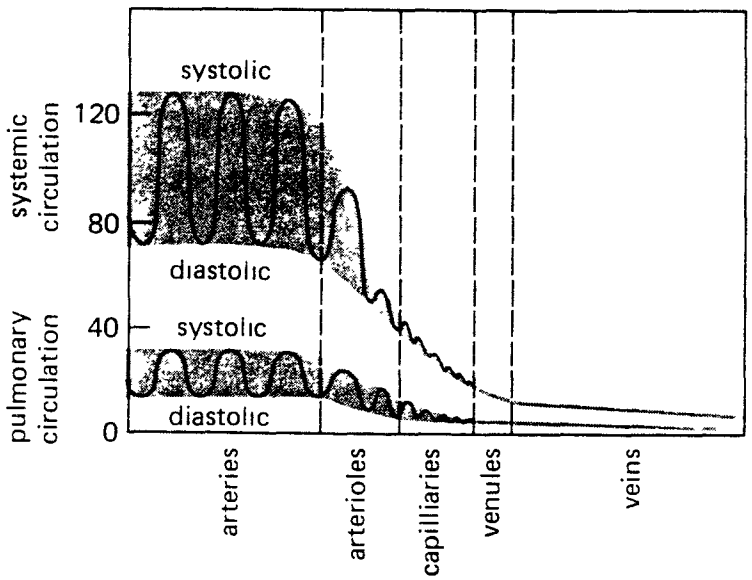

Figure 9 Various Blood Pressures Throughout the Circulatory System[15]

As noted on **Figure 9**, the most significant decrease in blood pressure (the greatest slope) occurs at the arterioles. Resistance in the arterioles is the highest in the circulatory system, accounting for about one-half the total resistance to blood flow.[12] Contributing factors to resistance include the blood's viscosity (the thicker the blood, the higher the pressure), vessel length (the longer the vessel, the greater the resistance), and the vessel's radius. Resistance is inversely proportional to the fourth power of the radius ($R \propto 1/r^4$).

Cardiac Output (CO) refers to the amount of blood ejected from each ventricle per minute (L/min). The average value for CO is approximately 5 L/min at rest. Since the body holds 5 liters of blood, this means that all of the blood in the system is pumped around in one minute. Cardiac Output is increased during periods of exercise. Cardiac Output is obtained using the following equation:

$$CO = HR \times SV \tag{1.1}$$

where: HR represents Heart Rate

SV represents Stroke Volume (the volume of blood ejected by each ventricle during each heart beat)

I-5 A Historical View of Hemodynamics

The first observation that the pulse of blood flow is a wave propagation was noted by the Greek physician Erasistratos (280 A.D.).[16] He remarked that the pulse appears in the arteries the furthest from the heart at a later time than those closer to the heart. His observation would have had more meaning had physicians at that time (Erasistratos included) had an understanding of blood circulation. Ancient Egyptian hieroglyphics dating as far back as 3000 B.C., indicate that there was a connection made between the peripheral pulse and the beating action of the heart.[17] It was not until studies in anatomy conducted during the Renaissance period that circulation began to be seriously studied. Leonardo da Vinci (1452-1519) was one of the early observers contributing to the knowledge of circulation with his detailed illustrations and notes on the cardiovascular system.[18]

Two major physicians contributing to the modern concept of circulation of blood were an English physician, William Harvey (1578-1658) and a Minister, Stephen Hales (1677-1761). The modern concept of circulation is attributed to William Harvey. Harvey was the first to demonstrate the presence of valves in the veins (**Figure 10**). As seen in the figure, he used a tourniquet wrapped around the arm to assist in making the veins protrude. Stephen Hales was the first to measure blood pressure.[19] Both men conducted geometric and kinematic quantitative calculations. They showed that flow was driven by pressure. Their work however was more

qualitative. The first mathematical paper on blood flow was by Leonhard Euler in 1775.[19]

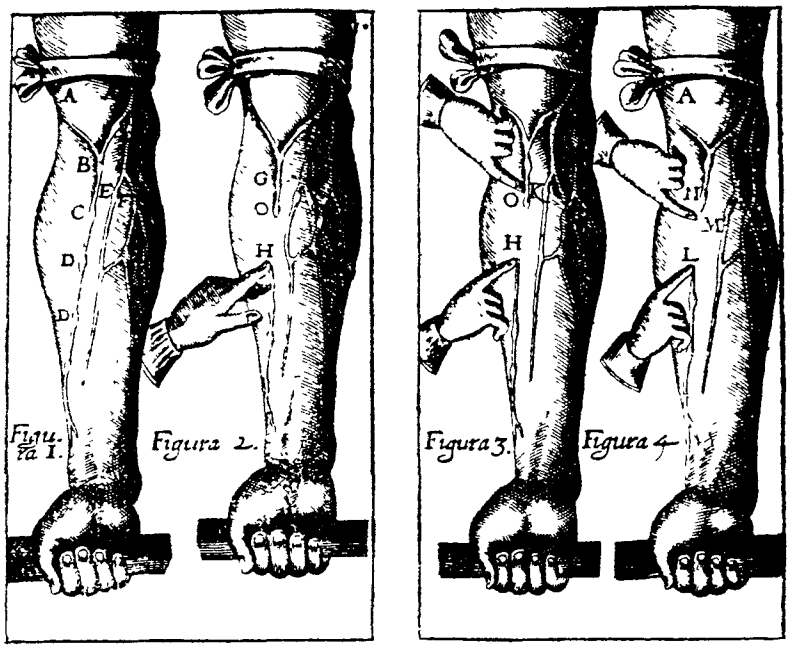

Figure 10 William Harvey's Vein Demonstration[7]

Euler developed one-dimensional equations for inviscid flow of an incompressible fluid in an elastic tube and postulated a nonlinear law relating the pressure at any point inside a blood vessel to its cross-sectional area. A physician and natural philosopher, Thomas Young (for whom ***Young's Modulus*** is named), was the first to derive the velocity of propagation of the pulse wave in blood flow.[20] Young also studied the pressure drop due to viscous losses across arterial segments. This viscous pressure loss was studied in much greater detail by Poiseuille in 1840.[19]

Poiseuille made precise measurements of pressure drops in glass tubes using water, alcohol, and mercury. His equation was expressed as:

$$Q=\frac{K(1+AT+A'T^2)PD^4}{L} \qquad (1.2)$$

where: P represents the pressure drop

L represents the length of the tube

D represents the diameter of the tube

T represents the temperature

K, A′, & A are constants depending on the fluid tested

Poiseuille's Law, as we know it today, was not developed until 1858 by Neumann and Hagenbach.[21] This equation is written in the following form:

$$Q=\frac{\pi PD^4}{128\mu L} \qquad (1.3)$$

where: μ represents the viscosity of the fluid

No advances were made in fluid mechanics until 1931. Fåhraeus and Lindqvist showed that the apparent viscosity of blood decreases as the tube diameter decreases from 500 to 40 micrometers.[22] This is referred to as the ***Fåhraeus-Lindqvist Effect*** and can be explained as a reduction in hematocrit caused by a migration of red blood cells away from the vessel wall due to shear effects. The coefficient of viscosity decreases as the diameter of the vessel becomes smaller. The hematocrit reduction is thus a result of the lower viscosity.

Studies concerning the mechanical aspects of flow in veins has not been studied as extensively as the arterial system. Veins are thinner and more flexible than arteries, and have significantly lower transmural pressure.

II. VASCULAR GRAFTS

II-1 A Brief History

Prosthetic vascular surgery did not develop clinically until after World War II although there had been some work dating back to the 1890's. An example of early pioneering work in vascular surgery occurred in America in the year 1897. Dr. Nitze used ivory cylinders as internal supports for arteries.[23] Dr. Nitze slipped the vessel ends over the ivory cylinder and held the ends of the artery in place with a circumferential ligature.

Along parallel lines, Dr. Payr, around 1907, used straight magnesium cylinders which were similar in design to Nitze's ivory cylinders. Dr. Payr's revised the magnesium cylinder. The revised prosthesis consisted of two magnesium tubes each possessing a flange (**Figure 11**). One tube had circumferential holes while the mating component had pins which would fit into the holes. The ends of the vessels were pulled back over the flanges and the two halves of the magnesium tubes were joined. The pins passed through the holes of the mating component and were then bent to provide a locking mechanism. Magnesium was chosen because it was known that it dissolved in tissue fluids. At that particular period in vascular surgery history, such a reaction was thought to be desirable because the magnesium metal disappeared in the process. It was observed that when the magnesium dissolved it produced a highly

inflammatory reaction. Fibrosis and distortion of the vessel was observed when these vessels were later examined.

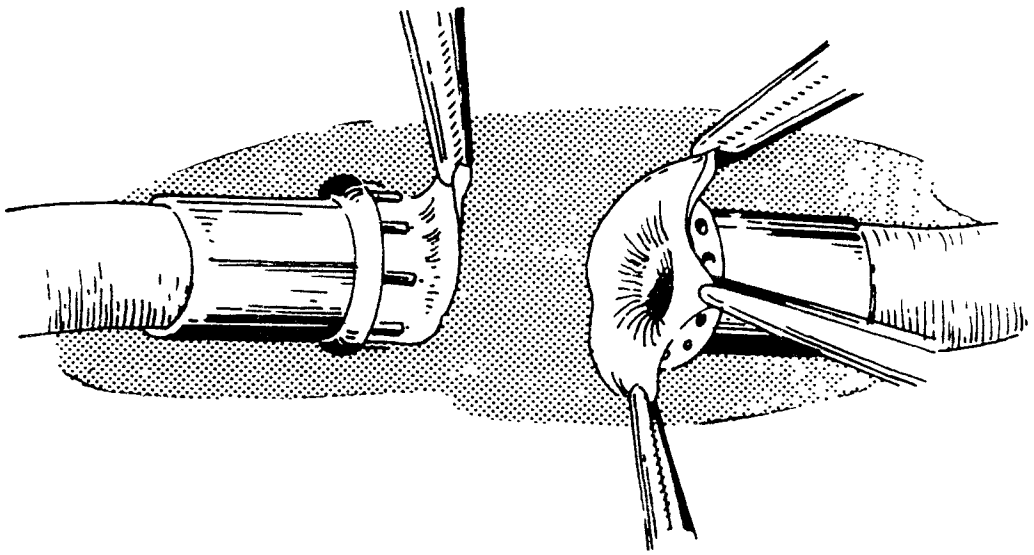

Figure 11 Dr. Payr's Magnesium Tubes[23]

Around 1907 in America, Dr. Carrel successfully interposed a jugular vein segment between the divided ends of the carotid artery, and the concept of the use of veins for the replacement of arterial segments was born.[24] Dr. Carrel won the Nobel Prize for his work in vascular surgery in 1912.

Other discoveries in vascular grafting continued to progress slowly in the early 1900's. During World War I, the number of large vessel wounds were great. Dr. Tuffier attempted to use silver tubes lined with paraffin to restore the circulation in

injured arteries. He had disappointing results and no limb salvage.[24] These results did not suppress further research with metals, for in 1942 Drs. Blakemore and Lord employed Vitallium tubes for non-suture type anastomosis of two tubular structures.[24] Vitallium, a Cobalt-Chrome-Molybdenum stainless steel alloy used at that time for dental prostheses, is now used in joint prostheses and is considered very biocompatible. This event marked the first successful permanent prosthesis in the thoracic aorta. Soon after this remarkable achievement more attention to the blood-prosthesis interface reaction began.

Earlier metal tubes were used somewhat successfully for non-sutured junctions (in which circumferential ligature was used). They were used in both the aorta and thoracic inferior vena cava. The metal used possessed a highly polished, cleaned surface which provided fewer focal points for the initiation of a ***thrombus*** (blood clot). Thrombus formation was limited due to the very smooth inner surfaces of these metal tubes.

Large vessel grafting began to prosper in the early 1950's with the use of harvested human aortas (***homografts***). These aortas were preserved by fresh antibiotic sterilization or freeze-drying. Eventually these grafts failed due to either aneurysm, calcification, thrombosis, or a combination of the above. An aneurysm is an abnormal dilation of a vessel, usually an artery. Calcification is a process by which calcium is deposited on the inside wall of the vessel. The vessel becomes hardened and its inner diameter reduced as a result.

Practical applications for synthetic vascular prostheses started in the 1950's when A.B. Voorhees discovered that the nylon used in parachutes could be used as an arterial substitute. In 1952, Voorhees, Blakemore, and Jaretzki demonstrated that hand-sewn tubes of Vinyon "N" fabric (a derivative of nylon) could successfully be used to replace the abdominal aorta of both dogs and humans. However, it was later discovered that Vinyon "N" lost its tensile strength quite rapidly after implantation. Shortly after these findings, Hufnagel and Rabil demonstrated that Orlon and Dacron were superior fibers to Vinyon "N" due to their extreme durability.

These early fabric vascular prostheses were crafted from flat pieces of cloth hand sewn to make a crude tube. The tubes required cuffing at the ends to avoid fraying of the cloth. The tubes were crimped because it allowed the prosthesis to bend without distortion, thus not inhibiting any flow restriction.

Much of the credit for the development of the Dacron arterial prosthesis belongs to Dr. Michael DeBakey, who in the 1950's introduced both knitted and woven Dacron. These grafts were crimped and heat shrunk. Dr. DeBakey and associates, in cooperation with Professor Thomas Edmond of the Philadelphia College of Textiles and Science, developed a new knitting machine that was designed to produce a seamless, knitted Dacron tube and bifurcation grafts.[24] It was later discovered that these Dacron grafts lost very little strength after implantation beyond their initial decrease of twenty percent.

II-2 Modern Day Grafts

Vascular grafts today are tube shaped prosthetics used to replace arteries. As blood conduits of medium and large diameters, the grafts perform well. A vascular prosthesis is not designed to be a rigid structure. The ideal design involves a graft which is both compliant and compressible for ease of handling and suturing. The graft may also be easily deformed by radial or longitudinal tension, as well as by internal pressure of the fluid. Once implanted, thrombus forms on the surfaces of the graft because it is a foreign body.

Vascular prostheses made from fabrics or polymers rapidly replaced metal tubing for arterial replacement. These prostheses, unlike their metal predecessors, could be sutured to the arterial segments. For this reason, the fabric and polymer grafts gained popularity over the metal grafts. It was also discovered that porous materials, when implanted as a vascular graft, became more completely incorporated by the surrounding tissue. Dacron possessed this quality along with being very durable, and hence became a favorable material for vascular prosthesis.

Other popular grafts included those made from polymers. One such polymer is Teflon, clinically configured as expanded Polytetrafluoroethylene (ePTFE). Local cells can adhere to the outer wall of this material, however they fail to penetrate through the outermost portion of the graft's wall. Kinking may be a problem associated with ePTFE grafts. The material can be too stiff for some body contours.

Polyurethane represents a wide variety of polymers, in which small variations in its chemical structure can make the difference between thrombogenicity and nonthrombogenicity. An example of this type of polymer implant was an electrostatically spun polyurethane graft developed at the University of Utah. Although the prosthesis first appeared promising, these grafts could not be tailored to meet the anatomical requirements which arose intraoperatively. They would deteriorate or uncoil following implantation.

Today's seamless vascular grafts are designed with surfaces ranging from filamentous and porous to smooth and impervious. One noticeable feature which has become popular in the vascular graft industry, is the incorporation of an external axial line. This guideline assists the surgeon in keeping the graft in proper alignment (avoiding twisting) during implantation. The possibility that blood flow will become obstructed if the graft is twisted is thus avoided. Not all vascular grafts possess this feature. Externally supported Dacron and Teflon prostheses are used to prevent kinking when crossing the joint creases, especially behind the knee. Recently there have been natural materials used as well, such as glutaraldehyde preserved human umbilical veins. However, such grafts are very expensive and have not proven as durable due to delayed aneurysmal degradation.

Porosity of the graft is a crucial design consideration. This determines the amount of cell ingrowth achieved. Porosity refers to the proportion of pores within the boundary of a solid material, compared to its total volume.[25] The tolerance for low porosity must be less than that which would permit excessive bleeding. Research

shows ideal pore size for support of ingrowth of capillaries and fibrohistocytic tissue lies between 10 and 45 micrometers; where at less than 10 micrometers ingrowth does not occur, and more than 45 micrometers causes the growth of undesirable fibrous tissue.[26] Porous grafts demonstrate the ability to completely heal. Healing clinically refers to the formation of a relatively smooth endothelial cell lining along the inner wall of the graft. Currently, the two types of porous grafts are ePTFE and Dacron. These textile vascular prostheses are available in structures which minimize blood loss, maximize handling and ingrowth, and have other special features. Dacron has the advantage of long clinical follow up with a high level of patency in aortoiliac-femoral implantations. While thrombosis may occur with any vascular prosthesis, ePTFE is more easily declotted. The ePTFE graft does not require pre-clotting and is preferred to Dacron for intrainguinal reconstruction. In addition to its smooth non-crimped flow surface, ePTFE appears to be less susceptible to infection.[27],[28] Some positive features of the ePTFE graft include the fact that pre-clotting is not required, they are easily sutured, and the inner wall possesses a smooth, non-crimped flow surface. However, it is not as popular as the Dacron graft because it is less compliant, possesses no longitudinal elasticity, it is prone to early occlusive thrombosis, and its wall impairs an organized form of cellular coverage.

II-3 Manufacture of Grafts

Dacron grafts are made from a texturized polyester yarn, which enhances tissue ingrowth. The Dacron yarns are multifilamentous, usually consisting from 20 to 54 filaments. The yarns are twisted together in order to hold them together during the fabrication process. Various graft designs are fabricated in different ways. The three types of commercially available Dacron porous grafts today are woven, knitted or velour. A few terms used to describe the manufacture of Dacrons grafts, as mentioned in the following paragraphs, should be defined. ***Weave*** refers to the making of a material (vascular graft) by interlacing Dacron fibers. ***Weft*** refers to one of the two fibers used to create a ***woven*** (past particle of the word *weave*) pattern. In manufacturing a woven product, the weft are the horizontal fibers which are interlaced perpendicularly through the ***warp*** (the fibers arranged lengthwise). The term ***velour***, as used by graft manufacturers, refers to a material with greater exposure of filaments on one or both surfaces through the use of texturized yarns. This emphasizes the filamentous surface characteristics of the velour graft.[29]

Figure 12 shows a crimped one-by-one woven (plain woven) Dacron graft. In the mid 1980's, woven grafts accounted for about 45% of the grafts being implanted each year.[29] This textile structure is formed by two sets of yarn interlacing at right angles to each other. Plain weave is the simplest of all the weaves. Since plain woven grafts have the most concentrated number of interlacings, they are the most dimensionally stable. Positive features regarding the woven tube include strength, low

porosity, high bursting strength, and minimum tendency to fatigue. Pre-clotting is not usually required since it can be fabricated tightly enough to lower blood leakage. Some negative features include the difficulty of handling and suturing, the cut edges have a tendency to fray, and its porosity may be too low for a given implanted area (which accounts for poor endothelial cell incorporation).

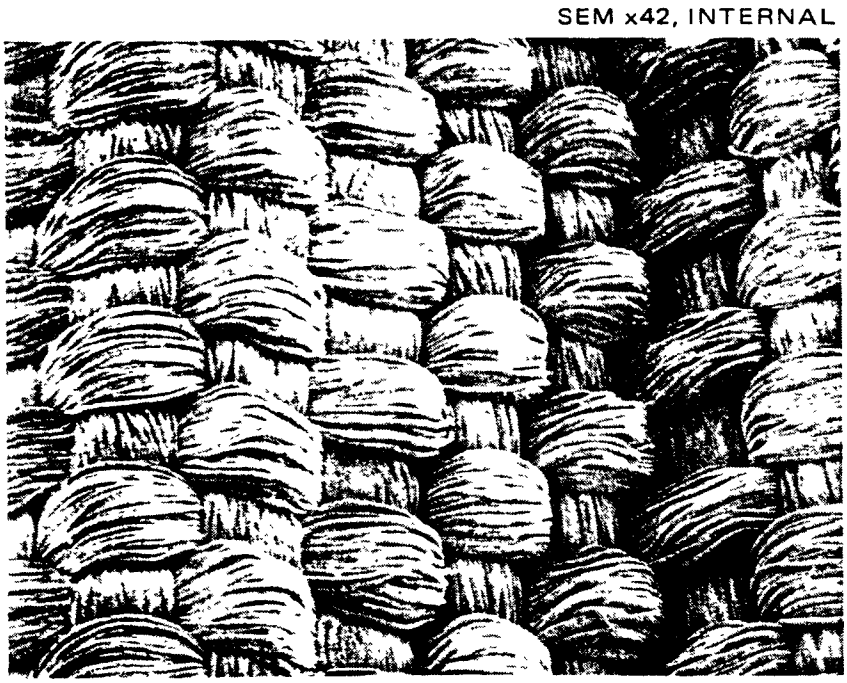

Figure 12 A Crimped One-by-One Woven Dacron Graft[30]

(DeBakey Graft, Internal Surface)

Figure 13 depicts a crimped weft-knit structure. Such a structure yields a more pliable graft because it is made with one continuous yarn (two yarns for a velour knit)

circumferentially interlooping to form a tube (unlike the interlacing process used with the woven grafts). Since the knitting is controlled by the raising and lowering of needles, many different structures can be derived.

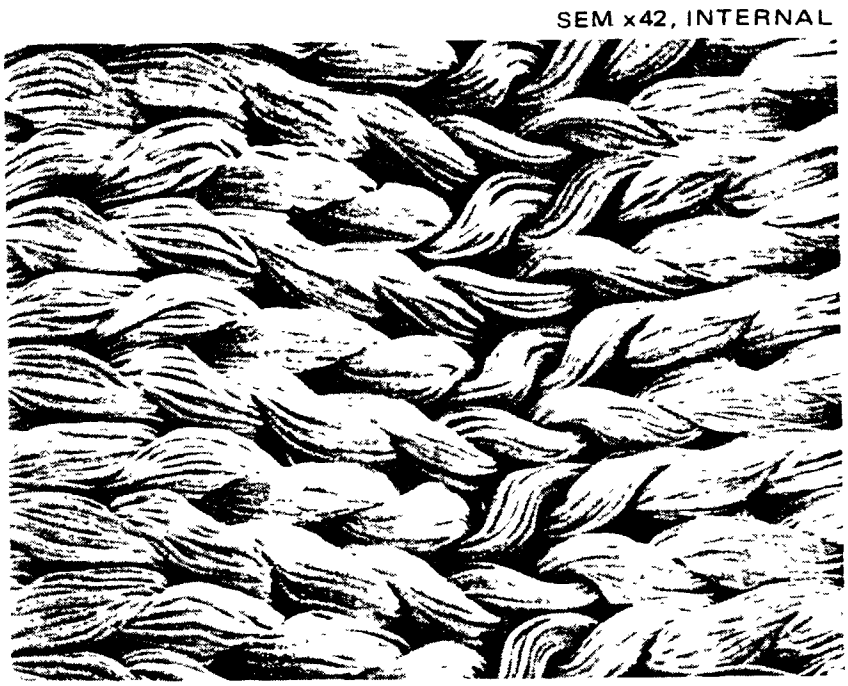

Figure 13 A Crimped Weft-Knit Dacron Graft[30]

(DeBakey Graft, Internal Surface)

One noticeable quality of a weft knitted graft is that the inner surface tends to be rougher in texture than the outer surface. For this reason, the material is turned inside out which allows the smoother surface to be the inside surface causing less turbulence

in blood flow. The desirable features include ease in suturing compared to the woven graft, cut edges which do not fray, and higher porosity. Due to its higher porosity, this style graft must be pre-clotted prior to implantation. Its undesirable features include difficulty pre-clotting, and the possibility of incomplete tissue incorporation. The weft knitted prosthesis is also available in a velour style. Although the weft knitted prosthesis' edges have a tendency to curl up, making suturing difficult, this style is generally sutured easily, more compliant, and easily handled. There is greater mobility in the circumferential direction than in the longitudinal direction, thus causing this graft to resemble its host artery.

A crimped external velour warp-knit graft is portrayed in **Figure 14**. It consists of the knitting of one or more sets of yarns. During the manufacturing process, each yarn forms a loop which is then intermeshed with another loop creating a zigzag pattern in the graft. Since it has smaller interstices than a weft knit, the warp knit has a lesser tendency to leak when arterial flow is restored. The advantages for this style include the ability for complex structures to be knit (such as branched structures), increased strength, reduced porosity for easier and more reliable during pre-clotting, a smoother flow surface, and improved surgical handling characteristics. The two most popular types are known as the locknit and reverse locknit, **Figure 15**). These grafts do not run, unravel, or curl up at the cut edges as the other styles of fabrication tend to do.

Figure 14 A Typical Warp-Knit Dacron Graft[30]

Top - External Surface

Bottom - Internal Surface

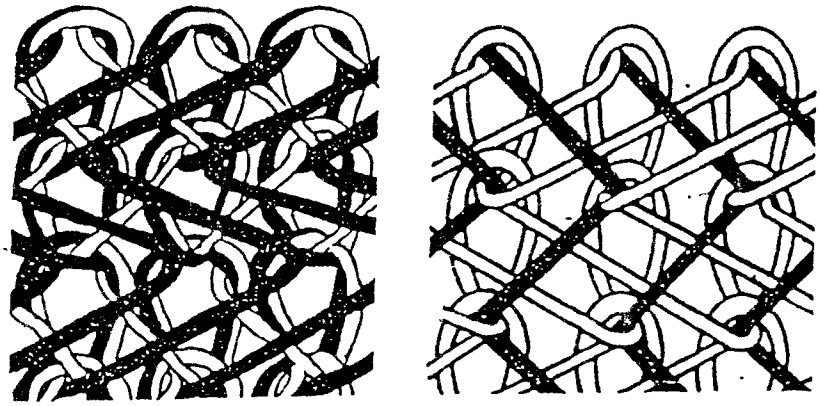

Figure 15 Thread Configurations for Locknit and Reverse Locknit Dacron Grafts

Left - Locknit Thread Configuration

Right - Reverse Locknit Thread Configuration

Figure 16 depicts an externally supported external velour, weft-knitted Dacron graft. The graft is not crimped and is supported by a spiral coil of polypropylene which is heat fused to the outer surface of the Dacron graft. The favorable advantages for this style include both kink and compression resistance, a smooth noncrimped flow surface, as well as a graft which is easily sutured. The external support coil does not allow the passage of X-Rays.

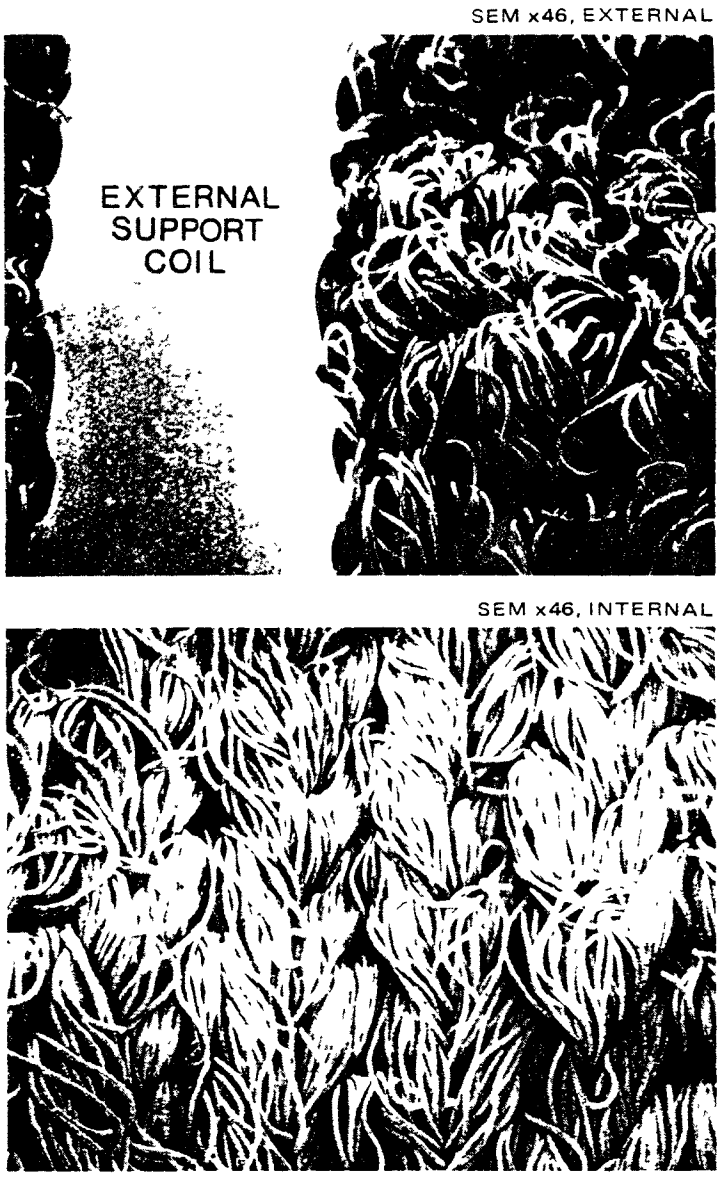

Figure 16 Externally Supported External Velour Weft-Knit Dacron Graft[30]

(USCI, Sauvage EXS)

Top - External Surface

Bottom - Internal Surface

All Dacron vascular grafts undergo three-stages after their basic manufacture before packaging. These stages are ***compaction***, ***crimping***, and ***cleaning***. Compaction is performed to reduce the fabric's natural porosity and stabilize the structure. There are several manufacturing techniques used to compact a graft.[31] The application of heat (using air or in a liquid heat transfer medium) will cause Dacron yarns to shrink. Dacron can also be compacted chemically by means of certain chemical solvents. These solvents cause the Dacron molecule to contract, thus shrinking the yarn. Excessive temperature using either of the two techniques must be avoided in order to avoid degradation of the Dacron yarns. The process of crimping involves the formation of corrugations along the graft which aids in bending the graft without restricting flow. Crimping of a weft-knitted prosthesis enlarges the interstices in the line of the crimp, and decreases the degree of filamentousness of the outer wall in the region of the crimp. These problems are not exhibited in the external velour, warp-knitted prosthesis; which is why this type graft preclots readily, yet allows itself to be penetrated and healed equally well. The final operation of cleaning the graft helps increase blood compatibility.

Polymeric grafts (such as ePTFE) are manufactured using an extrusion technique.[32] The polymeric solution is pushed under pressure through a small orifice. A polymeric fiber is formed as a result. The fiber being extruded is wound on a rotating mandril. The orifice is also moving with respect to the rotating mandril. The fiber is hot when it reaches the mandril causing fiber to fiber bonding. A long tubular shape is created as a result of the orifices axial translation along the rotating

mandril. The circumferential velocity of the mandril is such that the extruded fiber undergoes considerable stretching. After numerous passes of the orifice over the mandril, a desired thickness is built. The formed tube is dried or cooled and removed from the mandril.

Expanded PTFE is Teflon which has undergone an expansion process. The expansion process transforms a full-density PTFE matrix into a structure composed of nodes of PTFE. The nodes are interconnected by fine PTFE fibrils. The node size and shape as well as the fibril length can be controlled by the manufacturing process. As a result of the expansion process, the ePTFE graft is composed of approximately 15% pure PTFE and 85% air by volume.[33]

II-4 Surgical Technique for Pre-clotting a Dacron Graft

Until recently, a vascular graft had to be pre-clotted by the surgeon immediately prior to implantation. Pre-clotting of the graft converts the material framework from the manufacturer into a material-fibrin channel whose walls can not be penetrated by blood, but allows desired tissue ingrowth. Blood and perigraft tissue only "see" native proteins when they come in contact with the graft. Unfortunately, pre-clotting activates platelets on the surface of the graft. The more platelets that adhere to the graft's surface, the greater the possibility of thrombus formation.

Pre-clotting is done in many different ways. The ***submersion method*** (the most common method for a Dacron prosthesis) is summarized here.[34] First, the graft is injected with some non-heparinized blood from the patient. The completely wetted graft is then placed in an empty pan where thrombin is formed on the graft. After a specified time interval, the graft is again injected with blood and completely wetted with non-heparinized blood. The excess blood is then stripped by running the thumb and index finger along the graft from top to bottom. This step is repeated again. During this procedure, the thrombin is being utilized to form fibrin which coats the Dacron fibers and seal the interstices. If performed properly, the flow surface should be impervious, smooth, and thrombin free. When a pre-clotted graft is allowed to sit longer than 15 to 20 minutes prior to its use as a conduit, the graft may lose some of its pre-clot and will bleed when exposed to blood under pressure.[35] If bleeding occurs during examination before implantation, the pre-clotting procedure must be repeated. Current Dacron prostheses now incorporate an albumin coating which is also slowly reabsorbed but does not require pre-clotting.

II-5 Design Considerations and Failures

In the 1960's it was discovered that no other benefits would come from making the vascular prostheses of Dacron lighter and more porous. As a result, researchers

focused their efforts to the needs of the surgeon as well as those of the patient's blood and perigraft tissue. The surgeon needs a graft which does not require pre-clotting or can be pre-clotted easily and one which has excellent handling characteristics. On the other hand, a graft which has an inner surface over which blood can flow without thrombotic complications of stenosis, occlusions, or embolisms is also needed. The graft must have a wall strong enough for indefinite dimensional stability and fatigue strength. The ideal vascular graft will have elastic properties matching those of the host vessel, and possess the ability to reorganize the thrombotic matrix developed during implantation. Many vascular grafts fail because they do not match the properties of the arteries which they are called upon to replace. Designers must pay careful attention to the structural architecture of blood vessels (its ***compliance***). Compliance refers to the relationship between vessel pressure and diameter. The blood flow characteristics must not be ignored. Flow determines the chemical environment which will be present near a thrombus forming location, and at which rate such formation will occur. High flow volumes create shear forces on the flow surfaces of the graft which tend to sweep these surfaces clean. Low flows allow the formation of thrombus (due to platelet adhesion) by creating high enough shear forces to scrape these flow surfaces.

When considering the biocompatibility of the graft, one important factor is the biomaterial's surface charge. A normal blood vessel's inner wall is negatively charged, while its outer coating is positive. Natural blood vessels have reduced thrombogenicity because the blood cells are also negatively charged, and they are

repelled from the inner lining of the vessel. Although surface charge is a good method for determining blood compatibility of a material, the distribution of the charge on the material's surface is also an equally important parameter. After thrombosis has occurred on the graft, the polarity reversal of the inner and outer wall in the thrombosis region has been observed.

Surface cleanliness is another important design criteria. Contamination can occur by the sterilization process or by improper intraoperative handling. The different chemical treatments used during compacting and crimping Dacron grafts can affect the implant's performance.

Dilation, suture line leakage (caused by fracture), and thrombosis are the major reasons for modern vascular graft failures, with ***dilation*** being the more prominent (and the most cited in research) of the three. Dilation refers to a permanent enlargement of the graft's diameter brought about by the pulsating stresses generated from blood flow. Although inherent in all grafts, it may be minimized by adding elastic yarns to a Dacron graft. External support rings on Teflon grafts are manufactured of ***FEP***, Fluorinated Ethylene Propylene (William L. Gore Company, Flagstaff, Arizona) prevent compression and resist kinking. Suture line fractures result from a separation of the graft from the host artery at or near the suture line. This condition is caused by excessive stress at the suture line, weakness of the prosthetic, suture breakage, faulty suturing technique, and (perhaps the most common) infection. Today's grafts are estimated to have an elastic modulus 10 times greater than that of a natural artery.[36] This in effect creates strains near the suture line, yielding turbulent blood

flow and causing additional shearing stresses on the prosthetic's wall. In addition, thrombosis along the inner surfaces of the graft cause a decrease in flow velocity, and increase in blood turbulence, eventually leading to suture line fractures. Structural failures, such as holes or perforations, may also lead to the eventual failure of a graft. Some sources cite insufficient quality control measures during manufacturing. Although gross physical defects are detected at time of inspection during the manufacturing process, other microscopic damages sustained during the manufacturing and subsequent processes and handling are generally not detected.[36] Most failures of this type are noticed clinically at 40 to 60 months after implantation.

III. MATERIALS AND METHODS

III-1 The NJIT Biofluid Laboratory's Flow Loop

The equipment used for this experiment was designed and previously utilized by Hans Pawel, Ph.D., Department of Mechanical Engineering, New Jersey Institute of Technology.[37] The original system was created in the 1970's, and made use of the new microcomputer technology. Since the system had been dormant for a few years prior to this project, some Plexiglass components had become brittle and needed to be remanufactured. Future researchers are encouraged to read the Masters Theses of Bauer[38], Shin[39], and Wu[40], as well as the hand written papers of Korurek[41] and DeMuth.[42] The latter two papers provide the most up-to-date information about the flow loop's modifications and history. They can not be found in the NJIT library, but instead may be viewed in the Biofluids Laboratory of NJIT's Mechanical Engineering Department.

This pulsatile flow system is a closed-loop system and was developed to emulate the physiological system of the left heart (**FIGURE 17**). The system consists of a positive displacement pump which creates pulsatile flow throughout the loop. This mechanical simulator differs from the actual physiological system. Unlike the baroreceptors of the human circulatory system, the NJIT system does not possess a

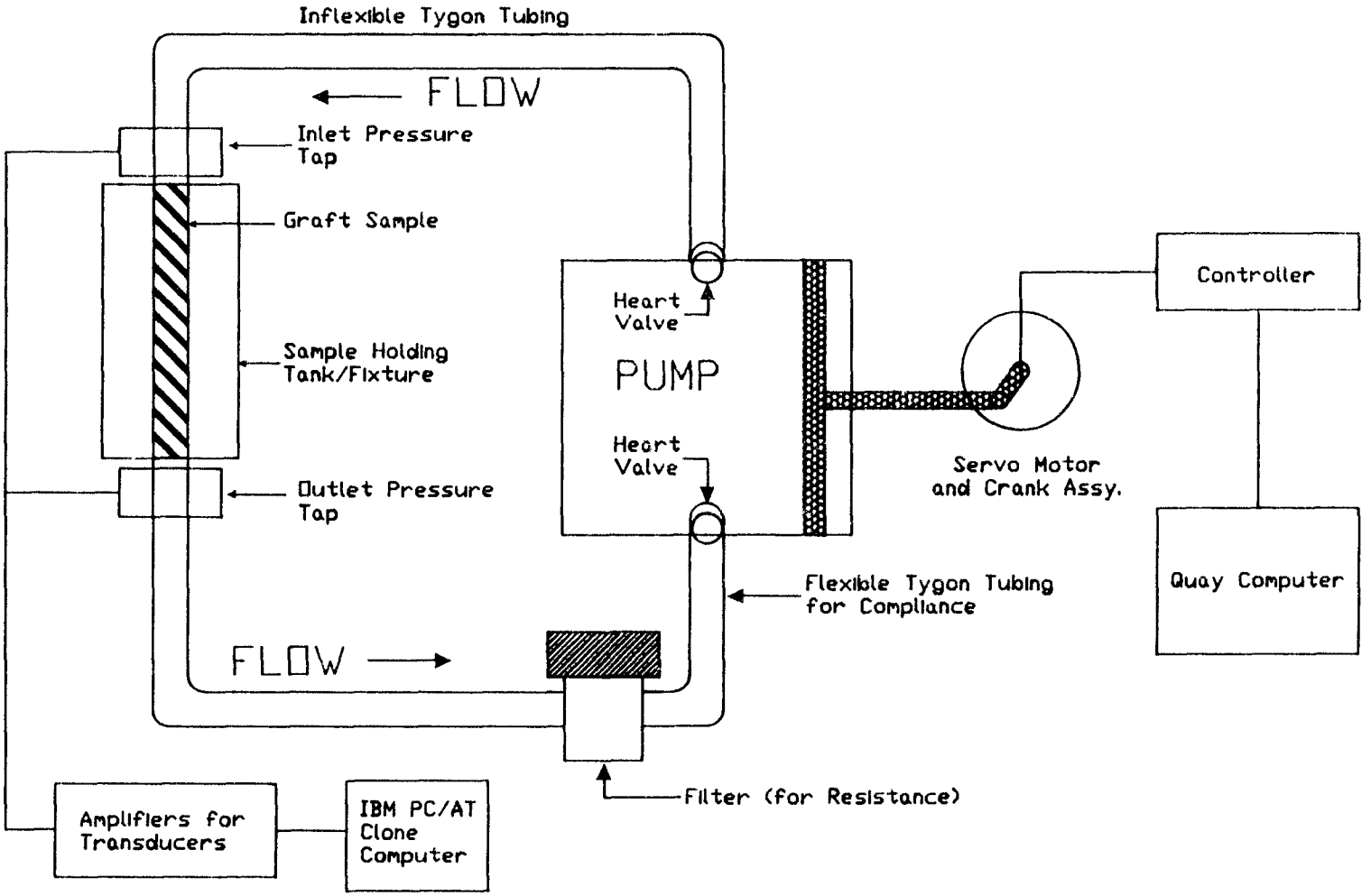

Figure 17 Representation of the NJIT Closed-Loop Pulsatile System

pressure feedback mechanism. The pump in the NJIT flow loop is a positive displacement pump. Despite the pressures present in the system, a predetermined amount of fluid will be ejected from the pump. To further imitate the heart's operation, the pump housing is comprised of two "ball and cage" type heart valve prostheses at the inlet and outlet fluid ports.

A rectangular container of approximate internal dimensions 3 inches high by 4 inches wide, the pump housing is manufactured from Plexiglass so that the viewing of the internal components, as well as any air bubbles which may be trapped within the housing is possible. Air bubbles dramatically the system by increasing damping within the chamber. Lower fluid volume ejected is the result. A new steel bleed valve was incorporated and locked in place using Loctite adhesive for easy removal of those air bubbles trapped in the pump housing. Silicone was added to the connection joints of the housing because the Plexiglass became brittle with age and dormancy and allowed fluid to seep through the housing joints.

The pump housing also consists of the fluid displacing piston. The piston utilizes a "rolling diaphragm" which eliminates the need for any type of lubrication to come in contact with the fluid enclosed in the closed-loop system (**FIGURE 18**). The piston pump is driven by a slider crank mechanism which in turn is controlled by a microprocessor controlled stepper motor (**FIGURE 19**). The stepper motor takes signals generated by the Quay microprocessor and converts these signals into rotary motion which drives the piston crank assembly, thus producing the desired displacement of the piston. The stepper motor shaft will rotate 1.8 degrees for every

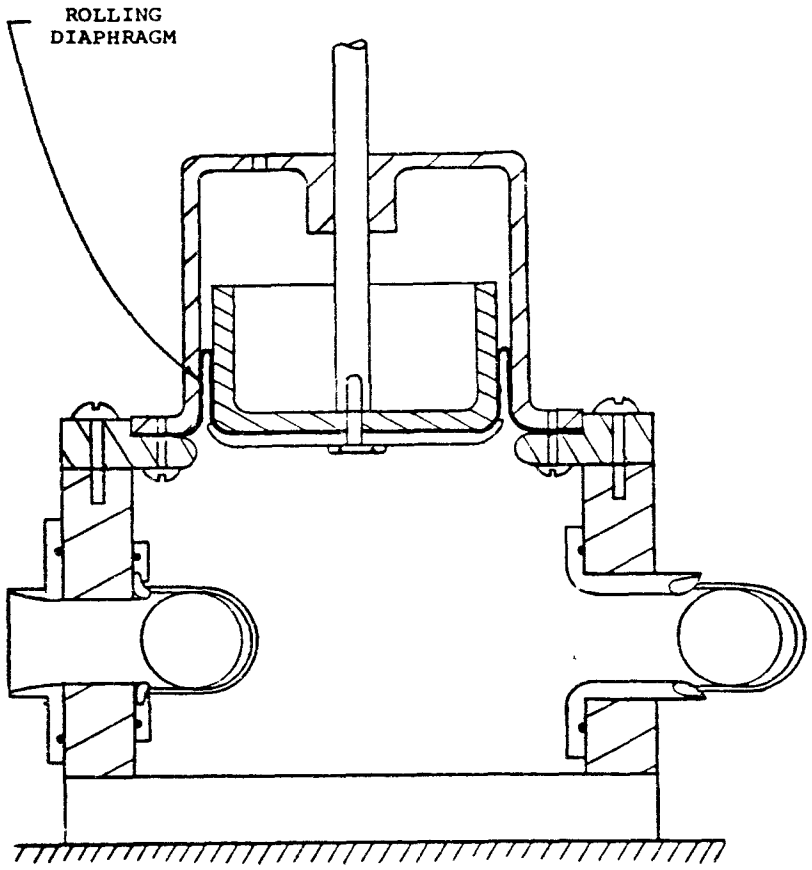

Figure 18 Location of the Rolling Diaphragm Inside the Pump Housing[37]

pulse generated by the microprocessor.[38,39,40,41,42] The program is written so that the crank shaft's wheel (which is at a 4:1 ratio with the stepper motor's wheel) will rotate 360 degrees for each pulse, thus returning the piston to its original starting position before the start of the next pulse.

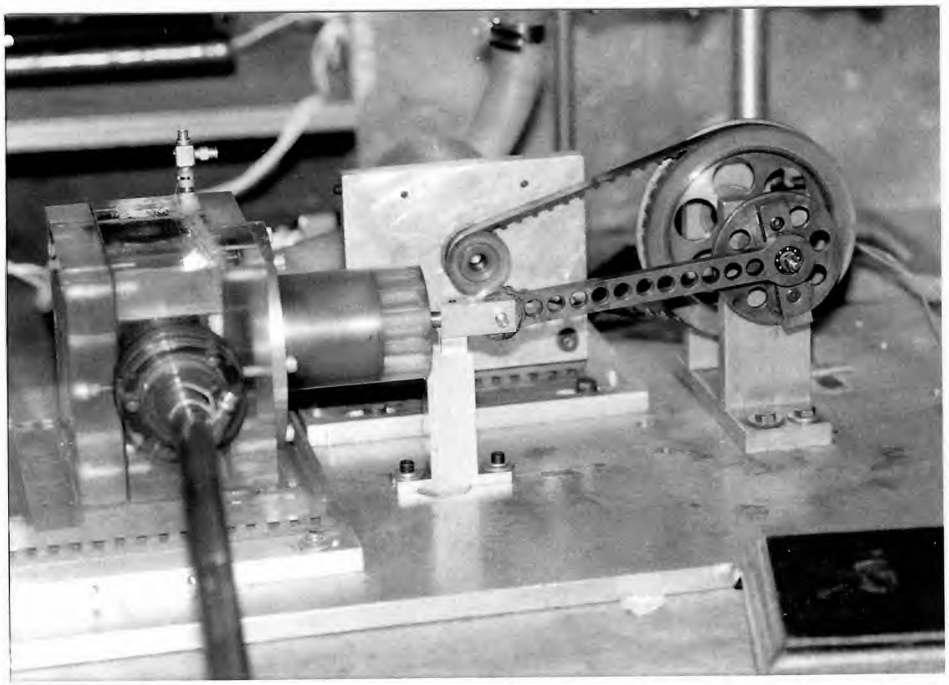

Figure 19 The Slider Crank Mechanism which Drives the Piston

(Slider Crank - right in photo)

(Pump Housing & Piston - left in photo)

The original QUAY computer program was developed circa 1982 and allowed for a fixed pulsatile flow of 72 beats per minute.[41] Later, in the fall of 1985, DeMuth modified the computer program allowing the user the ability to incorporate additional piston displacements so that various diseases of the heart could be emulated.[42]

An additional program written by DeMuth for the Comadore 64 computer assisted the user with developing new displacement curves. This program generated

a report of displacement versus time so that the new data points describing the desired piston displacement versus time curve could be entered into the QUAY computer program.[42]

The flow loop system is composed of clear Tygon tubing sections. The different diameters, wall thicknesses, and lengths (determined by Dr. Pawel and previous investigators) establish resistance to the flow loop system in order to develop the proper pressures. Clear tubing was employed to verify that air bubbles were not trapped within the system.

The original method for securing the vascular graft within the flow loop system involved the use of a Plexiglass tube assembly which served as a housing for a hot film velocity flow probe (**FIGURE 20**). As with the pump housing, this Plexiglass became very brittle over time, and despite repeated repair attempts was no longer functional. As a result, the vascular graft samples were connected to the system via slightly barbed plastic CPC connectors (**FIGURE 21**). These quick connectors are designed with internal spring valves. The valves are in the open position when the two halves of the connection are made to allow flow and are closed when the sections are disconnected (preventing any leakage of fluid from either half). The internal spring valves were removed to prevent possible flow obstructions. The tapered barbs of these connectors proved to be very functional. They secured the graft in such a way as not to damage the samples. Hose clamps were used to secure the graft sample to the CPC connector's barbed ends. Silicone tubing was placed between the hose clamp and graft so as not to damage the samples.

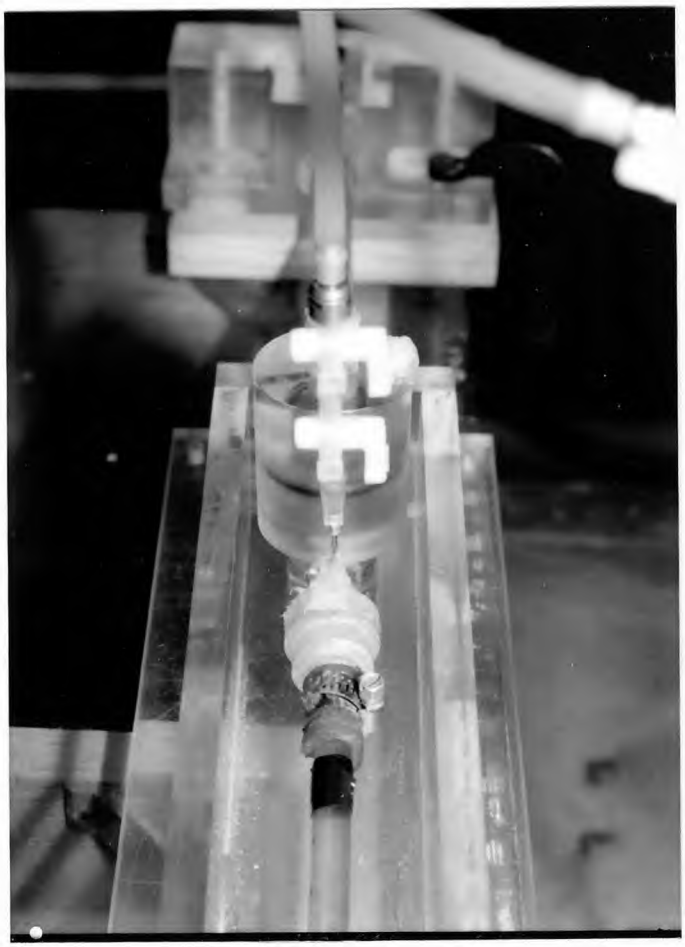

Figure 20 Hot Film Probe Holder-Tube Assembly

(Shown in test fixture holding Tygon tubing sample)

The graft's outlet connector is attached to the mating female connector; which in turn is secured to a 180 degree template-Tygon tubing assembly. A metal pointer

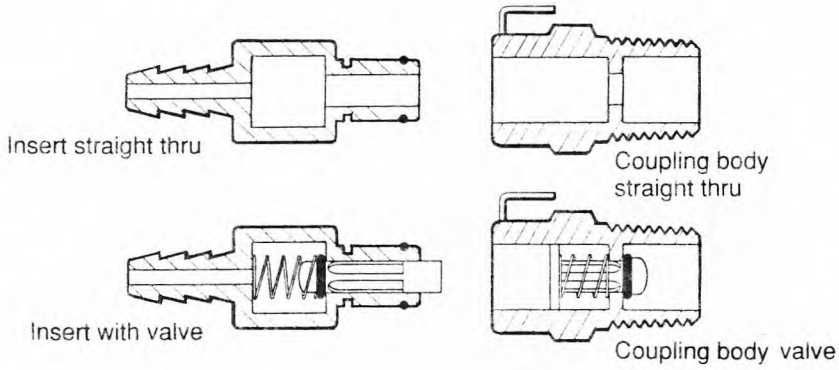

Figure 21 CPC Connectors Used to Secure the Graft Samples

CPC Colder Products, St. Paul, Minnesota

fastened to the template-Tygon tubing assembly (which rotates through 180 degrees) is used to measure the angular rotation of the vascular graft sample (**FIGURE 22**).

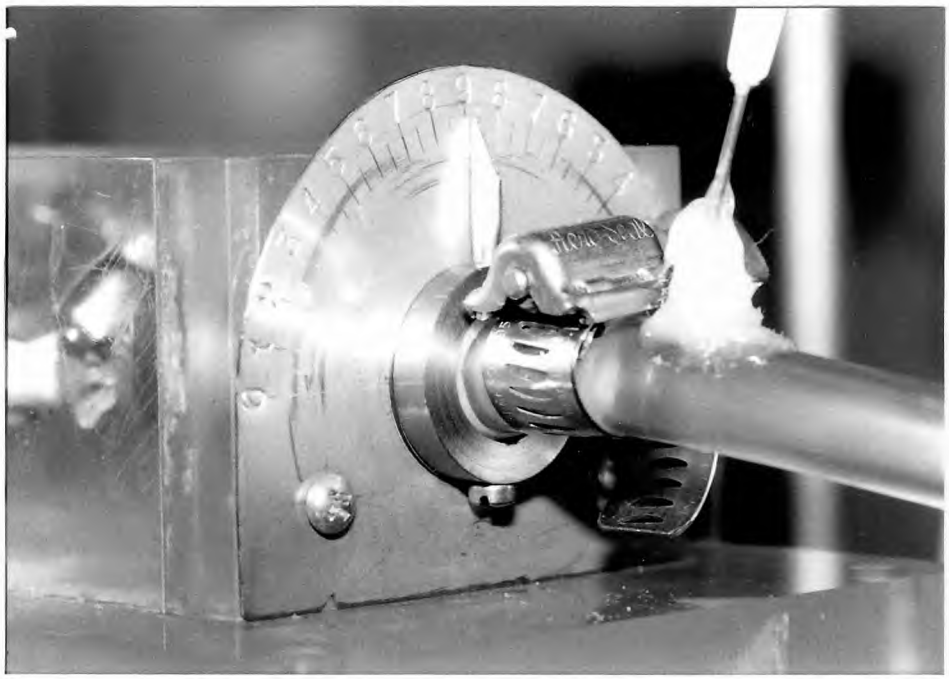

Figure 22 Metal Pointer and Protractor Used to Measure Twist Angle

Intraluminal pressure was measured utilizing two medical grade pressure transducers. Two hypodermic needles (inner diameter 0.031 inch) were inserted into the Tygon tubing on both the inlet and outlet sides of the graft sample and secured permanently into place. The sharp beveled points of the needles had been carefully removed using a grinding wheel prior to insertion into the Tygon tubing. After the insertion of these needles into the tubing, distilled water was injected through the needles in order to verify that they were not obstructed by small particles of Tygon tubing which may have clogged the needles during insertion. Clear rigid plastic tubing was connected between the needles and pressure transducers. Air bubbles in this tubing would drastically effect test results, damping the pressures prior to detection by the transducers.

Each transducer is connected to Wheatstone bridge amplifiers (BAMS), one for the input pressure and one for the output pressure. The output jacks from the BAMS are connected to an eight channel Metrabyte A/D converter installed within an IBM PC/AT style microcomputer. The input pressure transducer is connected to channel 0, and the output pressure transducer is connected to channel 1. The A/D converter samples the data from the channels 0 and 1 and stores an analogous integer for each channel within its corresponding buffer for that channel. The data from the A/D board is accessed utilizing a Microsoft QBasic program. Metrabyte provided the core QBasic program lines which access the A/D board. Unlike interpretive basic which greatly reduces the time that the A/D board can be sampled, a QBasic program is compiled

before it is run, thus providing a board sampling rate similar to any other compiled program.

A new addition to the closed-loop flow system involves the incorporation of a dual flip-flop switch, Radio Shack part number 276-2413 (**FIGURE 23**). This chip is connected inline between the A/D board and a toggle switch attached to the piston's crank assembly (**Table III**). As the wheel of the crank assembly rotates, a small pin on the crank comes in contact with the toggle switch. As the toggle switch is triggered during the first stroke of the piston, a 5 volt dc pulse from the microcomputer's motherboard (fed through the line via the A/D board) flows through the circuit activating the flip-flop switch.

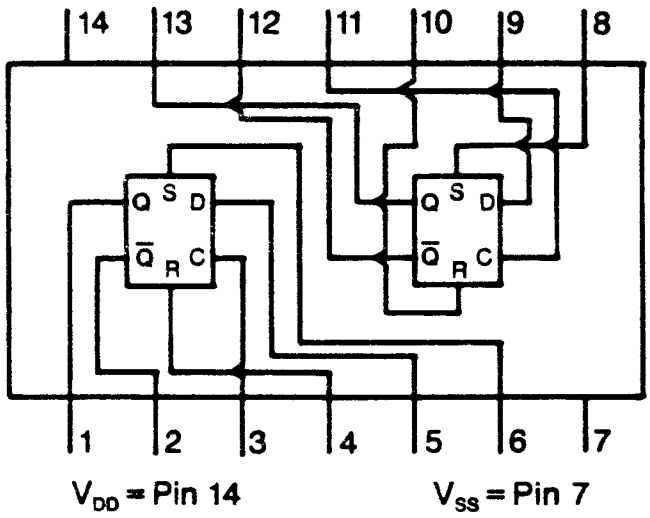

Figure 23 Schematic of the Radio Shack Dual Flip-Flop (P/N 276-2413)

Tandy Corporation, Fort Worth, Texas

TABLE III FLIP-FLOP PIN CONNECTIONS
(for Radio Shack P/N 276-2413 Dual Flip-Flop)

Pin Number	Connection To:
1	Pin #23 of Dash-8 A/D Board's Connector
3	Pulse Source (Trigger Switch)
4	Digital Output of Dash-8 (Pin #7 of Dash-8 A/D's Connector)
5	+5 Volt (Pin #14 of Flip-Flop)
6	Ground (Pin #7 of Flip-Flop)
7	Ground (Pin #11 of Dash-8 A/D's Connector)
8, 9, 10, & 11	+5 Volt (Pin #14 of Flip-Flop)
14	1) +5 Volt (Pin #29 of Dash-8 A/D's Connector) and 2) Pulse Source (Trigger Switch)
3 & 7	Install a 1K Resistor between these Pins

As the flip-flop switch is triggered, the signal activates the A/D board thus signaling the start of data collection. In digital logic, this 5 volt dc output is referred to as the signal going high; alternately no voltage is referred to as the signal being low. In order to begin the collection of the next set of data, a software switch must be used to reset the dual flip-flop, forcing the signal low. Since it was desired to sample the data of a full piston stroke beginning at the same piston position each time, a compromise was made. Data is taken slightly longer than the full piston stroke. This was purposely done to ensure that all data for full piston stroke was collected,

and relates to the capacity Metrabyte's eight channel A/D converter boards. As the piston begins its second stroke, the toggle switch is again activated. Data collection does not begin at this point because the QBasic program's data loop (started from the first stroke of the piston) has not yet completed. Once the data loop is complete, the flip-flop is reset via software and the system waits for the next impulse. The A/D board does not collect data until the start of the third stroke of the piston. These events continue until ten waves have been read. It would be a very difficult programming problem to have the switch perform the function of discontinuing data collection and beginning another sample run with one impulse (or click of the toggle switch). Metrabyte technical support personnel were consulted and the system used in this research was the best solution.

III-2 Test Description

This project was developed to investigate the effects of twist on the performance of ePTFE vascular grafts. An angle of twist between 0 and 180 degrees was studied. Another important criteria was to observe when "catastrophic failure" of the graft occurred; that is, when the twist in the graft is actually pushed toward the outlet side of the graft like a cork screw. When this happens, flow becomes severely restricted or obstructed, and pressure in the graft rises dramatically.

Distilled water was used as a fluid medium for this experiment. A pulse rate of 72 beats per minute was selected. The first test consideration involved testing the graft sample in its fully extended, taut position; however, not applying a large amount of tension to the sample (**FIGURE 24**).

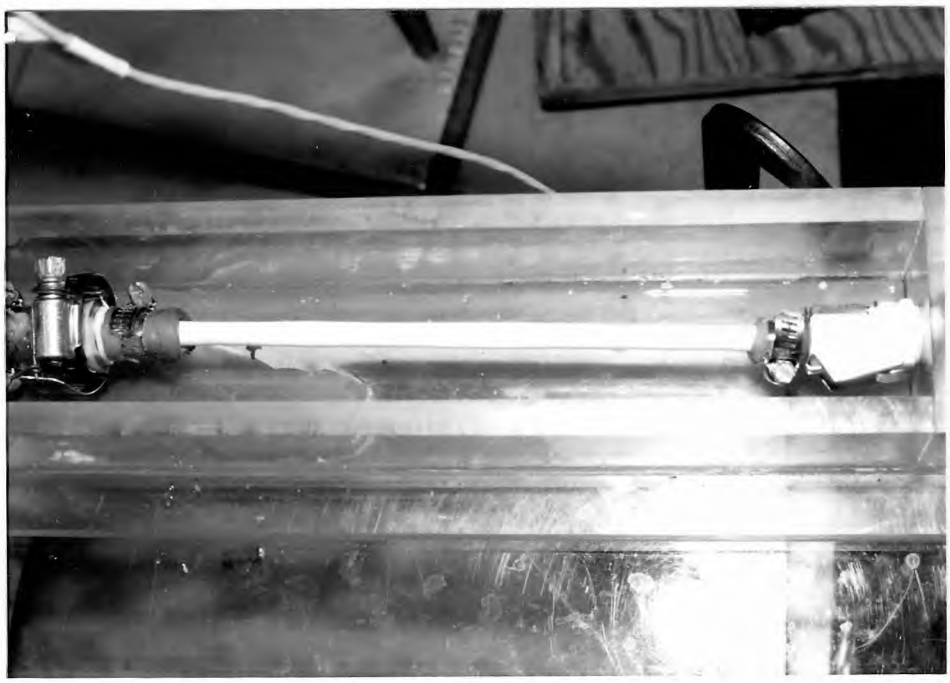

Figure 24 Graft Segment held Taut in the Test Fixture

The second focus of this test involved testing the ePTFE graft samples with up to two inches of slack introduced. Slack is obtained by bringing the fixture ends closer

together (**FIGURE 25**). Although two inches of slack should not occur clinically, it was theorized that if any slight changes had occurred with a minimum amount of slack (results which may have been difficult to observe), it would be drastically exaggerated with such a large amount of slack.

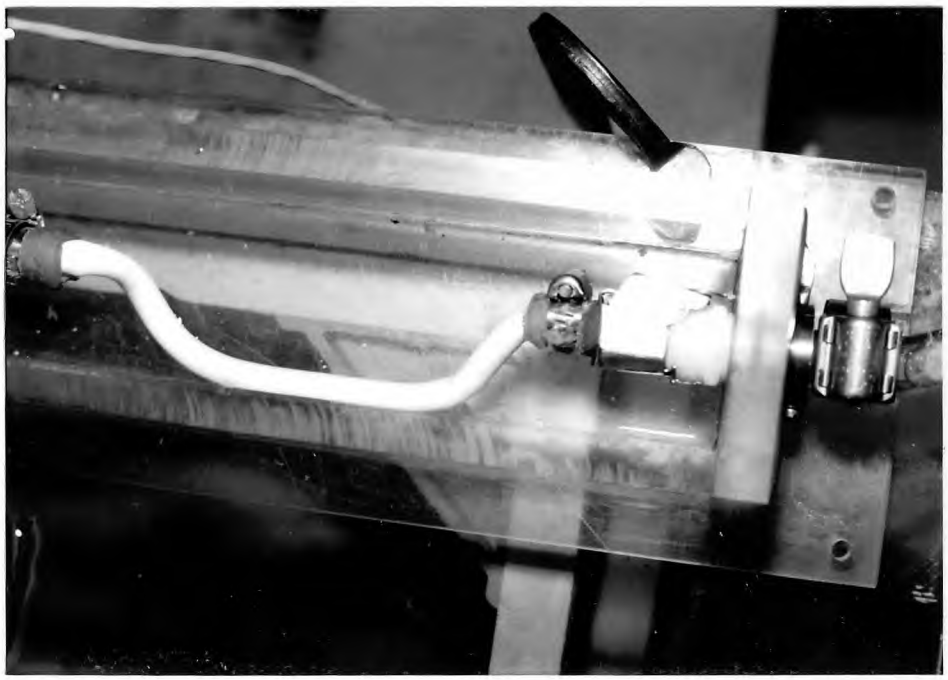

Figure 25 Graft Segment with 50 mm Slack Induced

Prior to testing any ePTFE grafts, a section of Tygon tubing was used. With this tubing in place, the system components' function, as well as the computer

software, was continually tested and modified. A record of sample numbers and descriptions were maintained for data analysis and future reference, **Table II**. The ePTFE graft segments (7 mm ID) were cut into 203 mm lengths. Each sample was first tested from 0 to 180 degrees of twist at its original 203 mm, zero slack (or taut), configuration. Slack was then introduced by bringing the fixture ends closer together, and the graft was re-tested. Once completed, the grafts were shortened and testing was repeated in several progressively reduced lengths.

Pressure versus time data for each individual sample and angle of twist was stored in the IBM PC/AT computer for both the inlet and outlet pressure curves (**Figure 26**). System pressures were accounted for using Bernoulli's equation by analyzing the displacement versus time curve of the piston. As described in **Section III-3.2.2**, the inlet and outlet pressures were calibrated and calculated utilizing a post processing program. Work across the graft segment was also calculated. The maximum outlet pressures were chosen to be the indicators for the changes in pressure across the graft as twist was induced. Should pressure be restricted, a decrease in outlet pressure would be noticed.

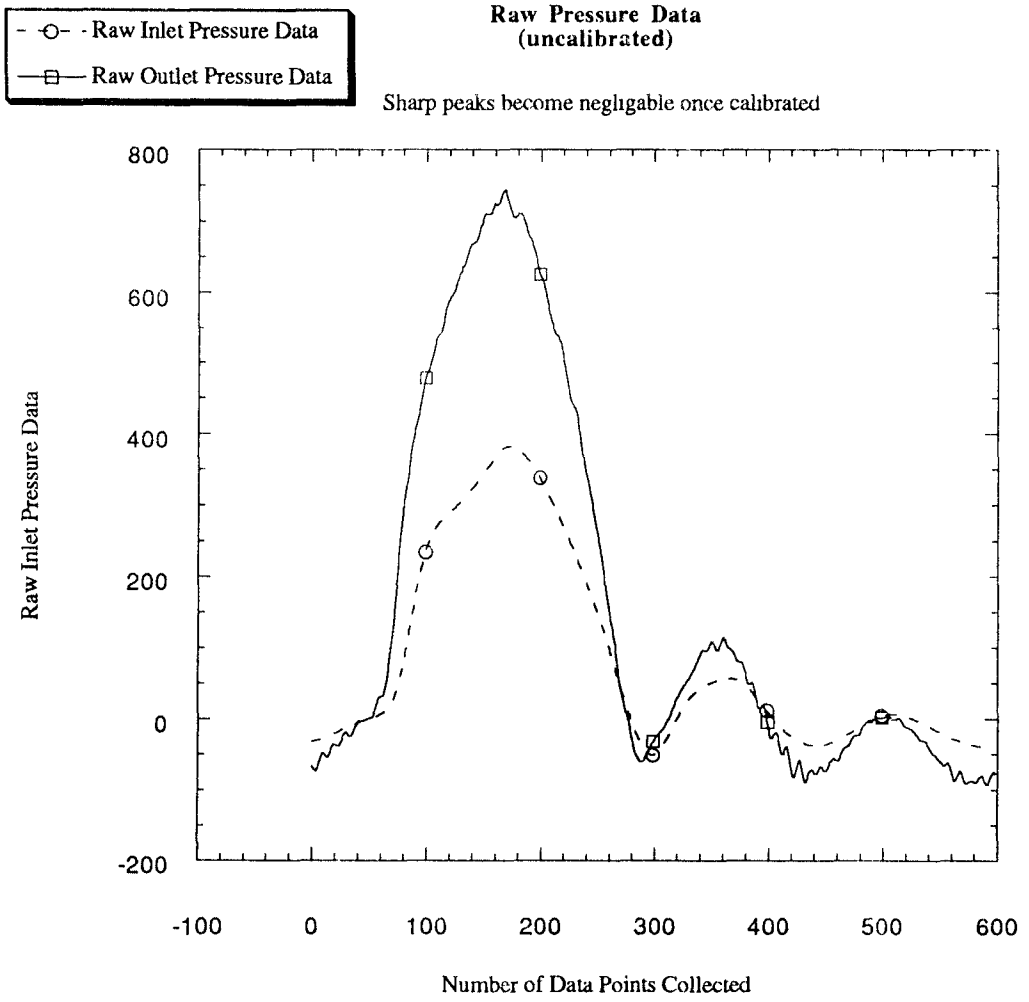

Figure 26 Example of Inlet and Outlet Pressure Waves Collected

TABLE IV SAMPLES TESTED

Sample Number	Length (mm)	Slack Induced (mm)	Description
0 & 1	304.8	0	Tygon Tubing
2 & 3	152.4	0	Tygon Tubing
4	76.2	0	Tygon Tubing
5, 8, & 18	203.2	0	Teflon Graft
6, 14, & 24	101.6	0	Teflon Graft
7 & 16	76.2	0	Teflon Graft
9 & 19	203.2	25.4	Teflon Graft
10 & 20	203.2	50.8	Teflon Graft
11 & 21	152.4	0	Teflon Graft
12 & 22	152.4	25.4	Teflon Graft
13 & 23	152.4	50.8	Teflon Graft
15 & 25	101.6	25.4	Teflon Graft
17	76.2	12.7	Teflon Graft
26	69.8	0	Teflon Graft
27	69.8	6.4	Teflon Graft
28	127	0	Teflon Graft
29	127	0	Teflon Graft

Note: All grafts (except 28 & 29) tested from 0 to 180 degrees of twist.
Sample 28 tested from 180 to 360 degrees of twist.
Sample 29 tested from 360 to 460 degrees of twist.
Catastrophic failure was noted at 460 degrees of twist.

III-2.1 Experiment Steps

The following steps list the procedures that were followed for running the test.

1. Turn on the BAMS (Wheatstone bridges) and allow them to warm for a minimum of 15 minutes. This accounts for any drift that may be present when the equipment is first turned on.

2. Turn on the Personal Computer and load the QBasic program.

3. Prepare the vascular graft sample and carefully secure it to the holding CPC connectors via hose clamps (using soft silicone tubing between the clamp and the graft, so as not to damage the graft). Before tightening the clamps verify that the graft is not pre-twisted in the fixture. this is easily achieved with the grafts because the manufacturer has provided a line on the product for this reason (Note: the angle indicator of the fixture should be set at zero degrees when setting up the graft).

4. Open the valve of the large filler tube of the flow system, and pour distilled water free of particles into tube. A coffee filter placed inside the funnel served as a safeguard in order to prevent any large particles from entering the system. Filling this tube to a high level will create a large pressure head which will be needed in the following steps (6 & 7) to aid in the removal of air bubbles.

5. Turn on the system and allow the pump to run for a couple of minutes. This will force any air bubble in the system to accumulate in areas which have been equipped with bleed valves. Also, walk around the system, examine the tubing, and verify that there are no leaks.

6. Turn off the pump and check the system for any air bubbles. It is especially important to check the pump housing itself. Bubbles can be easily removed via the bleed valve on the top of the housing (some slight tipping of the pump housing assembly to move the bubbles towards the valve may be necessary). It was observed by myself, during the preliminary checkout of the system, that if bubbles were allowed to remain in this housing, the full pumping potential of the piston will not be achieved, the trapped air serves as a damper to the system. This is easily recognized by viewing the output artificial heart valve. When the bubbles are present this valve is sluggish and does not operate properly.

7. Open the valves to the transducers and allow the water to flow in order to eliminate any air bubbles which may be trapped in the lines leading to the pressure transducers from the needles in the Tygon tubing. Next check and clear any air bubbles from the pressure transducers themselves. The best method to achieve this is to remove the transducers from their holders, move them around and tap until all air bubbles are removed.

8. Once it is certain that all the air bubbles have been removed from the system, calibrate each transducer against a sphygmomanometer in order to correlate the reading from the A/D board to mmHg.

9. Lower the water level in the large filler tube to the selected level marked on the tube. This will provide the system with a slight pressure head. The selected level is slightly above the valve on the filler tube. This level was selected so that when the valve is closed there would be no air trapped under the valve, thus creating a point of damping in the closed loop flow system. After the water in the system is at its proper height, close the valve, this will make the system a closed loop system.

10. Balance the Wheatstone bridges (note: it will be necessary to remove the cable which connects the BAM to the A/D board, in order to read the analog meter on the BAM and balance the whetstone bridge). Once the BAMS are balanced, reconnect the cable to the A/D board.

11. Run the program and answer the prompts provided. These first prompts will establish the file names for easy identification and storage of the raw data. The first step of the program is going to set the zero baseline of the system, this was programmed in to account for any reading other than zero from the BAMS when the system is at rest.

12. After the zero baseline has been established, turn on the pump and allow it to run for a couple of pulses (as directed by the computer prompts). Once the computer is activated, ten samples will be taken and averaged together. As described in the equipment section, the samples are taken on the odd interval (pulse 1, 3, 5, etc.) until ten have been collected. The switch on the pumps wheel, working in conjunction with the flip-flop switch, will make certain that data collection is started at the same piston position for each sample.

13. Once data collection is complete, shut off the pump. Twist the graft to the next degree increment. Open the valve on the large filler tube and verify that the water level remains at the selected marking. It may be necessary to add a small amount of water using a syringe and plunger (minus the hypodermic needle). Once complete, close the valve.

14. Steps 10 through 13 are then repeated until all testing is completed (180 degrees).

III-3 Computer Software

III-3.1 Test Data Collection Software

The main computer program begins by prompting the user to enter the sample number for the graft being tested. Each graft tested is given a sequential sample number (recorded in a laboratory notebook) so that data storage is kept organized. The next step of the program prompts the user as to whether a calibration run is necessary. A calibration run should be completed prior to each sample tested. At the time of this research, the available sphygmomanometer was irreparable. As a result, the calibration routine was written in a manner as to allow for the calibration of one transducer against the other. The inlet and outlet transducers are shut off from the system pressures via plastic inline three-way medical connectors. Both transducers are connected by two pieces of clear, rigid plastic tubing joined together by another connector valve. The valve is placed inline so that pressure may be introduced to the transducers using a plastic syringe and injecting distilled water. Each transducer is subjected to the same pressure applied by the syringe into this common plastic tubing. Five separate pressures are introduced into the system. The values of the pressure are not known, however they were kept reasonable enough by applying small forces with the syringe so as not to damage the transducers. The values generated by the two transducers are recorded by the A/D converter and corresponding values from the converter are stored in the computer's memory (and diskette in ASCII file format for

future reference). The inlet transducer was calibrated with respect to the outlet transducer using a linear regression routine. Performing this procedure prior to every sample tested accounted for any daily or monthly fluctuations in the two transducers' output. Data from sample testing was stored in integer format having no units associate with them. It was intended that a future calibration between the outlet transducer and a new sphygmomanometer would be performed to obtain the desired units, mmHg. The inlet transducer would not have to be calibrated against this new sphygmomanometer since it had been already calibrated against the outlet transducer.

After a calibration run, the main menu appears on the terminal. This menu contains the options for each angle of twist to be tested, plus an option for exiting the program (**FIGURE 27**).

```
                    MAIN MENU

[A]          0 DEGREES          [K]        100 DEGREES
[B]         10 DEGREES          [L]        110 DEGREES
[C]         20 DEGREES          [M]        120 DEGREES
[D]         30 DEGREES          [N]        130 DEGREES
[E]         40 DEGREES          [O]        140 DEGREES
[F]         50 DEGREES          [P]        150 DEGREES
[G]         60 DEGREES          [Q]        160 DEGREES
[H]         70 DEGREES          [R]        170 DEGREES
[I]         80 DEGREES          [S]        180 DEGREES
[J]         90 DEGREES          [T]        QUIT PROGRAM

              ENTER DEGREE BEING TESTED?
```

Figure 27 Example of the Main Menu Used in the Data Collection Software

As an angle is selected, the computer program automatically creates a file name for the storage of data. File names have been standardized for ease of reference at a later date as well as preventing the overwriting of any previous data recorded. A file name appears as "S##A###.PRN"; where S## indicates the sample number (for example, S09 for sample number 9) and A### for the angle of twist (for example, A180 for 180 degrees of twist). Each file was given the "PRN" prefix in order that the ASCII data be easily read by Lotus 123's import function (for graphing purposes). As each angle of twist is tested, the angles previously tested appear highlighted on the main menu, thus making the user aware that certain angles have already been tested. The program does not require that either the angles be sampled sequentially or that all angles be tested. The "QUIT" option allows the user to exit at any time.

Once an angle is chosen from the main menu, a series of detailed prompts begin the process of data collection. The transducers are zeroed manually on the BAMS, and a baseline pressure value is taken to account for small offsets above or below the zero baseline. Once data collection begins, the program records ten waveforms for a given angle of twist. After this, the data are averaged and stored in a file on the computer's hard disc in an ASCII file format for future reference. The main menu reappears and the next sample is tested in a similar fashion until all angles of twist of interest to the researcher have been investigated.

Both the inlet and outlet transducers had been calibrated with respect to the sphygmomanometer. Values for the inlet pressure transducer (one when it was calibrated using only its raw data, and one for the values which were obtained due to

the linear regression against the outlet transducer) were compared. A slight difference did develop and the values for the transducer prior to calibration with respect to the outlet transducer were chosen. Review of the raw data from each transducer revealed that no significant changes in output values had taken place over time.

III-3.2 Post Processing Programs

Two post processing programs which analyze the raw testing data were created. The first program calculates pressures in the system using Bernoulli's Equation. This was done since the inlet and outlet cross sectional areas of the Tygon tubing differed. This program was written separate because it only needed to be run once. Data from this program is stored in ASCII file format and is utilized by the second post processing program. The second program calibrates the raw test data, placing it into units of pascals. The waveforms are then analyzed as described in the following sections.

III-3.2.1 Calculating Bernoulli's Equation

Because the cross sectional areas of the Tygon tubing on both the inlet and outlet side of the graft varied, the pressures had to be corrected using Bernoulli's Equation. The amount of fluid ejected from the housing is easily calculated. Multiplying the

displacement of the piston (for given time interval, t) by the piston's cross sectional area will give a volume versus time curve.

$$\text{Volume(t)} = \text{Piston Disp} \times \text{Piston Area} \qquad (3.1)$$

piston displacement data points were obtained by Korurek's thesis (**FIGURE 28**).[41] In Korurek's thesis, displacement was identified on a scale between 0 and 1, with the latter being the maximum piston displacement. The maximum piston displacement was measured to be 0.3 inches (.0075 meters). **Table V** lists the displacement data points.

A total of 596 data pairs (for the inlet and outlet test data) had been collected by the main program. The A/D board sampled the two channels at 682 Hz. The total time for the collection of these 596 points is easily calculated as 0.874 seconds. To create a table of piston displacement versus time for this time interval ($\Delta t = 0.0014666$ second), the known piston displacements contained within **Table V** were utilized by a subroutine within the program. This subroutine performed interpolation calculations in order to obtain a piston displacement versus time curve to be used in calculating Bernoulli's Equation.

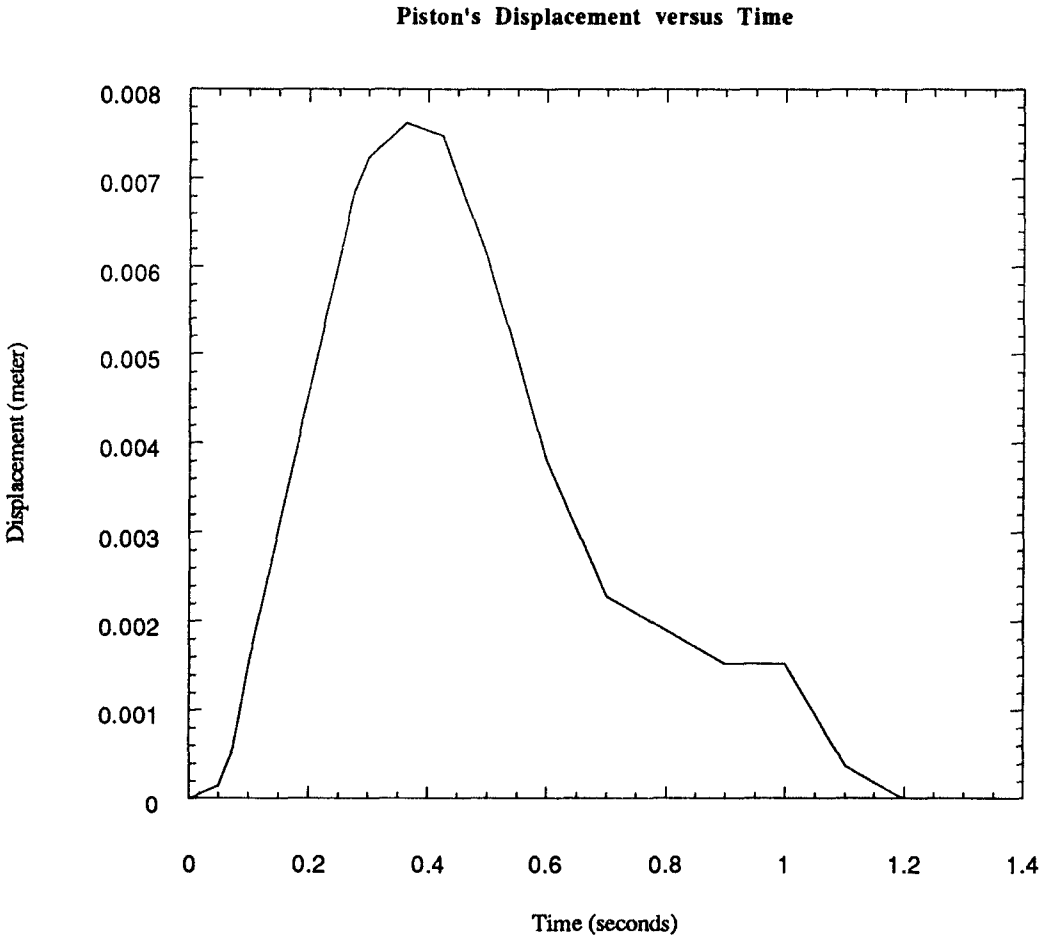

Figure 28 Piston's Displacement versus Time

TABLE V PISTON DISPLACEMENT VERSUS TIME

Percentage of Total Displacement (%)	Time (seconds)	Displacement (meters)
0	0	0
0.02	0.05	0.0001524
0.076	0.076	0.0005791
0.20	0.10	0.0015240
0.60	0.20	0.0045720
0.90	0.276	0.0068580
0.95	0.30	0.0072390
1.00	0.364	0.0076200
0.98	0.425	0.0074777
0.80	0.50	0.0060960
0.50	0.60	0.0038100
0.30	0.70	0.0022860
0.25	0.80	0.0019050
0.20	0.90	0.0015240
0.20	1.0	0.0015240
0.05	1.2	0.000381
0.0	1.2	0.0

The calculation for pressure in the system at a given point (using Bernoulli's Equation) is as follows:

$$\frac{P_1}{Rg}+\frac{V_1^2}{2g}=\frac{P_2}{Rg}+\frac{V_2^2}{2g} \tag{3.2}$$

Knowing that:

$$V=\frac{Q}{A} \tag{3.3}$$

the above equation (3.3) can be manipulated into the following form:

$$P_1-P_2=\frac{RQ}{2}\left(\frac{1}{A_2^2}-\frac{1}{A_1^2}\right) \tag{3.4}$$

where: P1 represents the inlet pressure

P2 represents the outlet pressure

A1 represents the inlet tubes cross sectional area (A1=7.126E-05 meters)

A2 represents the outlet tube's cross sectional area (A2=3.167E-05 meters)

The density of water is 998 Kg/m^3 at 20°C. The mean room temperatures for the laboratory taken at testing was 23.86°C. Therefore, the density of the water from interpolation is 997 Kg/m^3. Utilizing Equation (3.4), the pressure change was then calculated and the following values resulted (**Figure 29**). These calculated data points and their corresponding time intervals were stored in an ASCII formatted file to be used by the second post-processing program.

III-3.2.2 Calculating Pressures

The second post processing program calculated inlet and outlet pressures. The pressure drop across the samples, and the maximum work performed on the graft segments were also calculated.

The first task of this program was to read in the data points calculated and stored to a file by the first post processing equation. This data was then stored in arrays for future calculations. Raw data from the testing files were individually read into the program, calculations were performed and the resulting data was stored on disc. Again, data was stored by sample number and angle of twist in a similar format as the raw data on the hard disc.

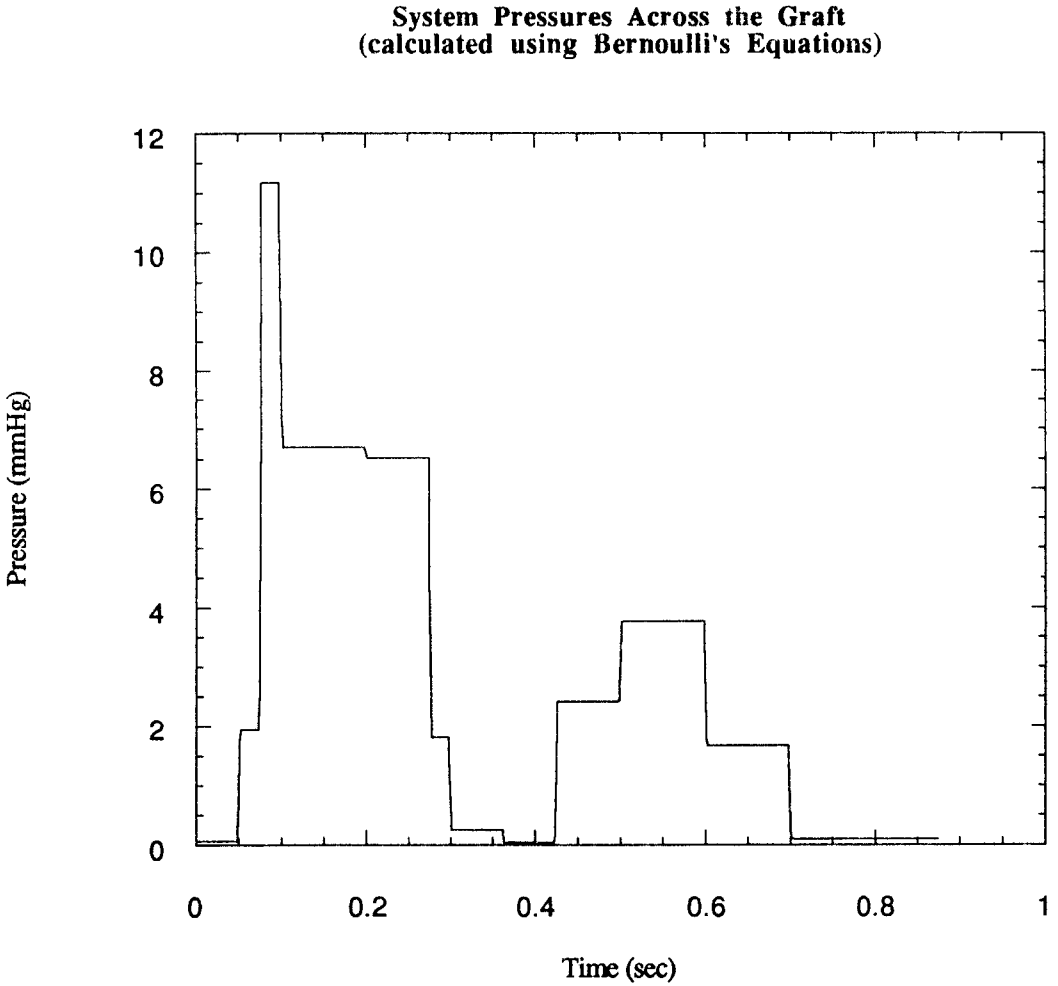

Figure 29 System Pressures versus Time Calculated using Bernoulli's Equation

As mentioned earlier, data was collected beyond the full stroke of the piston's travel (reference **Figure 28**). It was decided to observe the major positive pressure pulse of the data. This is the point when the distilled water pulse wave is passing through the graft and applying the most pressure to the sample. Two smaller waves of significantly lesser value than the major pressure pulse can be seen. The wave represent the pressures created in the pulse by the pump housing's outlet prosthetic heart valve. Despite repeated adjustment attempts. the stainless steel ball would strike the cage portion of the heart valve with significant force. This action would cause the ball to bounce back against the valve's seating ring with such a force as to prevent the ball from properly seating. The ball would strike the cage and seat twice before the piston's next positive fluid displacing stroke.

The program trimmed away the leading and trailing edges of the pressure wave, thus leaving the desired positive pressure pulse. The remaining data which represented the major pressure pulse was then converted into pressure units (**FIGURE 30**). This was achieved by utilizing the transducer versus sphygmomanometer calibration data. The outlet pressure data was subtracted from the inlet pressure to calculate the pressure drop across the graft. Work across the sample for each time interval was calculated utilizing Equation (3.5).

$$W(t) = \Delta P \times A \times L \tag{3.5}$$

where: ΔP represents the pressure drop across the graft

A represents the cross sectional area of the 7 mm graft

L represents the length of the graft

The program also identified the maximum work value, in the same manner that it had identified the maximum inlet and outlet pressures. Once all the calculation had been obtained for a given sample and angle of twist, the results were stored in two ASCII format files. One file stores the calibrated pressure data of the major pressure pulse while the other stores all the maximum pressure values, including the maximum work values, for each angle of twist. The files were analyzed by plotting.

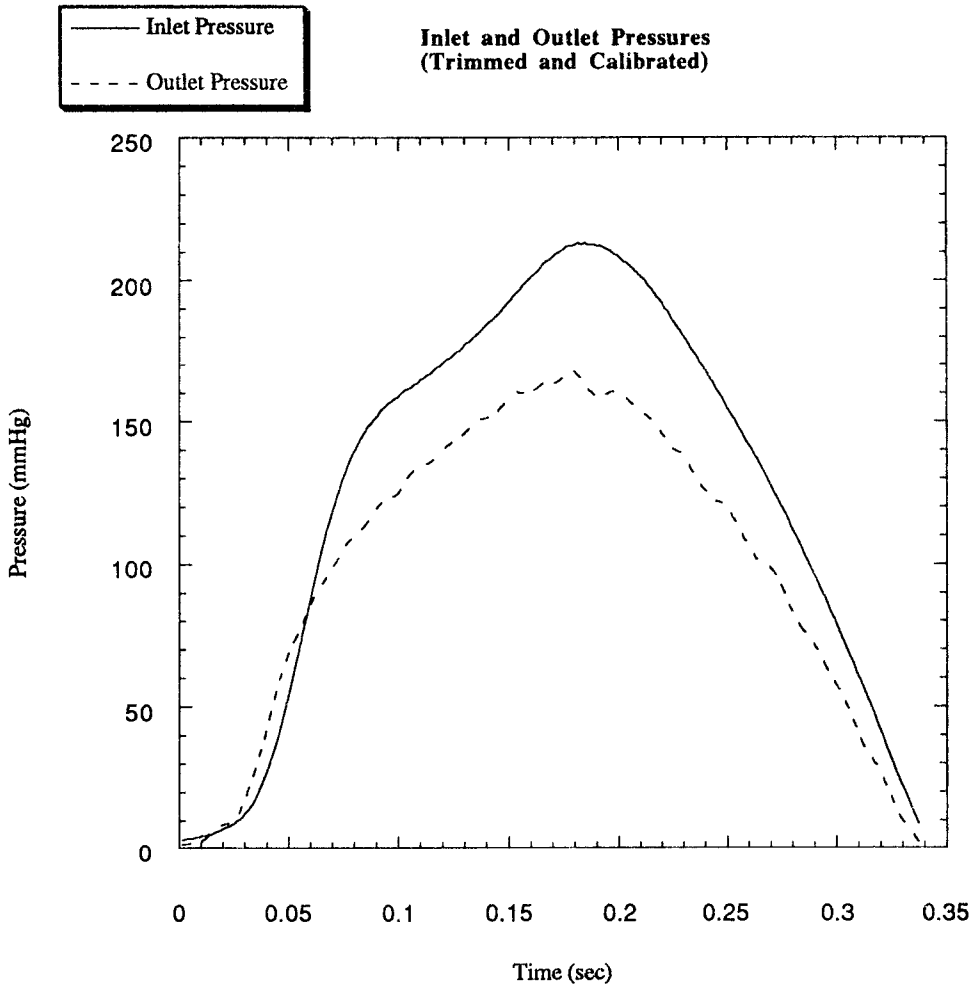

Figure 30 Example of the Major Trimmed and Calibrated Pressure Pulses

IV. RESULTS

IV-1 Previous Research

There has been very little similar research to this project published on vascular grafts. One set of investigators conducted a study on the effects of twist on flow. Endean, E., et al. examined the effect of twist on the flow of a canine vein graft using a non-pulsatile, steady flow setup.[43] Their in-vitro system consisted of a large reservoir containing perfusate suspended above the sample. Vein segments were tested at 25, 50, 75, 100, and 150 mmHg. These pressures were obtained by altering the height of the reservoir. The vein segments were held horizontally by cannulas at both the inlet and outlet sides. Outflow resistance was also varied to simulate one, two, and three vessel outflow in patients by using 19, 18, and 15 gauge hypodermic needles. A hairline mark was made on the distal cannula and twist was measured using a protractor. The distal end of the vein received a single suture to verify the amount of twist imposed. Twists of 0, 45, 90, 135, and 200 degrees were studied. The liquid from the tank, which flowed through the twisted sample, was collected in a beaker over a one minute period. This volume was then measured to determine the effect that twist had on the flow of fluid through the sample. Their findings show that blood flow was not reduced until 140 degrees of twist; slightly greater degrees of twist produced a sharp reduction in flow through the canine vein graft. Notably, they did not investigate pressures across the vein segment, and did not use a pulsatile system.

IV-2 Results

The pressures observed were higher than those seen physiologically. The pressure will have to be lowered in future tests to more closely resemble physiological conditions. No change in pressure occurred for the taut sections of graft as they were tested through 180 degrees. **Figure 31** shows the values for the four lengths tested (203 mm, 152 mm, 102 mm, and 76 mm) with no slack induced, while **Figure 32** shows the same samples with 25.4 mm of slack induced. Despite the shortening lengths of graft segments tested (from 203 mm to 70 mm), there appears to be no change in pressure when twisting the graft through 0 to 180 degrees. Creating slack in the system produced no change in pressure across the graft as well. Pressure values for all grafts tested can be found in Appendix A along with their corresponding graphs.

Catastrophic failure was achieved at 460 degrees of twist. When this occurred, flow was obstructed due to excessive warping of the tube surface, and leakage through the graft's wall was excessive (**Figure 33**). **Figure 34** is the photographic representation of the warped graft prior to the catastrophic failure. This degree of twist is too extreme and is unlikely to exist in an implanted graft.

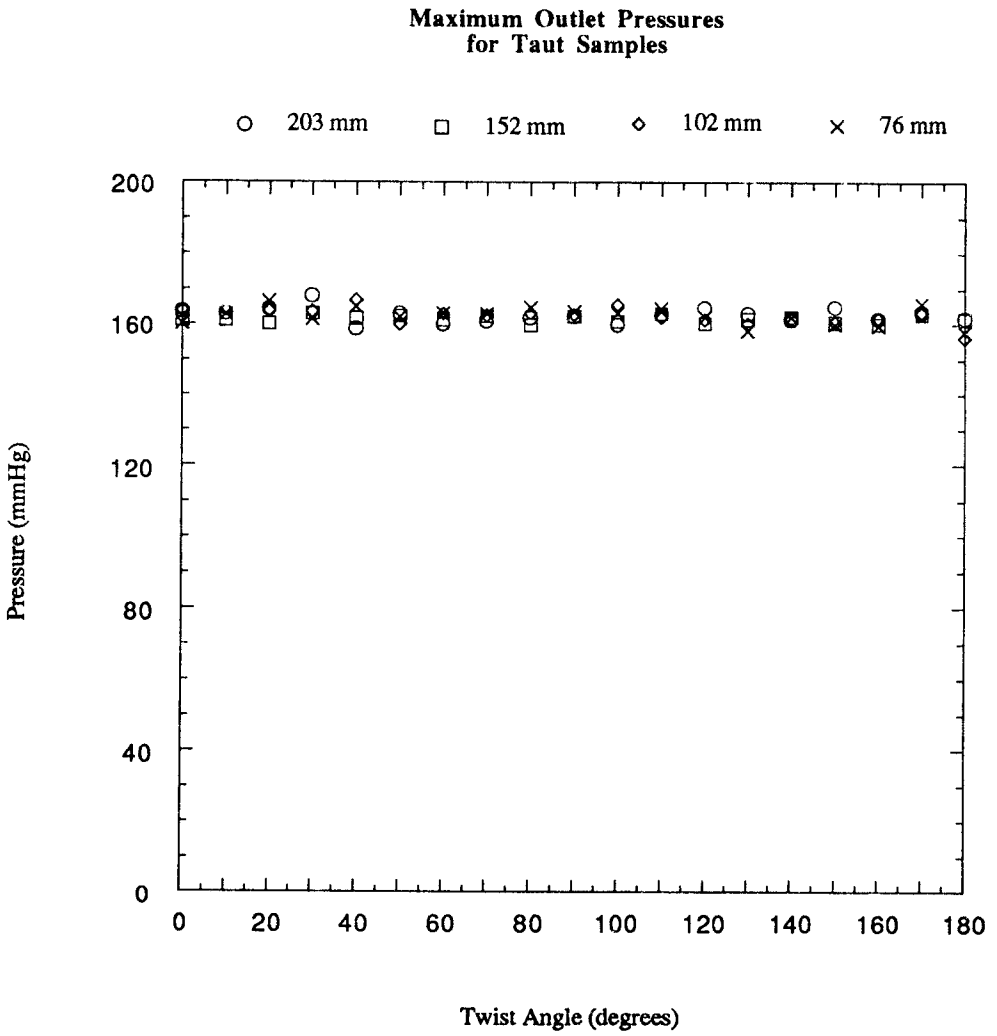

Figure 31 Maximum Outlet Pressure Obtained for a Taut Sample

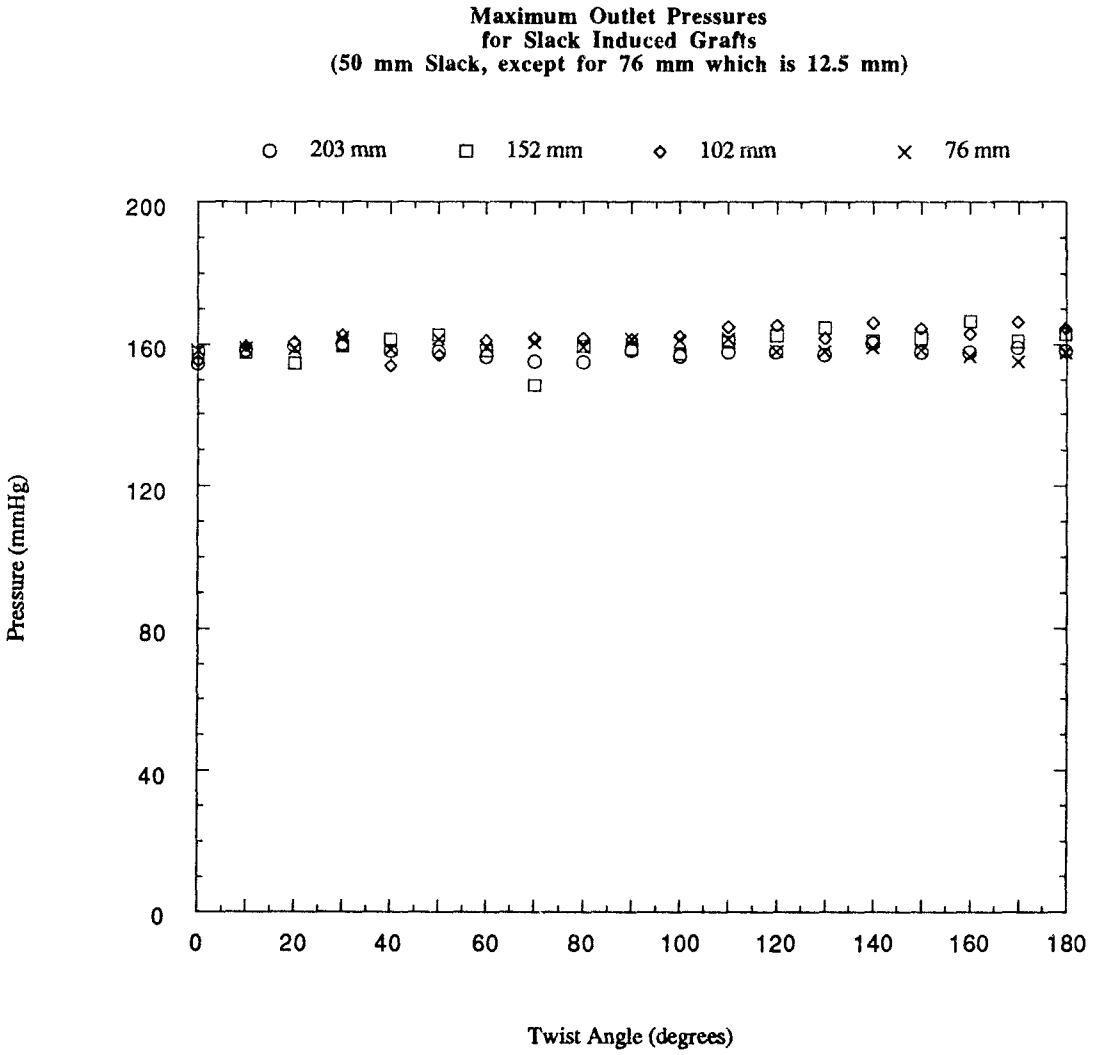

Figure 32 Maximum Outlet Pressure Obtained for a Sample With Slack Induced

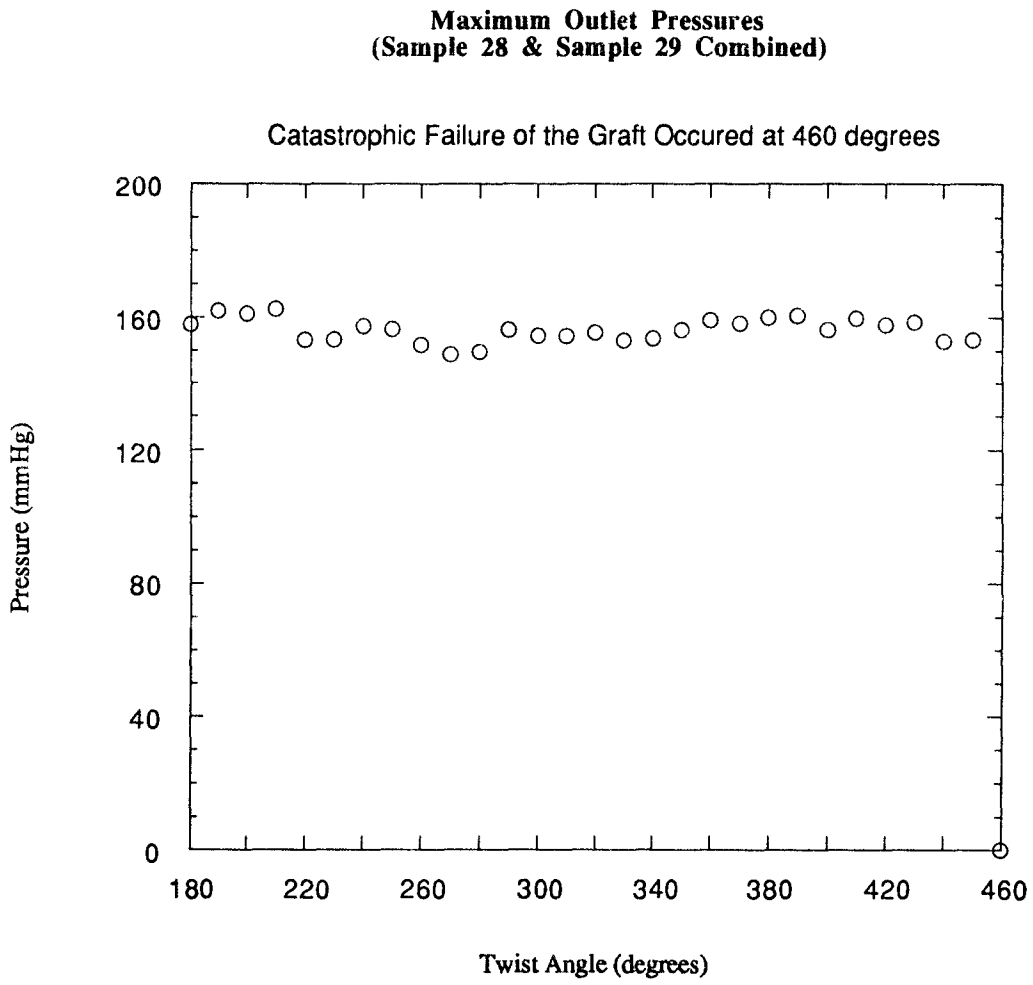

Figure 33 Maximum Pressures - Catastrophic Failure Occurring

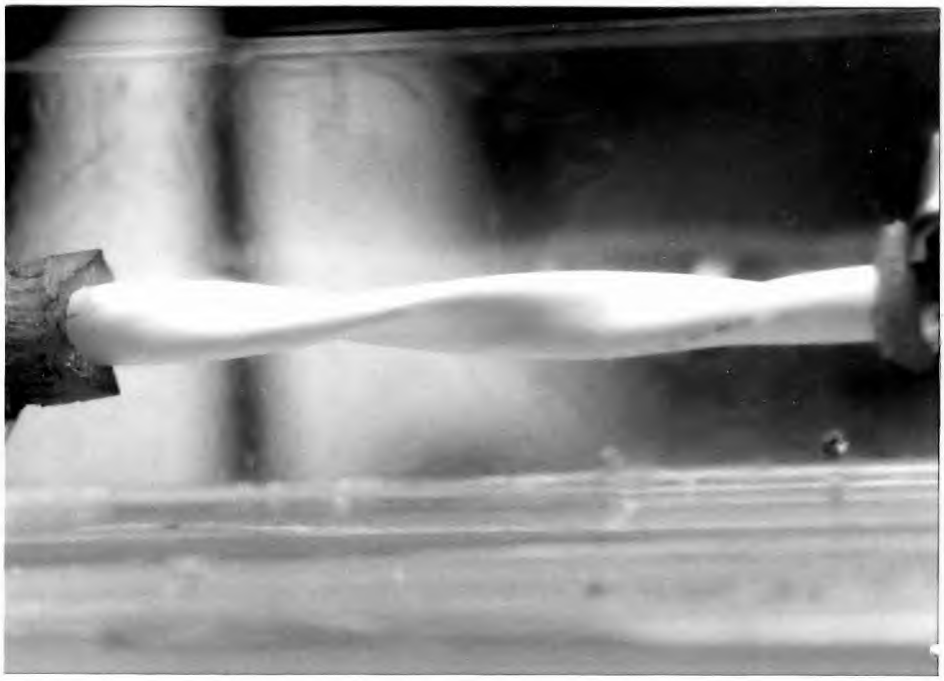

Figure 34 Teflon Graft (460 Degrees of Twist)

Prior to Catastrophic Failure

Note excessive warping of graft

V. CONCLUSION

At the elevated pressures tested, twisting ePTFE vascular grafts through 180 degrees appears to have no effect on function as measured by these pressure flow relationships. There were no adverse effects when using shorter test segments in taut or slack configurations. These observations indicate that it may be possible to twist a graft in a human subject without any detrimental effects to the patient. Further testing of the grafts is suggested. These results will serve as a basis for future research which will focus on the changes in the flow profiles due to twisting of the vascular grafts.

It was observed during testing that the twisted graft would collapse on itself during the period when the piston was creating was returning from its full stroke position to its neutral position (creating a negative pressure). The graft would balloon outward and swell during the positive stroke of the piston (the period in which the main pressure pulse is occurring, reference **Figure 30**). This action of collapsing and ballooning could cause the fatigue failure of the graft over time. The NJIT Flow Loop system is capable of performing a fatigue test.

VI. RECOMMENDATIONS FOR FUTURE RESEARCH

In order to reestablish a functioning NJIT flow loop system, we remanufactured the equipment and investigated pressure differences across vascular grafts. This research has established a foundation for continuing graft research using the NJIT Biofluids Laboratory. The following paragraphs list some recommendations for future research which would expand upon the research performed for this thesis. System pressures should be corrected as mentioned previously in **Section IV-2.**

Future investigators should examine the flow across the graft. This can be accomplished with equipment in the laboratory. The first method for determining flow across the graft makes use of the Disa anamometry equipment. Hot wire probes, as opposed to hot film probes, could be used; however these require a more delicate technique since the wire which runs across the probe is extremely small in diameter. These wires tend to break sooner than their hot film counterparts. The Plexiglass holding fixture and tube for the hot film probe must be remanufactured. Despite repeated attempts to repair this fixture, the Plexiglass has become too brittle over time.

The second technique for measuring flow involves the use of the pulse doppler machine on loan to the Biofluids Laboratory by Dr. Frank T. Padberg, Jr. of the VA Hospital, East Orange, NJ. This testing technique will require some training before using the pulse doppler machine. In order to perform such tests while using distilled

water in the flow loop, machining oil will have to be added to the system. This oil breaks up into small droplets, and causes the signal sent from the transmitter of the doppler probe to be reflected back from the moving fluid and received by the receiver of the probe.

It is recommended that all of the above testing techniques be attempted using distilled water before animal blood is utilized. The entire test setup will have to be dismantled and cleaned thoroughly at the conclusion of each test. Using blood will require the use of anticoagulants, such as heparin, and careful handling techniques in order to avoid any bacteria, etc. which may be present in the blood.

After the program was written and data was being collected, the Metrabyte technical support staff was generous enough to provide diskettes containing programs which can access the eight channel A/D board in Pascal, Fortran, and C. Depending on the discretion of future researchers, the present program created for this project may be converted into any of the latter programs. If all eight channels are used in the future, it would be advisable to create a program written in C. Doing such would increase the speed at which the A/D board is accessed.

APPENDIX

TABLES AND GRAPHS OF DATA COLLECTED

TABLE VI MAXIMUM PRESSURES - SAMPLES 0 & 1
Sample 0, Sample 1

Plastic Tubing (Length = 304.8 mm, Slack = 0 mm)				
Twist Angle (degrees)	Max. Inlet Pressure (mmHg)	Max. Outlet Pressure (mmHg)	Max. Delta Pressure (mmHg)	Max. Work ($mmHg \cdot m^3$)
0	228.2, 222.2	168.6, 164.8	56.4, 56.6	0.0018, 0.0018
10	227.7, 219.5	169.7, 164.8	52.8, 50.8	0.0017, 0.0017
20	227.2, 218.9	170.8, 165.7	51.9, 51.0	0.0017, 0.0017
30	226.6, 217.8	172.8, 165.5	51.0, 49.9	0.0017, 0.0016
40	225.0, 220.6	171.9, 164.3	49.4, 51.5	0.0016. 0.0017
50	224.4, 223.9	167.0, 167.9	51.1, 50.4	0.0017, 0.0016
60	227.2, 224.4	170.6, 169.0	51.9, 51.2	0.0017, 0.0017
70	221.1, 220.6	167.9, 167.2	50.5, 48.6	0.0016, 0.0016
80	224.4, 220.0	170.8, 166.1	48.9, 51.4	0.0016, 0.0017
90	219.5, 221.7	167.9, 167.5	51.0, 48.6	0.0017, 0.0016
100	223.9, 225.0	169.2, 168.1	51.5, 50.8	0.0017, 0.0017
110	226.1, 225.0	172.1, 168.4	49.9, 52.8	0.0016, 0.0017
120	225.0, 225.0	171.0, 169.0	50.5, 52.6	0.0016, 0.0017
130	227.2, 223.9	172.6, 167.5	50.8, 54.4	0.0017, 0.0018
140	225.5, 225.5	170.6, 169.0	52.4, 50.5	0.0017, 0.0016
150	224.4, 218.4	167.0, 164.3	54.4, 51.1	0.0018, 0.0017
160	218.9, 222.2	165.2, 165.9	50.2, 54.1	0.0016, 0.0018
170	226.1, 220.0	171.3, 164.8	50.6, 53.3	0.0016, 0.0017
180	223.3, 226.1	168.6, 168.8	51.2, 52.7	0.0017, 0.0017
Reference **Figure 35** (next page) for a graph of maximum outlet pressures				

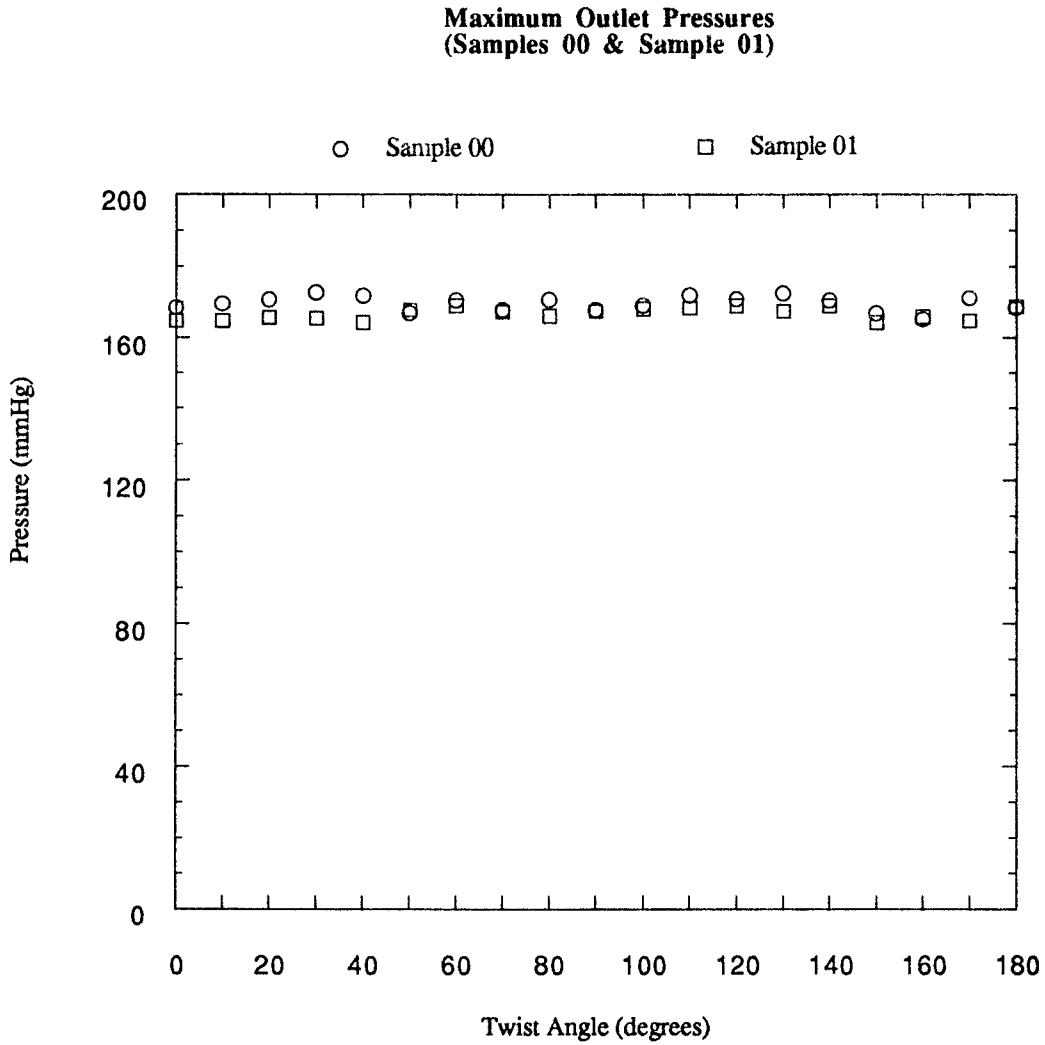

Figure 35 Maximum Outlet Pressures for Sample 00 & Sample 01

TABLE VII MAXIMUM PRESSURES - SAMPLES 2 & 3
Sample 2, Sample 3

Teflon Vascular Graft (Length = 152.4 mm, Slack = 0 mm)

Twist Angle (degrees)	Max. Inlet Pressure (mmHg)	Max. Outlet Pressure (mmHg)	Max. Delta Pressure (mmHg)	Max. Work ($mmHg \cdot m^3$)
0	210.12, 231.00	165.01, 173.71	40.18, 52.10	0.0008, 0.0011
10	216.71, 226.05	170.14, 171.03	47.32, 52.60	0.0010, 0.0011
20	217.81, 228.25	170.36, 173.26	53.29, 52.88	0.0011, 0.0011
30	217.26, 230.45	171.03, 172.81	46.67, 56.75	0.0010, 0.0012
40	209.57, 231.55	165.01, 172.14	41.84, 58.93	0.0009, 0.0012
50	216.16, 231.00	169.02, 173.48	52.95, 53.50	0.0011, 0.0011
60	217.81, 231.55	169.69, 173.71	49.00, 57.25	0.0010, 0.0012
70	218.91, 223.85	170.36, 166.35	50.46, 55.46	0.0010, 0.0011
80	215.06, 229.90	168.35, 171.25	43.58, 57.30	0.0009, 0.0012
90	216.16, 229.90	169.02, 171.03	45.39, 58.55	0.0009, 0.0012
100	211.76, 225.50	167.91, 168.35	40.48, 55.60	0.0008, 0.0011
110	217.26, 227.70	170.14, 166.57	51.42, 58.14	0.0011, 0.0012
120	216.71, 225.50	168.35, 167.69	56.40, 56.51	0.0012, 0.0012
130	215.06, 225.50	167.91, 167.69	45.34, 57.19	0.0009, 0.0012
140	216.71, 228.80	169.25, 170.81	50.53, 56.91	0.0010, 0.0012
150	219.46, 231.00	171.48, 172.81	47.66, 55.28	0.0010, 0.0011
160	213.41, 227.70	166.79, 170.81	41.54, 54.57	0.0009, 0.0011
170	215.06, 232.64	167.91, 175.04	45.63, 53.81	0.0009, 0.0011
180	212.31, 229.35	166.12, 173.26	42.14, 53.80	0.0009, 0.0011

Reference **Figure 36** (next page) for graph of maximum outlet pressures

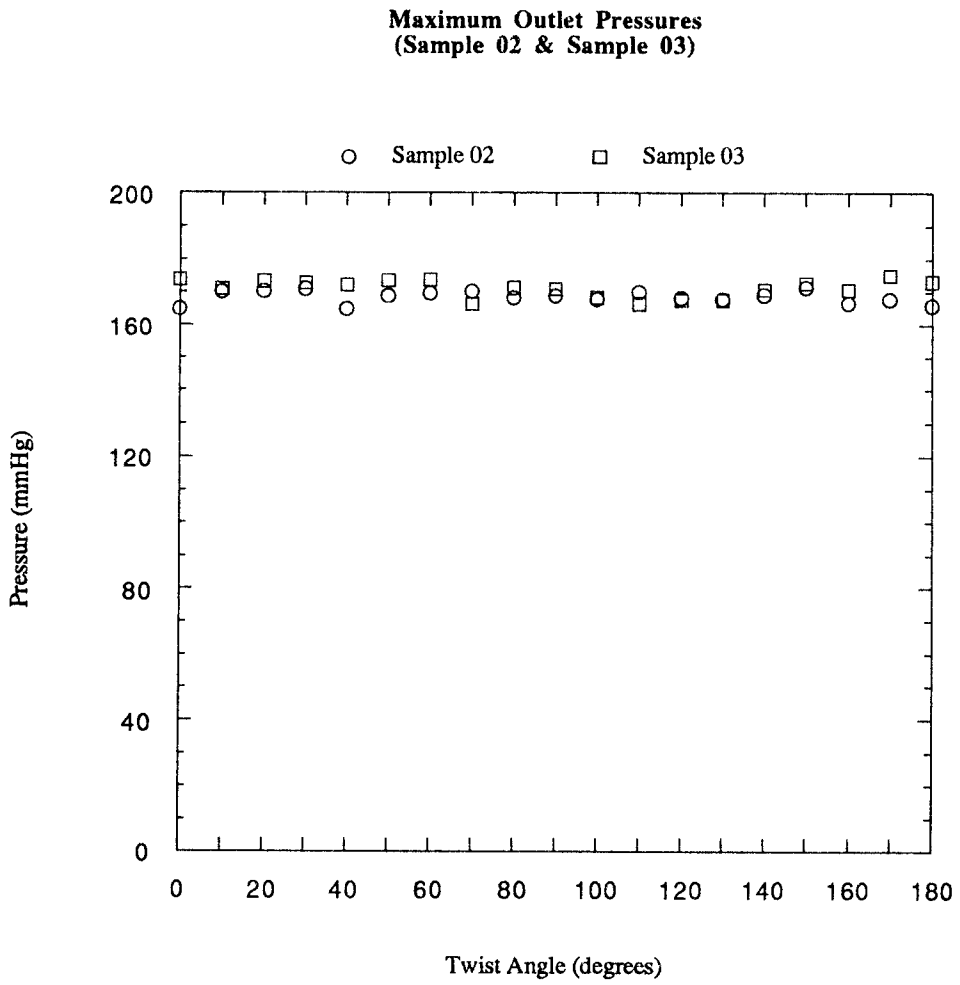

Figure 36 Maximum Outlet Pressures for Sample 02 & Sample 03

TABLE VIII MAXIMUM PRESSURES - SAMPLE 4

Teflon Vascular Graft (Length = 76.2 mm, Slack = 0 mm)

Twist Angle (degrees)	Max. Outlet Pressure (mmHg)	Max. Inlet Pressure (mmHg)	Max. Delta Pressure (mmHg)	Max. Work ($mmHg \cdot m^3$)
0	221.11	167.46	49.66	0.0007
10	222.75	172.59	46.21	0.0007
20	224.95	175.27	45.94	0.0007
30	221.66	173.48	44.55	0.0006
40	226.60	177.05	44.88	0.0006
50	225.50	175.49	45.54	0.0007
60	224.95	175.71	44.82	0.0006
70	218.36	171.70	44.13	0.0006
80	228.25	178.61	47.40	0.0007
90	217.26	169.02	46.01	0.0007
10	221.11	172.37	44.00	0.0006
11	222.75	174.38	44.14	0.0006
12	224.40	175.49	46.93	0.0007
13	222.20	173.93	45.17	0.0007
14	219.46	172.59	44.83	0.0006
15	222.75	174.38	45.33	0.0007
16	225.05	175.71	46.15	0.0007
17	227.15	176.83	48.21	0.0007
18	223.30	175.04	46.69	0.0007

Reference **Figure 37** (next page) for graph of maximum outlet pressures

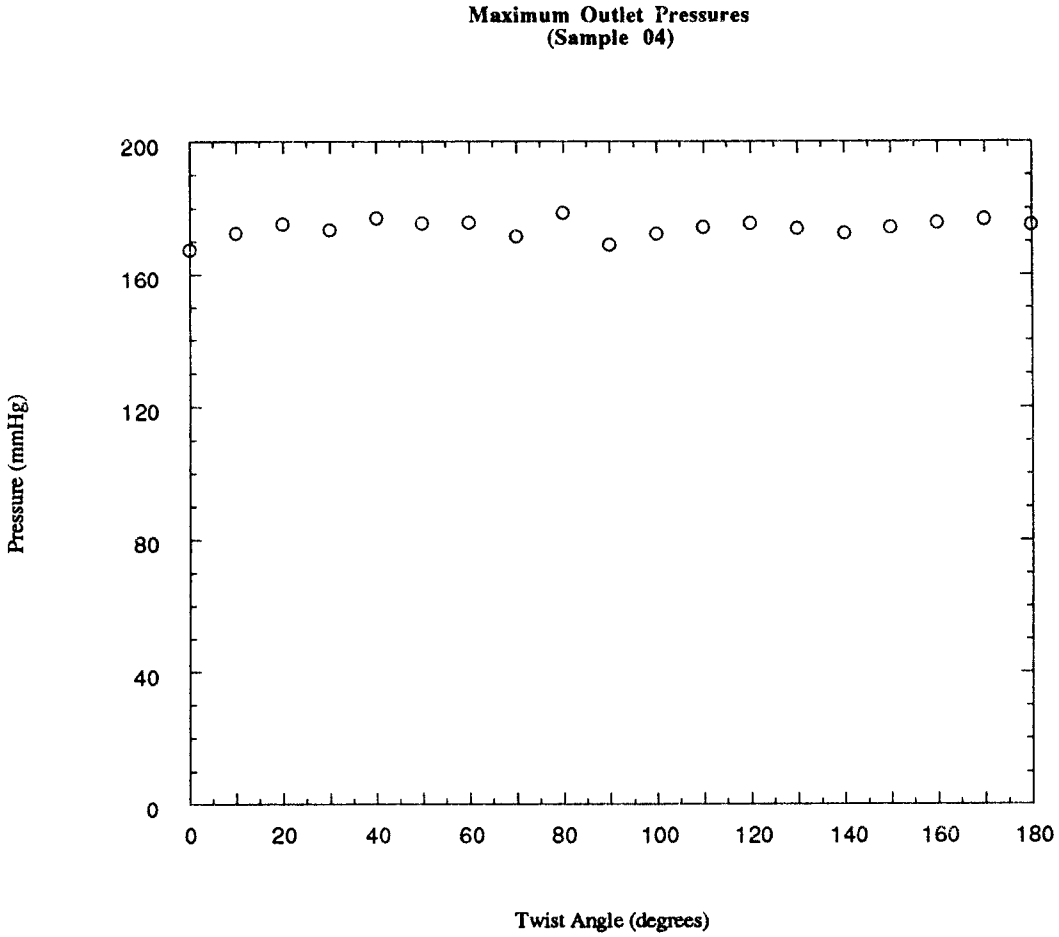

Figure 37 Maximum Outlet Pressure for Sample 04

TABLE IX MAXIMUM PRESSURES - SAMPLES 5, 8, & 18
Sample 5, Sample 8, Sample 18

Teflon Vascular Graft (Length = 203.2 mm, Slack = 0 mm)				
Twist Angle (degrees)	Max. Inlet Pressure (mmHg)	Max. Outlet Pressure (mmHg)	Max. Delta Pressure (mmHg)	Max. Work ($mmHg \cdot m^3$)
0	210.12, 222.20, 219.46	163.67, 164.56, 161.44	40.32, 53.85, 55.11	0.0010, 0.0013, 0.0013
10	210.12, 220.01, 226.05	163.00, 165.01, 165.68	41.70, 51.55, 55.48	0.0010, 0.0013, 0.0014
20	211.21, 217.81, 223.85	164.34, 165.45, 166.79	42.15, 50.89, 56.76	0.0010, 0.0012, 0.0014
30	215.06, 217.26, 226.60	168.13,,157.20, 170.36	44.31, 56.62, 52.56	0.0011, 0.0014, 0.0013
40	209.57, 212.86, 221.66	158.77, 159.21, 168.13	44.93, 50.93, 55.50	0.0011. 0.0012, 0.0014
50	213.96, 220.56, 226.05	163.00, 165.68, 165.90	46.62, 55.07, 54.71	0.0011, 0.0013. 0.0013
60	205.72, 220.01, 223.85	160.10, 164.56, 166.35	42.87, 51.99, 53.06	0.0010, 0.0013, 0.0013
70	207.37, 220.01, 220.56	161.00, 165.01, 165.23	42.37, 51.13, 52.10	0.0010, 0.0013, 0.0013
80	210.12, 216.16, 223.85	161.89, 157.87, 168.80	42.22, 56.05, 53.49	0.0010, 0.0014, 0.0013
90	209.57, 217.26, 221.66	162.33, 161.00, 165.23	43.78, 54.08, 54.95	0.0011, 0.0013, 0.0013
100	206.27, 220.01, 221.11	159.88, 162.78, 165.68	40.16, 52.10, 50.86	0.0010, 0.0013, 0.0012
110	209.57, 212.86, 224.40	162.78, 159.43, 167.69	42.67, 50.94, 57.39	0.0010, 0.0012, 0.0014
120	213.41, 218.91, 225.50	164.79, 162.56, 169.02	45.31, 51.67, 51.59	0.0011, 0.0013, 0.0013
130	211.21, 215.06, 222.75	163.00, 160.10, 167.46	44.76, 51.42, 51.07	0.0011, 0.0013, 0.0012
140	206.82, 218.36, 223.85	161.44, 163.00, 167.46	42.71, 52.84, 52.60	0.0010, 0.0013, 0.0013
150	211.76, 213.96, 224.95	165.01, 161.89, 167.69	43.54, 51.63, 54.50	0.0011, 0.0013, 0.0013
160	212.31, 217.81, 226.60	161.66, 163.23, 169.47	43.96, 50.84, 52.94	0.0011, 0.0012, 0.0013
170	210.12, 219.46, 221.66	163.67, 163.00, 166.57	42.32, 53.54, 52.20	0.0010, 0.0013, 0.0013
180	208.47, 220.56, 222.75	161.89, 164.79, 166.57	42.80, 52.20, 51.94	0.0010, 0.0013, 0.0013
Reference **Figure 38** (next page) for graph of maximum outlet pressures				

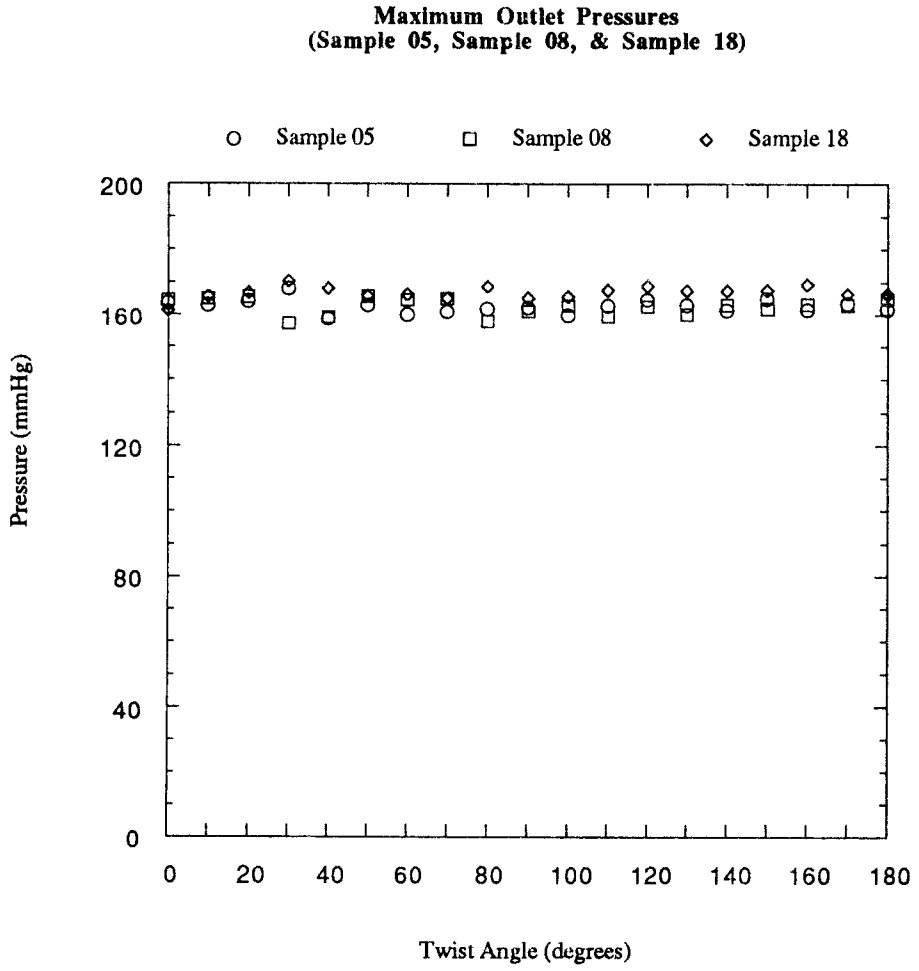

Figure 38 Maximum Outlet Pressures for Sample 05, Sample 08, & Sample 18

TABLE X MAXIMUM PRESSURES - SAMPLES 6, 14, 24
Sample 6, Sample 14, Sample 24

Teflon Vascular Graft (Length = 101.6 mm, Slack = 0 mm)

Twist Angle (degrees)	Max. Inlet Pressure (mmHg)	Max. Outlet Pressure (mmHg)	Max. Delta Pressure (mmHg)	Max. Work (mmHg . m^3)
0	202.42, 218.91, 224.95	161.00, 164.56, 158.77	36.46, 52.53, 61.77	0.0006, 0.0009, 0.0010
10	199.67, 221.11, 228.80	161.00, 168.35, 162.33	33.94, 47.96, 62.35	0.0006, 0.0008, 0.0010
20	198.03, 218.91, 226.60	160.10, 166.79, 161.89	35.60, 52.76, 59.58	0.0006, 0.0009, 0.0010
30	202.97, 217.26, 226.60	163.00, 167.69, 162.78	37.08, 46.89, 57.83	0.0006, 0.0008, 0.0009
40	204.07, 220.01, 227.15	161.66, 166.79, 163.89	40.84, 48.70, 58.12	0.0007, 0.0008, 0.0010
50	202.97, 217.26, 223.85	162.33, 164.56, 154.75	38.30, 51.73, 64.77	0.0006, 0.0008, 0.0011
60	203.52, 220.01, 227.15	161.22, 168.58, 155.87	37.67, 47.43, 66.53	0.0006, 0.0008, 0.0011
70	204.62, 216.71, 226.05	162.33, 167.46, 156.31	38.06, 44.34, 64.16	0.0006, 0.0007, 0.0011
80	200.77, 216.71, 223.85	159.66, 164.12, 157.43	37.01, 48.13, 62.63	0.0006, 0.0008, 0.0010
90	205.72, 218.36, 222.75	162.33, 166.12, 158.10	41.39, 47.24, 58.89	0.0007, 0.0008, 0.0010
100	203.52, 218.91, 223.30	160.77, 168.13, 153.19	38.44, 50.33, 64.45	0.0006, 0.0008, 0.0011
110	206.27, 217.81, 222.75	163.00, 167.69, 153.41	39.07, 53.34, 66.16	0.0006, 0.0009, 0.0011
120	201.87, 218.36, 222.75	160.33, 169.47, 154.97	37.89, 45.01, 63.33	0.0006, 0.0007, 0.0010
130	208.47, 218.91, 224.40	161.44, 165.90, 161.44	43.38, 46.78, 58.63	0.0007, 0.0008, 0.0010
140	211.21, 216.71, 221.66	162.11, 166.35, 155.20	43.77, 46.91, 61.45	0.0007, 0.0008, 0.0010
150	208.47, 217.26, 223.30	160.55, 168.35, 156.76	47.04, 46.02, 62.77	0.0008, 0.0008, 0.0010
160	210.67, 217.81, 222.20	160.10, 167.02, 158.32	49.25, 49.64, 59.68	0.0008, 0.0008, 0.0010
170	211.76, 220.56, 221.66	162.78, 171.25, 154.30	46.01, 45.95, 63.14	0.0008, 0.0008, 0.0010
180	211.76, 216.16, 224.40	161.44, 168.13, 156.76	45.86, 49.84, 63.30	0.0008, 0.0008, 0.0010

Reference **Figure 39** (next page) for graph of maximum outlet pressures

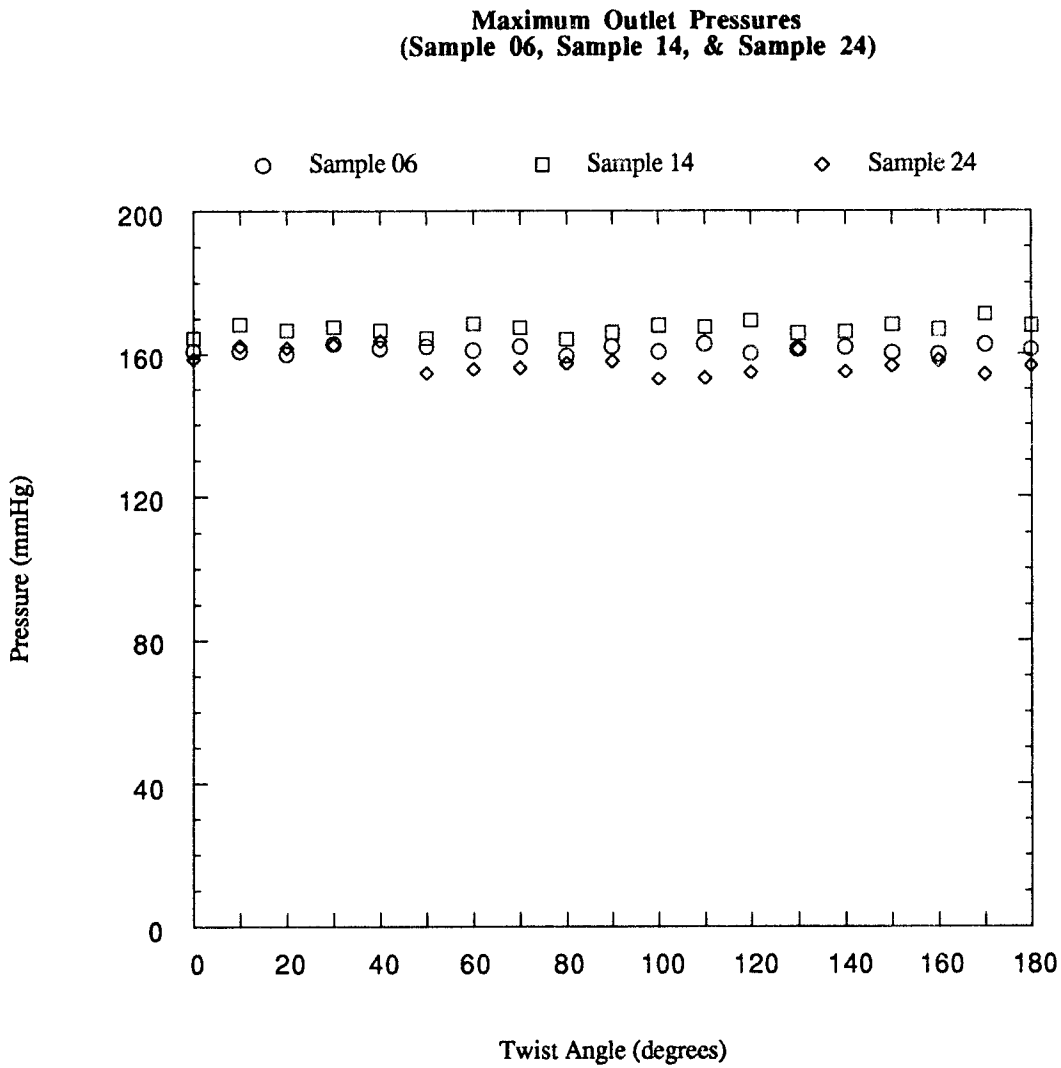

Figure 39 Maximum Outlet Pressures for Sample 06, Sample 14, & Sample 24

TABLE XI MAXIMUM PRESSURES - SAMPLES 7 & 16
Sample 7, Sample 16

Teflon Vascular Graft (Length = 76.2 mm, Slack = 0 mm)

Twist Angle (degrees)	Max. Inlet Pressure (mmHg)	Max. Outlet Pressure (mmHg)	Max. Delta Pressure (mmHg)	Max. Work ($mmHg.m^3$)
0	205.72, 213.41	160.10, 167.46	41.60, 46.96	0.0006, 0.0011
10	209.57, 213.96	162.78, 167.24	42.32, 45.59	0.0006, 0.0011
20	211.21, 213.96	166.57, 167.46	43.32, 42.68	0.0006, 0.0010
30	202.97, 211.76	161.44, 167.69	39.08, 39.20	0.0006, 0.0010
40	209.57, 211.21	165.01, 163.45	42.22, 43.87	0.0006, 0.0011
50	208.47, 211.76	162.11, 165.68	44.69, 44.16	0.0006, 0.0011
60	210.12, 213.41	163.23, 168.13	41.76, 42.50	0.0006, 0.0010
70	206.82, 211.76	163.00, 168.35	40.59, 42.39	0.0006, 0.0010
80	211.21, 214.51	164.79, 168.58	40.76, 43.03	0.0006, 0.0011
90	205.72, 213.41	163.67, 167.46	39.06, 42.04	0.0006, 0.0010
100	210.67, 212.31	163.23, 166.79	42.32, 44.56	0.0006, 0.0011
110	212.86, 206.82	164.56, 164.12	42.72, 43.18	0.0006, 0.0011
120	209.02, 210.12	162.11, 168.35	41.67, 40.16	0.0006, 0.0010
130	204.07, 211.21	158.32, 164.79	42.02, 42.48	0.0006, 0.0010
140	208.47, 208.47	162.11, 164.79	42.59, 43.38	0.0006, 0.0011
150	207.92, 212.31	160.10, 166.35	42.51, 41.33	0.0006, 0.0010
160	205.72, 211.76	159.66, 167.24	42.73, 43.34	0.0006, 0.0011
170	215.61, 216.16	165.90, 170.36	45.69, 40.44	0.0007, 0.0010
180	207.37, 209.57	157.87, 165.23	47.04, 43.78	0.0007, 0.0011

Reference **Figure 40** (next page) for graph of maximum outlet pressures

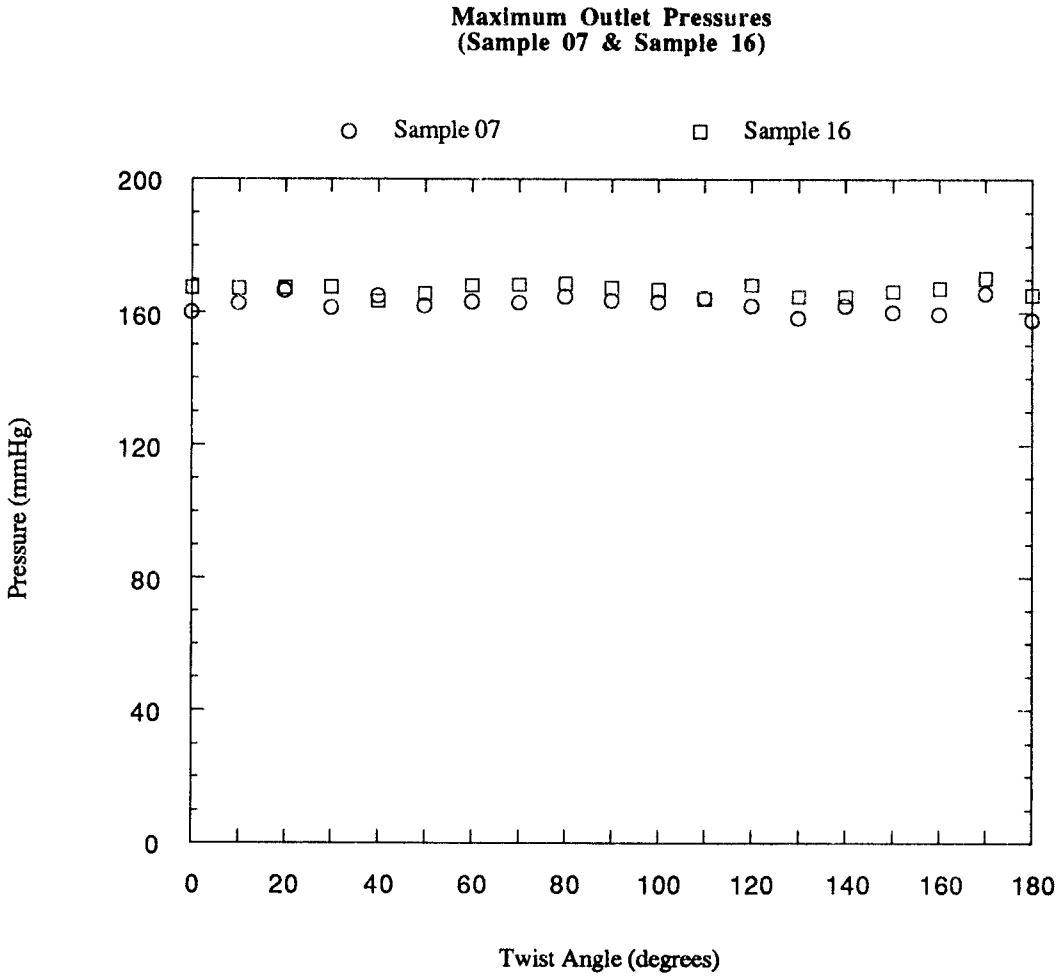

Figure 40 Maximum Outlet Pressures for Sample 07 & Sample 16

TABLE XII MAXIMUM PRESSURES - SAMPLES 9 & 19
Sample 9, Sample 19

Teflon Vascular Graft (Length = 203.2, Slack = 25.4 mm)

Twist Angle (degrees)	Max. Inlet Pressure (mmHg)	Max. Outlet Pressure (mmHg)	Max. Delta Pressure (mmHg)	Max. Work ($mmHg.m^3$)
0	215.61, 222.20	154.75, 163.23	57.37, 56.44	0.0013, 0.0013
10	218.91, 220.56	158.54, 162.56	57.53, 53.98	0.0013, 0.0012
20	217.26, 221.11	159.66, 162.78	58.05, 53.31	0.0013, 0.0012
30	220.01, 224.40	160.33, 166.12	54.10, 54.10	0.0012, 0.0012
40	216.16, 220.01	158.32, 159.43	54.95, 54.22	0.0012, 0.0012
50	219.46, 222.75	158.10, 162.11	57.46, 55.30	0.0013, 0.0012
60	216.16, 221.66	156.76, 161.22	56.84, 55.97	0.0013, 0.0013
70	214.51, 221.11	155.42, 162.78	55.76, 54.00	0.0013, 0.0012
80	216.71, 223.30	155.20, 164.12	55.97, 53.61	0.0013, 0.0012
90	218.36, 222.75	158.54, 160.55	55.80, 56.63	0.0013, 0.0013
100	217.26, 222.75	156.76, 161.89	55.39, 56.42	0.0012, 0.0013
110	215.61, 224.95	157.87, 165.01	53.62, 56.83	0.0012, 0.0013
120	218.36, 220.01	157.87, 162.11	56.02, 55.68	0.0013, 0.0013
130	215.61, 222.20	157.20, 163.23	54.35, 55.85	0.0012, 0.0013
140	222.20, 218.36	160.55, 161.00	57.22, 53.14	0.0013, 0.0012
150	221.11, 223.85	157.87, 163.45	58.01, 54.95	0.0013, 0.0012
160	218.91, 218.91	157.87, 161.44	59.02, 53.24	0.0013, 0.0012
170	222.20, 220.01	159.21, 161.44	60.66, 53.45	0.0014, 0.0012
180	219.46, 224.95	158.32, 165.90	56.35, 55.48	0.0013, 0.0012

Reference **Figure 41** (next page) for graph of maximum outlet pressures

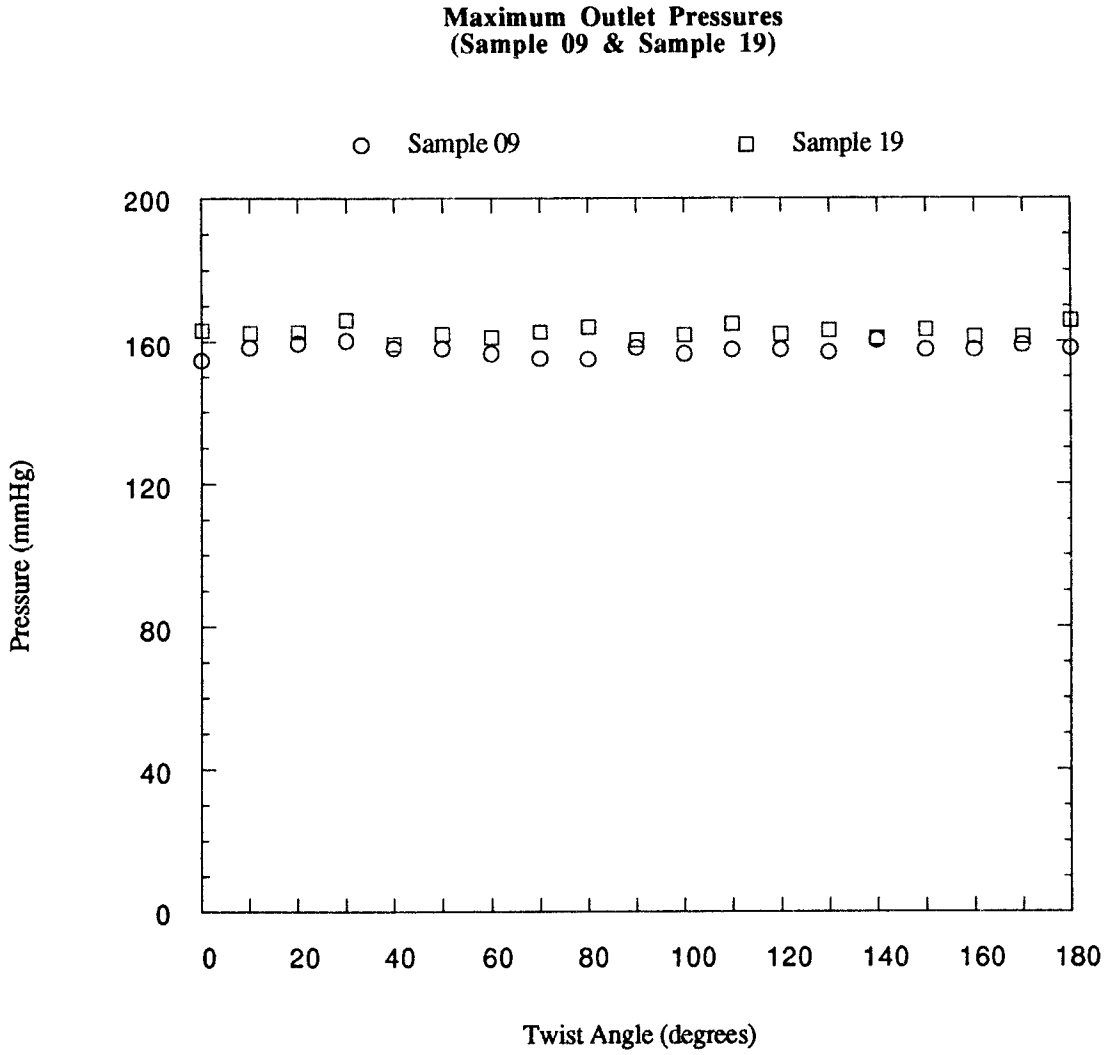

Figure 41 Maximum Outlet Pressures for Sample 09 & Sample 19

TABLE XIII MAXIMUM PRESSURES - SAMPLES 10 & 20
Sample 10, Sample 20

Teflon Vascular Graft (Length = 203.2 mm, Slack = 50.8 mm)

Twist Angle (degrees)	Max. Inlet Pressure (mmHg)	Max. Outlet Pressure (mmHg)	Max. Delta Pressure (mmHg)	Max. Work ($mmHg.m^3$)
0	218.36, 224.40	155.20, 158.54	57.93, 61.29	0.0012, 0.0013
10	223.85, 221.11	160.77, 157.20	59.41, 62.58	0.0012, 0.0013
20	221.11, 225.50	158.99, 162.33	57.65, 61.72	0.0012, 0.0013
30	218.91, 226.05	155.87, 164.79	60.62, 60.66	0.0012, 0.0012
40	223.85, 225.50	160.33, 163.67	59.85, 60.45	0.0012, 0.0012
50	223.85, 227.70	159.21, 163.45	58.84, 58.71	0.0012, 0.0012
60	221.11, 227.15	158.54, 163.45	61.00, 62.81	0.0012, 0.0013
70	224.95, 225.50	160.55, 165.23	58.84, 59.68	0.0012, 0.0012
80	226.05, 225.50	162.33, 158.54	58.84, 63.28	0.0012, 0.0013
90	224.95, 226.60	159.88, 160.33	61.29, 61.48	0.0013, 0.0013
100	222.20, 223.30	157.87, 159.66	59.11, 58.53	0.0012, 0.0012
110	223.85, 226.05	159.21, 163.23	61.29, 63.77	0.0013, 0.0013
120	226.05, 222.20	160.77, 161.44	59.82, 58.53	0.0012, 0.0012
130	220.56, 225.50	156.54, 162.56	58.79, 57.71	0.0012, 0.0012
140	225.50, 224.40	159.21, 162.56	61.16, 57.52	0.0013, 0.0012
150	221.66, 226.60	156.98, 164.34	61.33, 60.52	0.0013, 0.0012
160	222.20, 227.70	157.65, 165.01	60.31, 56.82	0.0012, 0.0012
170	222.20, 226.60	158.32, 163.89	58.08, 56.48	0.0012, 0.0012
180	227.70, 226.60	160.77, 165.01	60.68, 59.14	0.0012, 0.0012

Reference **Figure 42** (next page) for graph of maximum outlet pressures

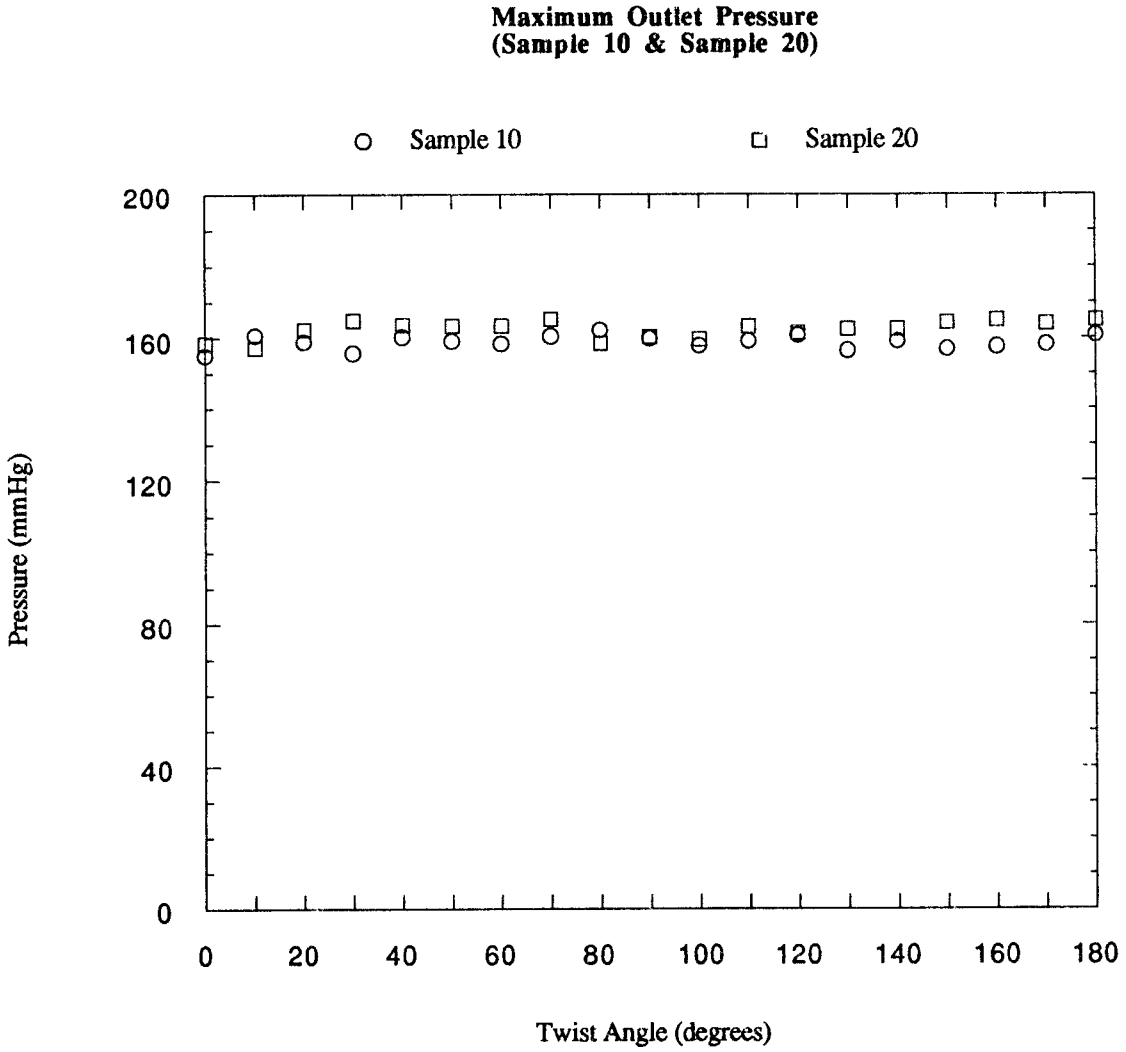

Figure 42 Maximum Outlet Pressures for Sample 10 & Sample 20

TABLE XIV MAXIMUM PRESSURES - SAMPLES 11 & 21
Sample 11, Sample 21

Teflon Vascular Graft (Length = 152.4 mm, Slack = 0 mm)

Twist Angle (degrees)	Max. Inlet Pressure (mmHg)	Max. Outlet Pressure (mmHg)	Max. Delta Pressure (mmHg)	Max. Work ($mmHg.m^3$)
0	223.85, 226.05	163.89, 165.23	56.40, 58.81	0.0012, 0.0012
10	220.56, 228.80	163.89, 168.13	53.55, 56.67	0.0011, 0.0012
20	220.56, 222.75	163.89, 165.90	51.20, 54.17	0.0010, 0.0011
30	220.56, 227.70	163.67, 167.02	52.76, 57.37	0.0011, 0.0012
40	219.46, 226.05	167.02, 167.46	51.67, 55.69	0.0011, 0.0011
50	218.36, 226.60	160.10, 167.69	57.11, 54.79	0.0012, 0.0011
60	222.20, 226.60	163.00, 170.14	59.56, 54.71	0.0012, 0.0011
70	218.36, 226.60	162.56, 169.92	51.12, 52.68	0.0010, 0.0011
80	216.16, 225.50	163.23, 170.36	53.43, 52.70	0.0011, 0.0011
90	222.20, 224.95	162.78, 168.58	54.53, 52.91	0.0011, 0.0011
100	225.50, 227.15	165.68, 170.14	57.38, 52.22	0.0012, 0.0011
110	218.36, 224.95	162.11, 169.47	54.36, 50.47	0.0011, 0.0010
120	215.06, 226.60	161.44, 169.92	52.50, 51.98	0.0011, 0.0011
130	214.51, 227.15	160.33, 171.03	51.75, 53.11	0.0011, 0.0011
140	216.71, 223.85	161.66, 170.81	51.03, 51.82	0.0010, 0.0011
150	217.81, 228.25	160.77, 172.81	54.39, 52.89	0.0011, 0.0011
160	218.36, 225.50	161.89, 169.69	52.45. 51.21	0.0011, 0.0010
170	222.20, 227.15	163.45, 170.58	55.42, 51.66	0.0011, 0.0011
180	211.76, 225.50	156.31, 170.58	51.43, 50.78	0.0011, 0.0010

Reference **Figure 43** (next page) for graph of maximum outlet pressures

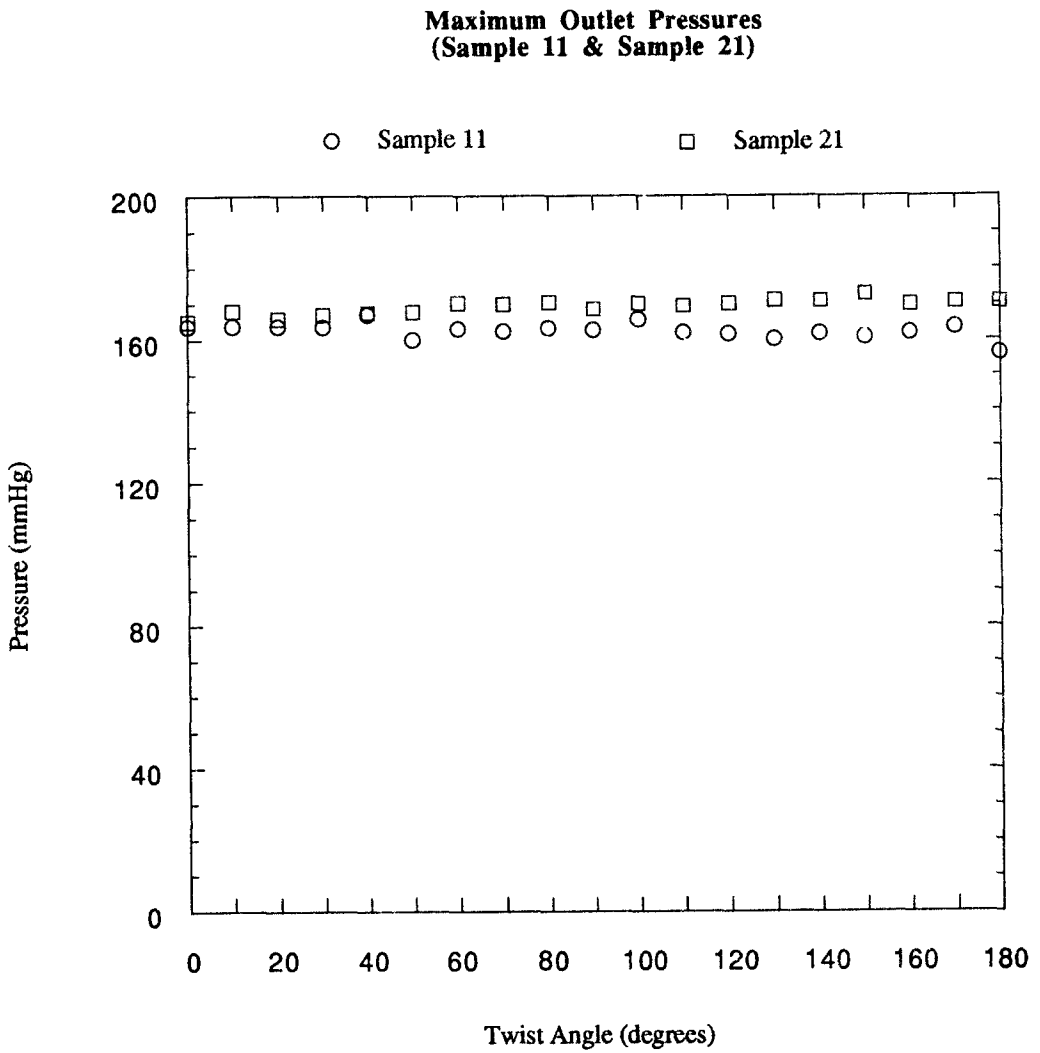

Figure 43 Maximum Outlet Pressures for Sample 11 & Sample 21

TABLE XV MAXIMUM PRESSURES - SAMPLES 12 & 22
Sample 12, Sample 22

Teflon Vascular Graft (Length = 152.4 mm, Slack = 25.4 mm)

Twist Angle (degrees)	Max. Inlet Pressure (mmHg)	Max. Outlet Pressure (mmHg)	Max. Delta Pressure (mmHg)	Max. Work ($mmHg.m^3$)
0	222.20, 224.40	157.65, 159.88	59.88, 68.29	0.0011, 0.0013
10	222.20, 226.60	157.87, 160.77	65.82, 64.75	0.0012, 0.0012
20	214.51, 228.80	154.75, 164.79	61.02, 60.80	0.0011, 0.0011
30	224.40, 227.70	159.66, 164.56	60.18, 62.74	0.0011, 0.0012
40	222.75, 231.00	161.44, 167.46	59.44, 63.24	0.0011, 0.0012
50	224.95, 227.70	162.78, 163.45	60.40, 60.01	0.0011, 0.0011
60	218.36, 229.35	158.32, 165.68	59.38. 58.66	0.0011, 0.0011
70	213.96, 230.45	148.51, 168.35	60.13, 59.21	0.0011, 0.0011
80	224.40, 228.80	159.66, 164.34	60.06, 60.13	0.0011, 0.0011
90	221.66, 228.80	158.99, 164.56	59.71, 58.45	0.0011, 0.0011
100	218.36, 228.80	157.43, 165.90	56.91, 58.67	0.0010, 0.0011
110	222.75, 224.95	160.77, 164.12	61.33, 55.82	0.0011, 0.0010
120	224.40, 228.80	162.56, 165.68	61.12, 59.77	0.0011, 0.0011
130	225.50, 228.25	164.79, 165.01	55.27, 57.46	0.0010, 0.0011
140	222.75, 226.60	161.00, 165.23	55.96, 55.81	0.0010, 0.0010
150	222.75, 231.00	161.89, 167.69	56.85, 57.53	0.0010, 0.0011
160	228.25, 227.15	166.57, 164.12	57.81, 57.69	0.0011, 0.0011
170	220.01, 228.25	161.00, 165.01	61.15, 57.11	0.0011, 0.0011
180	224.40, 227.15	163.00, 165.23	57.28, 58.02	0.0011, 0.0011

Reference **Figure 44** (next page) for graph of maximum outlet pressures

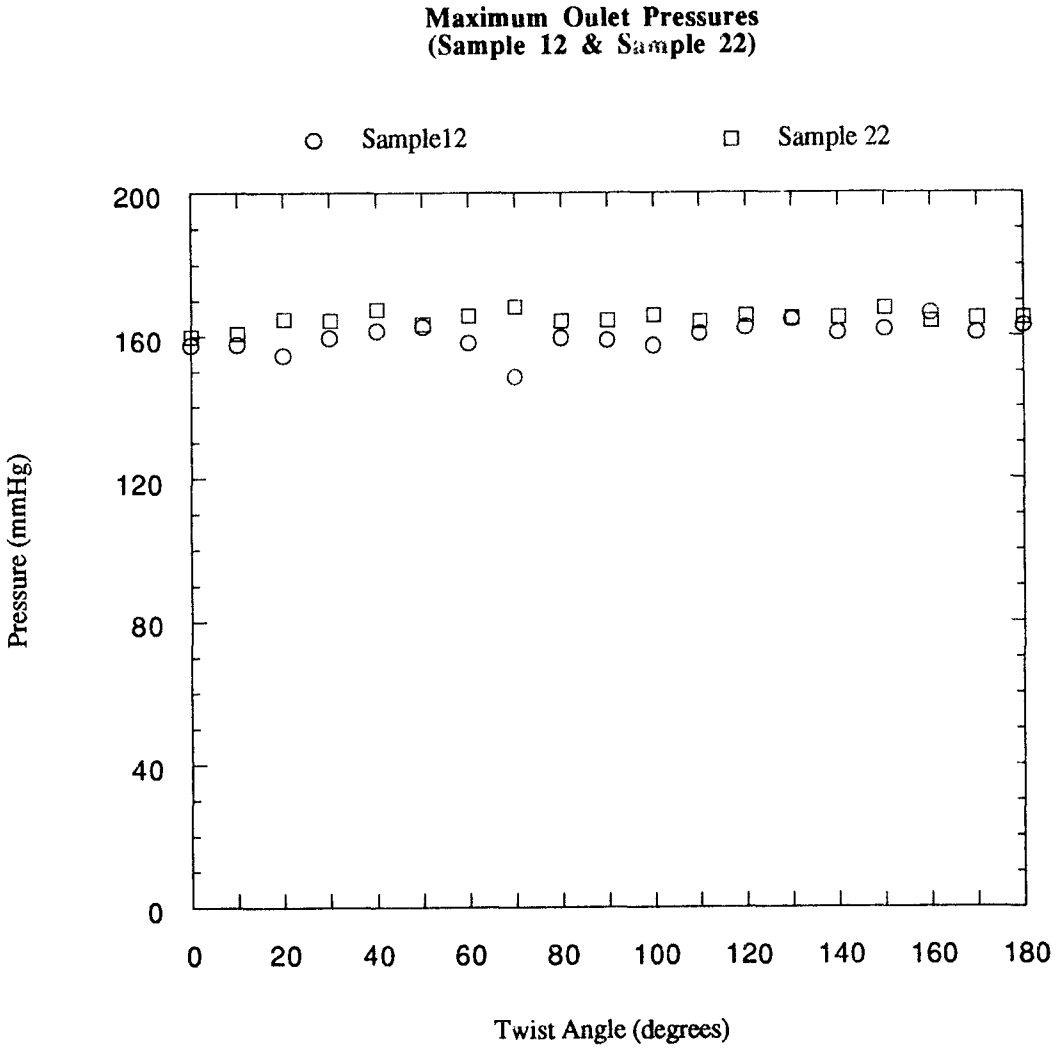

Figure 44 Maximum Outlet Pressures for Sample 12 & Sample 22

TABLE XVI MAXIMUM PRESSURES - SAMPLES 13 & 23
Sample 13, Sample 23

Teflon Vascular Graft (Length = 152.4 mm, Slack = 50.8)

Twist Angle (degrees)	Max. Inlet Pressure (mmHg)	Max. Outlet Pressure (mmHg)	Max. Delta Pressure (mmHg)	Max. Work ($mmHg.m^3$)
0	222.20, 205.72	156.54, 145.16	67.32, 57.45	0.0011, 0.0009
10	227.70, 230.45	159.43, 162.33	62.51, 64.54	0.0010, 0.0011
20	224.40, 228.80	159.43, 160.55	65.24, 62.67	0.0011, 0.0010
30	226.05, 228.80	162.56, 161.22	60.16, 62.67	0.0010, 0.0010
40	226.60, 231.55	162.78, 163.23	59.60, 65.33	0.0010, 0.0011
50	227.70, 226.05	163.23, 158.54	59.79, 63.61	0.0010, 0.0010
60	226.05, 227.15	162.78, 161.00	59.72, 62.58	0.0010, 0.0010
70	225.50, 227.70	161.44, 162.33	58.84, 60.68	0.0010, 0.0010
80	226.60, 228.25	163.45, 162.56	60.70, 61.35	0.0010, 0.0010
90	229.90, 226.60	163.89, 165.23	61.09, 58.47	0.0010, 0.0010
100	226.05, 221.66	160.55, 161.22	59.70, 57.31	0.0010, 0.0009
110	231.00, 224.95	165.01, 163.89	61.52, 56.42	0.0010, 0.0009
120	231.55, 226.60	166.35, 161.22	60.29, 60.47	0.0010, 0.0010
130	230.45, 223.30	165.45, 160.77	58.74, 56.97	0.0010, 0.0009
140	229.90, 226.60	166.57, 164.34	58.54, 57.40	0.0010, 0.0009
150	230.45, 222.75	166.12, 158.99	58.97, 57.98	0.0010, 0.0010
160	229.90, 226.05	163.00, 162.33	61.09, 58.81	0.0010, 0.0010
170	227.15, 204.62	164.12, 147.84	59.02, 61.03	0.0010, 0.0010
180	230.45, 220.01	165.45, 158.32	59.19, 57.02	0.0010, 0.0009

Reference **Figure 45** (next page) for graph of maximum outlet pressures

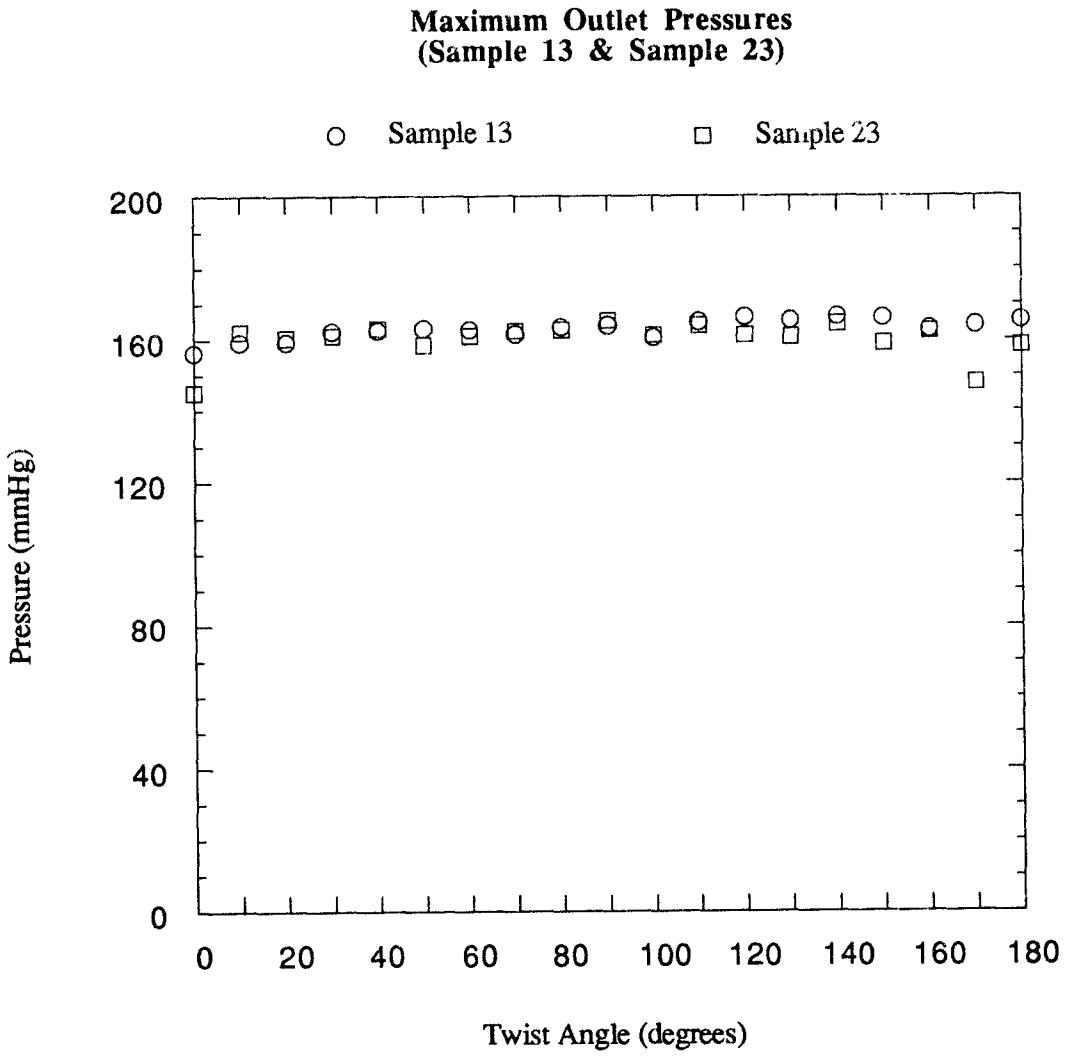

Figure 45 Maximum Outlet Pressures for Sample 13 & Sample 23

TABLE XVII MAXIMUM PRESSURES - SAMPLES 15 & 25
Sample 15, Sample 25

Teflon Vascular Graft (Length = 101.6 mm, Slack = 25.4 mm)

Twist Angle (degrees)	Max. Inlet Pressure (mmHg)	Max. Outlet Pressure (mmHg)	Max. Delta Pressure (mmHg)	Max. Work ($mmHg.m^3$)
0	219.46, 229.35	155.42, 152.52	59.57, 73.06	0.0015, 0.0011
10	224.40, 228.80	159.66, 153.41	64.66, 73.18	0.0016, 0.0011
20	222.75, 229.90	160.77, 156.31	56.08, 70.61	0.0014, 0.0010
30	224.40, 227.70	162.78, 156.54	55.84, 68.60	0.0014, 0.0010
40	220.01, 229.35	154.08, 153.86	62.15, 72.17	0.0015, 0.0010
50	220.01, 229.90	156.98, 154.75	61.05, 71.59	0.0015, 0.0010
60	222.75, 229.90	161.22, 156.76	59.20, 69.27	0.0014, 0.0010
70	222.75, 228.25	161.89, 157.20	55.85, 68.72	0.0014, 0.0010
80	220.01, 227.15	161.89, 157.87	54.33, 66.94	0.0013, 0.0010
90	221.66, 229.90	161.66, 163.23	55.75, 65.81	0.0014, 0.0009
100	220.56, 228.80	162.33, 153.41	54.33, 73.17	0.0013, 0.0011
110	221.11, 228.80	165.01, 154.53	53.42, 71.40	0.0013, 0.0010
120	220.56, 229.90	165.45, 155.87	54.21, 71.33	0.0013, 0.0010
130	218.36, 227.70	161.89, 155.64	51.71, 67.63	0.0013, 0.0010
140	221.11, 229.35	166.12, 152.74	52.76, 73.84	0.0013, 0.0011
150	220.01, 227.15	164.56, 152.74	50.33, 71.40	0.0012, 0.0010
160	217.81, 228.80	163.00, 154.53	50.30, 70.18	0.0012, 0.0010
170	222.20, 227.15	166.35, 156.09	52.56, 68.15	0.0013, 0.0010
180	218.36, 229.35	164.56, 159.66	50.15, 65.59	0.0012, 0.0009

Reference **Figure 46** (next page) for graph of maximum outlet pressures

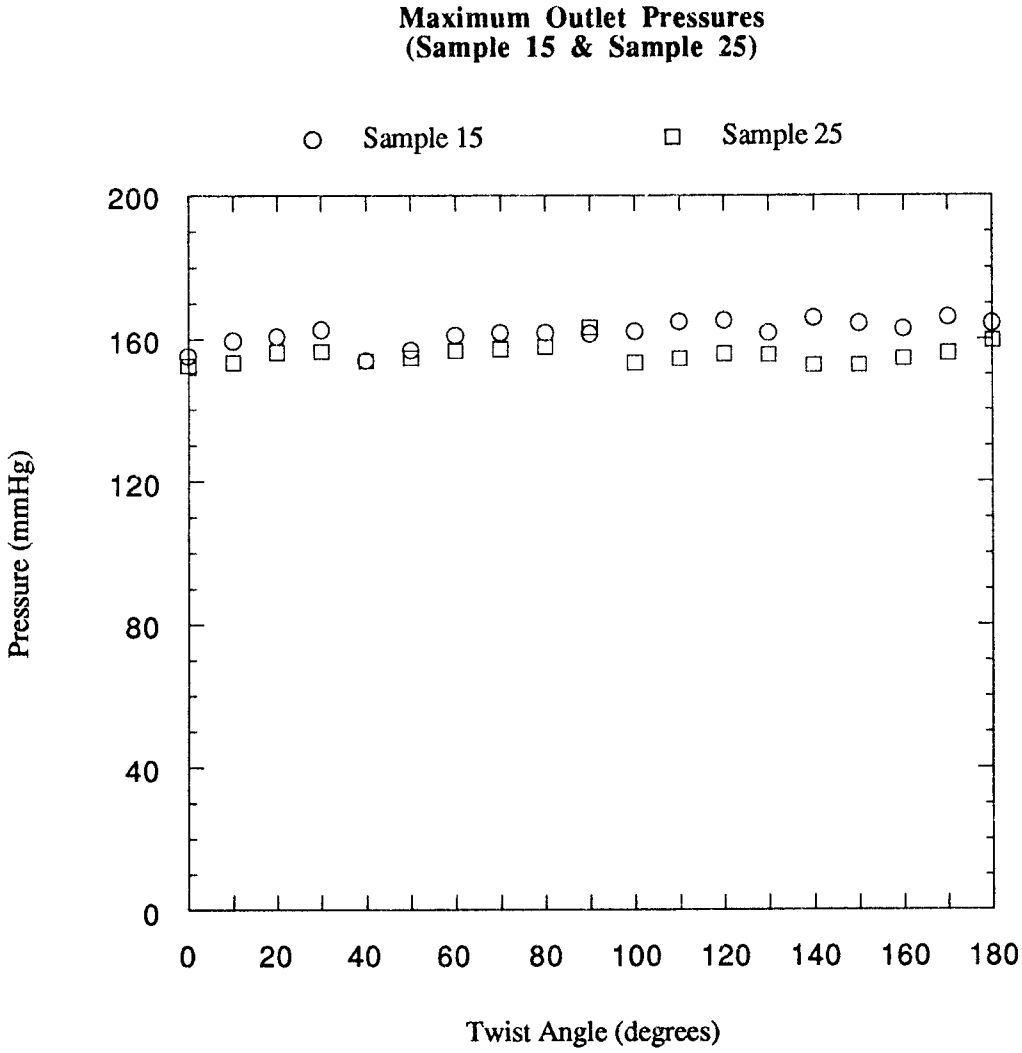

Figure 46 Maximum Outlet Pressures for Sample 15 & Sample 25

TABLE XVIII MAXIMUM PRESSURES - SAMPLE 17

Teflon Vascular Graft (Length = 76.2 mm, Slack = 12.7 mm)

Twist Angle (degrees)	Max. Inlet Pressure (mmHg)	Max. Outlet Pressure (mmHg)	Max. Delta Pressure (mmHg)	Max. Work ($mmHg.m^3$)
0	219.46	158.32	61.26	0.0008
10	218.91	158.99	58.13	0.0008
20	217.26	158.77	58.21	0.0008
30	222.20	161.89	55.97	0.0007
40	217.81	158.77	59.59	0.0008
50	221.11	161.66	60.74	0.0008
60	217.81	159.43	57.73	0.0008
70	219.46	160.77	57.13	0.0008
80	213.96	159.43	53.55	0.0007
90	220.01	161.66	57.81	0.0008
100	220.01	161.22	54.99	0.0007
110	219.46	161.66	54.24	0.0007
120	216.71	158.10	54.85	0.0007
130	216.16	158.10	56.05	0.0008
140	220.56	159.21	58.67	0.0008
150	219.46	158.54	58.59	0.0008
160	222.20	156.76	62.49	0.0008
170	219.46	155.20	59.78	0.0008
180	222.20	157.87	61.19	0.0008

Reference **Figure 47** (next page) for graph of maximum outlet pressures

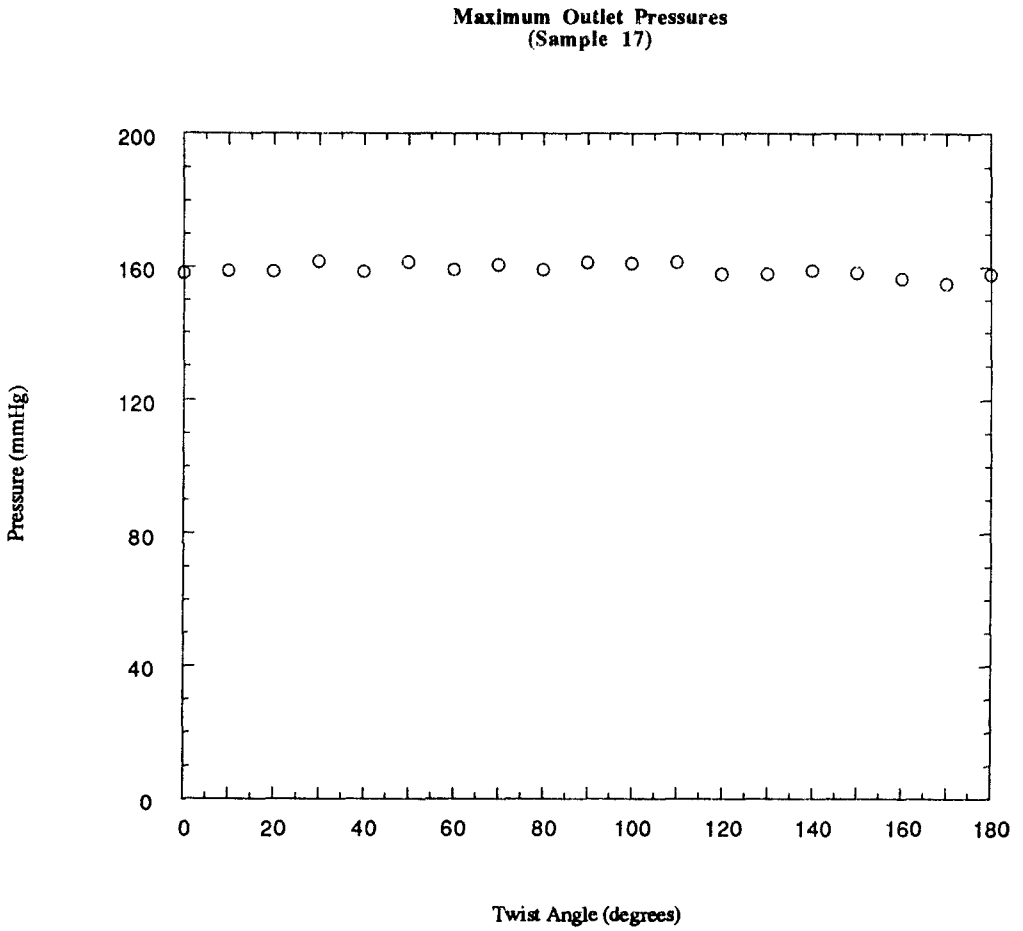

Figure 47 Maximum Outlet Pressures for Sample 17

TABLE XIX MAXIMUM PRESSURES - SAMPLE 26

Teflon Vascular Graft (Length = 69.8 mm, Slack = 0 mm)

Twist Angle (degrees)	Max. Inlet Pressure (mmHg)	Max. Outlet Pressure (mmHg)	Max. Delta Pressure (mmHg)	Max. Work ($mmHg.m^3$)
0	221.66	157.20	59.76	0.0008
10	224.40	159.43	60.64	0.0008
20	225.50	161.44	59.53	0.0008
30	220.56	160.33	55.66	0.0008
40	223.30	155.20	62.66	0.0009
50	222.75	156.54	60.66	0.0008
60	222.75	157.20	60.09	0.0008
70	218.36	157.43	55.25	0.0008
80	222.75	161.66	55.97	0.0008
90	222.75	154.75	64.24	0.0009
100	225.50	157.43	62.20	0.0009
110	224.95	158.77	62.08	0.0009
120	223.30	159.66	57.62	0.0008
130	221.66	154.08	63.68	0.0009
140	224.95	156.31	63.54	0.0009
150	224.40	158.54	62.10	0.0009
160	222.75	158.54	60.21	0.0008
170	221.66	154.53	61.68	0.0009
180	229.90	155.42	71.18	0.0010

Reference **Figure 48** (next page) for graph of maximum outlet pressures

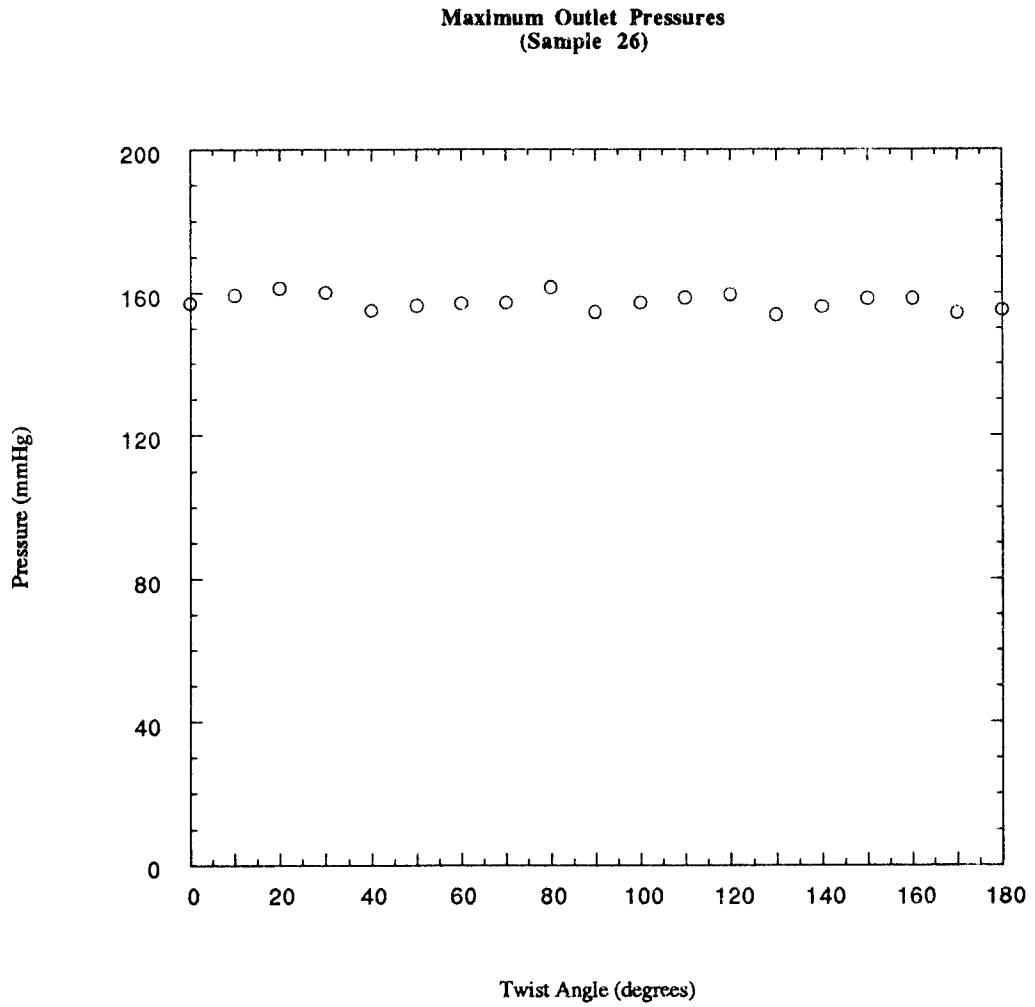

Figure 48 Maximum Outlet Pressures for Sample 26

TABLE XX MAXIMUM PRESSURES - SAMPLE 27

Teflon Vascular Graft (Length = 69.8 mm, Slack = 6.4 mm)

Twist Angle (degrees)	Max. Inlet Pressure (mmHg)	Max. Outlet Pressure (mmHg)	Max. Delta Pressure (mmHg)	Max. Work ($mmHg.m^3$)
0	227.70	153.86	71.18	0.0010
10	227.70	155.64	70.30	0.0009
20	230.45	157.87	71.46	0.0010
30	227.15	156.98	68.28	0.0009
40	223.85	151.41	68.43	0.0009
50	226.60	154.08	69.62	0.0009
60	228.80	156.31	68.25	0.0009
70	227.70	148.73	74.21	0.0010
80	228.80	151.18	76.27	0.0010
90	228.25	152.30	72.17	0.0010
100	226.60	152.30	72.01	0.0010
110	229.35	155.42	71.97	0.0010
120	223.30	152.74	70.19	0.0009
130	224.40	146.95	76.59	0.0010
140	228.25	148.06	78.76	0.0011
150	229.90	148.51	78.21	0.0010
160	228.80	146.95	79.40	0.0011
170	228.80	146.28	79.87	0.0011
180	231.55	148.28	80.94	0.0011

Reference **Figure 49** (next page) for graph of maximum outlet pressures

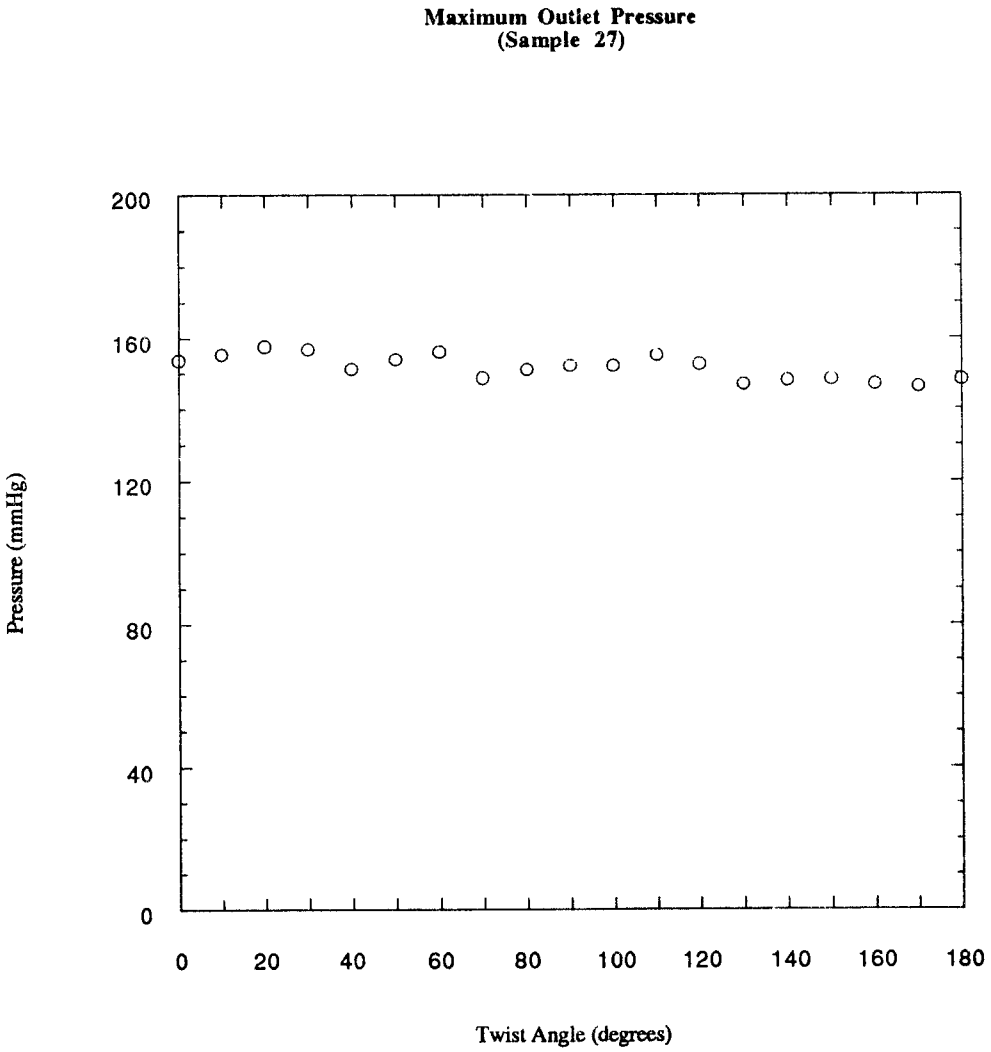

Figure 49 Maximum Outlet Pressures for Sample 27

TABLE XXI MAXIMUM PRESSURES - SAMPLE 28

Teflon Vascular Graft (Length = 127 mm, Slack = 0 mm)

Twist Angle (degrees)	Max. Inlet Pressure (mmHg)	Max. Outlet Pressure (mmHg)	Max. Delta Pressure (mmHg)	Max. Work ($mmHg.m^3$)
180	223.30	157.87	60.52	0.0011
190	226.05	162.11	59.94	0.0011
200	224.40	161.22	59.29	0.0011
210	224.95	162.56	56.59	0.0010
220	221.11	153.41	62.34	0.0011
230	220.01	153.41	62.35	0.0011
240	223.85	157.65	60.63	0.0011
250	222.75	156.54	60.31	0.0011
260	225.50	151.85	67.57	0.0012
270	222.20	148.95	74.80	0.0014
280	222.20	149.62	66.56	0.0012
290	223.85	156.54	63.75	0.0012
300	223.30	154.53	69.97	0.0013
310	223.30	154.53	68.97	0.0013
320	222.75	155.64	61.88	0.0011
330	221.66	153.19	71.90	0.0013
340	222.75	153.86	69.27	0.0013
350	223.85	156.31	63.42	0.0012
360	225.50	159.21	62.72	0.0012

Reference **Figure 50** for graph of maximum outlet pressures (note: Sample 28 & Sample 29 combined on graph)

TABLE XXII MAXIMUM PRESSURES - SAMPLE 29

Teflon Vascular Graft (Length = 127 mm, Slack = 0 mm)

Twist Angle (degrees)	Max. Inlet Pressure (mmHg)	Max. Outlet Pressure (mmHg)	Max. Delta Pressure (mmHg)	Max. Work ($mmHg.m^3$)
360	224.95	159.21	60.63	0.0011
370	223.85	158.32	63.09	0.0012
380	224.95	160.10	61.21	0.0011
390	222.20	160.55	57.86	0.0011
400	221.11	156.54	61.89	0.0011
410	222.75	159.88	61.98	0.0011
420	220.56	157.87	57.39	0.0011
430	218.36	158.77	57.61	0.0011
440	217.81	152.97	62.95	0.0012
450	217.81	153.41	62.50	0.0012
460	736.54	000.00	43.40	0.0082

Reference **Figure 50** (next page) for graph of maximum outlet pressures for Sample 28 & Sample 29

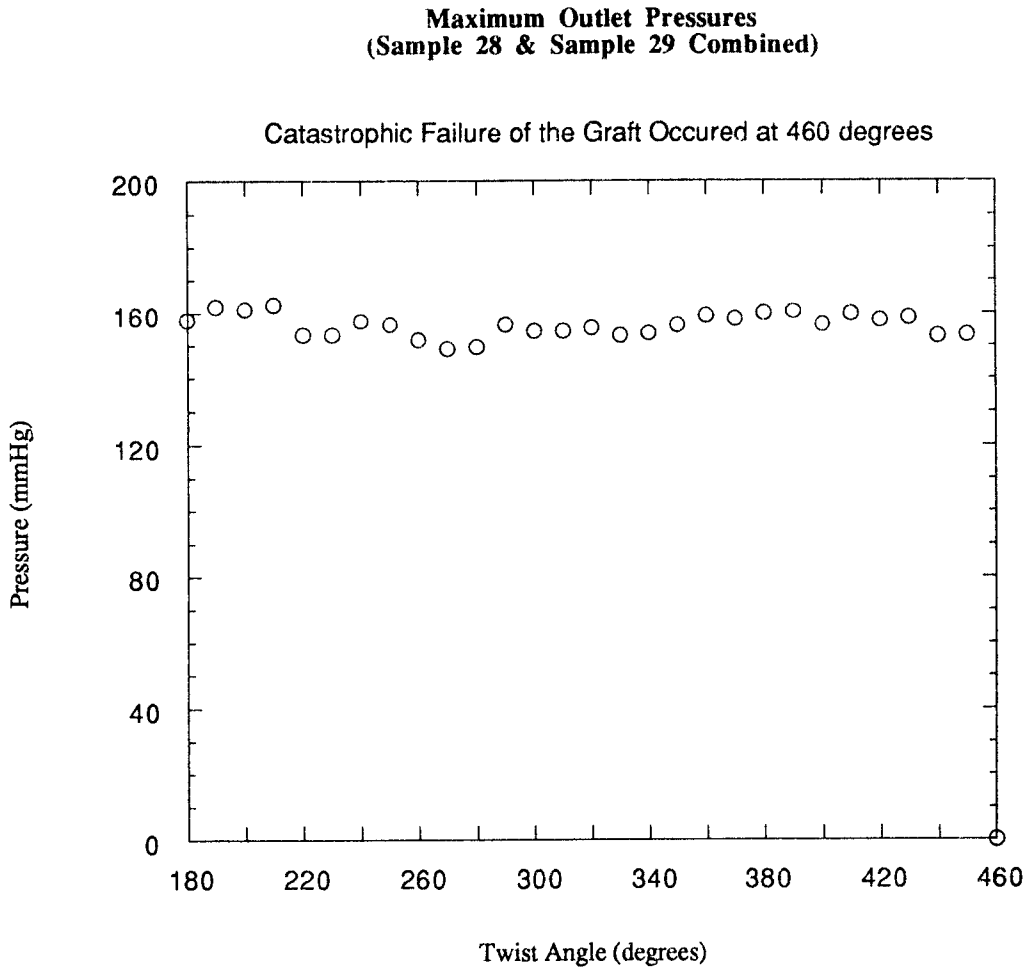

Figure 50 Maximum Outlet Pressures for Sample 28 & Sample 29

REFERENCES

1. Vander, A., et al. Human Physiology: The Mechanisms of Body Function, 4th Edition, New York: McGraw-Hill Book Company, 1985, pages 311.

2. Deykin, D. "Thrombogenesis," New England Journal of Medicine, Boston, 1967, pages 276:621.

3. Collins, G.J. "Thromboembolic Complications of Vascular Prostheses," in Wright, C.B., et. al Vascular Grafting: Clinical Applications and Techniques, Boston: John Wright PSG, Inc., 1983, page 246.

4. Vander, A., et al. Human Physiology: The Mechanisms of Body Function, 4th Edition, New York: McGraw-Hill Book Company, 1985, page 303.

5. Ibid, page 8.

6. Tortora, G., and Anagnostakos, N. Principles of Anatomy and Physiology, 6th Edition, New York: Harper & Row, Publishers, 1990, page 546.

7. Wallace, R., et al. Biology: The Science of Life, Illinois: Scott, Foresman and Company, 1981, pages 752-760.

8. Tortora, G. and Anagnostakos, N. Principles of Anatomy and Physiology, 6th Edition New York: Harper & Row Publishers, 1990, page 583.

9. Thomas, C., Taber's Cyclopedic Medical Dictionary, Philadelphia: F.A. Davis Co., 1981, page 643.

10. Kroemer, K.H.E. "Ergonomics," in Plog, B.A., et al. Fundamentals of Industrial Hygiene, Third Edition, Illinois: The National Safety Council, 1988, page 288.

11. Fung, Y.C. Biomechanics: Mechanical Properties of Living Tissues, New York: Springer-Verlag New York, Inc., 1981, page 261.

12. Tortora, G., and Anagnostakos, N. Principles of Anatomy and Physiology, 6th Edition, New York: Harper & Row, Publishers, 1990, pages 606-611.

13. Ibid, page 312.

14. Lichtenstein, O., and Dinnar, U. "Experimental Analysis of Pulsatile Flow Through Elastic Collapsible Tubes: Application to Cardiac Assist Device," Journal of Biomechanical Engineering, Vol. 112, Feb., 1990, page 76.

15. Vander, A., et al Human Physiology: The Mechanisms of Body Function, 4th Edition, New York: McGraw-Hill Book Company, 1985, page 332.

16. Skalak, R., et al. "Mechanics of Blood Flow," Transactions of the ASME, Vol. 103, May 1991, page 102.

17. Hamburger, W. W., "The Earliest Known Reference to the Heart and Circulation, The Edwin Smith Surgical Papyrus, circa 3000 B.C.," American Heart Journal, Vol. 17, 1939, pages 259-274.

18. O'Malley, C.D., and Saunders, J.B. de C.M., Leonardo da Vinci on the Human Body, New York: Henry Schuman Co., 1952, pages 216-326.

19. Skalak, R., et al. "Mechanics of Blood Flow," Transactions of the ASME, Vol. 103, May 1991, page 103.

20. Young, T., "Hydraulic Investigations," subservient to an intended Croonian lecture on the motion of the blood, Philosophical Transactions of the Royal Society of London, Vol. 98, 1808, pages 164-186.

21. Rouse, H., and Ince, S., History of Hydraulics, Iowa Institute of Hydraulic Research, Iowa City, Iowa, 1957, page 161.

22. Fåhraeus, R. "The Suspension Stability of the Blood," Physiology Review, Vol. 9, 1929, pages 241-274.

23. Voorhees, A.B., "How It All Began," in Sawyer, P., and Kaplitt, M. Vascular Grafts, New York: Appleton-Century-Crofts, 1978, pages 5-22.

24. Hufnagel, C.A. "History of Vascular Grafting," in Wright, C.B., Vascular Grafting, Boston: John Wright PSG, Inc., 1983, pages 1-12.

25. Guidoin, R., King, M., Marceau, D., and Cardou, A., "Textile Arterial Prostheses: Is Water Permeability Equivalent to Porosity?," Journal of Biomedical Materials Research, New York: John Wiley & Sons, Inc., Vol. 21, 1987, page 68.

26. Sawyer, P., Modern Vascular Grafts, New York: McGraw-Hill Book Company, 1987, page 93.

27. Padberg, F.T., et al. "Management of Hemoaccess Site Infection," Surgery, Gynecology & Obstetrics, February, 1992, Vol. 174, pages 103-108.

28. Padberg, F.T., et al. "Optimal Method for Culturing Vascular Prosthetic Grafts," Accepted for Publication, Journal of Surgical Research, Vol. 53, 1992.

29. Pourdeyhimi, B., and Wagner, D., "On the Correlation Between the Failure of Vascular Grafts and Their Structural and Material Properties: A Critical Analysis," Journal of Biomedical Materials Research, New York: John Wiley & Sons, Inc., Vol. 20, 1986, page 385.

30. Sauvage, L. R., et al Grafts for the 80's, Washington: The Bob Hope International Heart Research Institute, 1980, pages 2-6.

31. Snyder, R. W. "Fabrication and Testing of Textile Vascular Prostheses," in Wright, C.B. et al. Vascular Grafting: Clinical Applications and Techniques, Boston: John Wright PSG, Inc., 1983, pages 13-22.

32. Leidner, J., and Wong, E., "A Novel Process for the Manufacturing of Porous Grafts: Process Description and Product Evaluation," Journal of Biomedical Materials Research, New York: John Wiley & Sons, Inc., Vol. 17, 1983, pages 231-232.

33. Cannon, J.A. "The Expanded Reinforced Polytetrafluoroethylene Prosthetic Vascular Graft," in Wright, C.B. et al Vascular Grafting: Clinical Applications and Techniques, Boston: John Wright PSG, Inc., 1983, pages 31-42.

34. Sauvage, L. R., et al Grafts for the 80's, Washington: The Bob Hope International Heart Research Institute, 1980, pages 10 - 11.

35. Sauvage, L.R. "Externally Supported, Noncrimped, External-Velour, Weft-Knitted Dacron Prosthesis for Axillofemoral, Femoropopliteal and Femorotibial Bypass," in Wright, C.B., Vascular Grafting, Boston: John Wright PSG, Inc., 1983, pages 167-186.

36. Pourdeyhimi, B., and Wagner, D., "On the Correlation Between the Failure of Vascular Grafts and Their Structural and Material Properties: A Critical Analysis," Journal of Biomedical Materials Research, New York: John Wiley & Sons, Inc., Vol. 20, 1986, page 385.

37. Lynch, T., Hobson, R., Pawel, H. "Microprocessor-Controlled Pulsatile Flow Loop for Hemodynamic Studies," Journal of Surgical Research, Vol. 40, 1986, pages 285-286.

38. Bauer, K.T. "An Investigation of Flow-Induced Sound in Partially Occluded Distensible Tubes," M.S. Diss., New Jersey Institute of Technology: Mechanical Engineering Department, 1979.

39. Shin, S. "Blood Pressure Signal Simulation in an Artificial Circulation System," M.S. Diss., New Jersey Institute of Technology: Electrical Engineering Department, 1982.

40. Wu, Y. "An Investigation of Characteristics of Blood Velocity in a Simulated Circulation System," M.S. Diss., New Jersey Institute of Technology: Electrical Engineering Department, 1984.

41. Korurek, M. "A Development of Pulsatile Flow in an Artificial Circulatory Model," New Jersey Institute of Technology: Mechanical Engineering Department, 1982.

42. DeMuth, M. "NJIT Flowloop," New Jersey Institute of Technology: Biomedical Engineering Department, 1985.

43. Endean, E.D., et al. "The Effects of Twist on Flow and Patency of Vein Grafts," Journal of Surgery, Vol. 9, No. 5, 1989, pages 651-655.